

# Morphological development after the July 2014 flow slide on the tidal flat of Walsoorden in the Western Scheldt



MSc Thesis  
Samantha van Schaick  
November 2015



Front cover: Areal view of the tidal flat of Walsoorden after the July 2014 flow slide  
Source: Rijkswaterstaat/Edwin Pree 2014 ©

# Morphological development after the July 2014 flow slide on the tidal flat of Walsoorden in the Western Scheldt

by

S.J. (Samantha) van Schaick

in partial fulfilment of the  
requirements for the degree of

**Master of Science**  
in Civil Engineering

at

**Delft University of Technology**

November 2015, Delft, The Netherlands

**Graduation committee:**

Prof.dr.ir. Z.B. Wang	Chairman, Delft University of Technology
Dr.ir. J.J. van der Werf	Deltares
Ir. D.R. Mastbergen	Deltares
Dr.ir. B.C. van Prooijen	Delft University of Technology
Ir. P.L.M. de Vet	Delft University of Technology/Deltares

An electronic version of this thesis is available at <http://repository.tudelft.nl>



## Preface

This thesis concludes the 'Hydraulic Engineering' master programme at the Delft University of Technology, faculty Civil Engineering and Geosciences. The research was conducted at Deltares in Delft, within the context of the Deltares project KPP Westerschelde, meso-scale morphology (project number 1220095).

I would like to thank all the members of my graduation committee for their commitment and feedback during my thesis work. A special thanks to my daily supervisors Dick Mastbergen and Jebbe van der Werf for the meetings and advice, as well as the time invested in me.

During this project I had the opportunity to work at Deltares every day. This was a valuable experience for me. I would like to thank Deltares for providing me this opportunity. Furthermore, I would like to thank the fellow students at Deltares for their help, suggestions and the coffee and lunch breaks.

Last, but not least, I would like to thank my family for providing me the possibility to study and for their unconditional support.

Samantha van Schaick  
Delft, November 2015



## Abstract

The overall behaviour of the tide-dominated Western Scheldt is in general well known. Its multichannel-system consists of ebb and flood channels, separated by intertidal areas; the tidal flats. The estuary shows a dynamic behaviour of erosion and sedimentation of the tidal flats. A large flow slide occurred at the tidal flat of Walsoorden in July 2014. A flow slide occurs when the slope is sufficient steep and a trigger starts the process of liquefaction or breaching. In a few hours a huge amount of sediment slides away, causing loss of surface and endangering safety. During this flow slide approximately 800,000 m<sup>3</sup> of sediment flowed to the navigation channel, leaving a large gap in the tidal flat. This flow slide is one of the largest known in this part of the Western Scheldt.

A measurement campaign was initiated to measure the bathymetry around the tidal flat, starting a few months before the flow slide. After the event monthly measurements were taken to monitor the development of the area. Dunes were formed on top of the accumulation of sediment, which travelled in flood (eastern) direction. A large part of the sediment accumulation was transported as bed load in flood direction, which is unexpected since the Zuidergat channel is known as an ebb channel. The sediment volume in the channel is decreasing, suggesting suspended load transport. The channel dominance is determined based on three characteristics: the water level, velocities and sediment transport. Based on water level data flood dominant behaviour is expected, while velocity and sediment transport data result in ebb dominance.

Based on the bathymetry measurements, the volume changes in the channel and in the gap were determined. Those showed an exponential change in time. The erosion rate in the channel was faster than the sedimentation rate in the gap. The recovery time of the system is estimated through extrapolation of this data. The recovery time for the channel is thus shorter than the recovery time for the gap, 9 months and 1.5 to 2 years respectively.

An existing Delft3D model schematisation of the Western Scheldt was used to calculate the morphological development. The model was setup around the tidal flat of Walsoorden. The boundary conditions were generated by a model schematization which describes the full Scheldt estuary; the validation was performed with observations of water level and velocity along the tidal flat. The morphological changes determined by the model are different from the bathymetric changes found in the measurements. In the model the sediment accretion smoothens out; the sediment is deposited on the sides of the accumulation. Most of the sediment from the channel is transported in ebb direction. The model shows almost no sedimentation in the gap, which is contradictive with the measurements.

The sensitivity of the model was tested to investigate the differences between the observations and the model. A varying sediment diameter in the model had effect on the amount of transported sediment only, not on the residual direction. The used model is a 2DH model, neglecting the secondary circulations. The sensitivity of these processes was tested using a 3D model. From this model it was found that the secondary circulations were not of significant importance concerning the areal development after the flow slide. Finally, a non-cohesive sediment fraction was implemented in the model. This showed sedimentation in the gap. Therefore, it is suggested that the sediment settling in the gap is a combination of cohesive and non-cohesive sediment, which is supported by the observations.

# Contents

<b>Preface</b>	<b>i</b>
<b>Abstract</b>	<b>iii</b>
<b>1 Introduction</b>	<b>1</b>
1.1 Background	1
1.2 Opportunities	2
1.3 Research objective and questions	3
1.4 Methodology and thesis outline	3
<b>2 Literature review</b>	<b>4</b>
2.1 Western Scheldt	4
2.1.1 Historical development	4
2.1.2 Hydrodynamics	5
2.1.3 Sediment transport	6
2.1.4 Morphology	7
2.2 Tidal flat of Walsoorden	8
2.2.1 Historical development	8
2.2.2 Hydrodynamics	9
2.3 Flow slides	10
2.3.1 Static liquefaction	10
2.3.2 Up-slope migrating breach	11
2.3.3 Dike safety and flood defence	12
2.3.4 Sensitive areas	12
2.4 Conclusion	13
<b>3 Analysis of velocity, sediment transport and morphological data</b>	<b>14</b>
3.1 Velocity	14
3.1.1 Discharge	15
3.2 Sediment composition	16
3.2.1 McLaren	16
3.2.2 IJkdijk	16
3.3 Sediment transport measurement	17
3.4 Bathymetry	18
3.4.1 Cross sections	19
3.4.2 Longitudinal section	20
3.4.3 Contour lines	21
3.4.4 Dune migration	22
3.4.5 Bed load transport	23
3.5 Morphology	23
3.5.1 Erosion and sedimentation pattern	23
3.5.2 Volume	24
3.5.3 Volume change over time	25
3.5.4 Suspended load transport from the deposited sediment in the channel	27
3.6 Dominant processes	27
3.6.1 Driving forces	27
3.6.2 Estuarine circulation	27
3.7 Discussion	29

3.8	Conclusion	29
3.8.1	Ebb/Flood dominance	29
3.8.2	Morphologic development	30
<b>4</b>	<b>Walsoorden model setup</b>	<b>31</b>
4.1	Delft3D	31
4.2	NeVla model	31
4.2.1	Grid	31
4.2.2	Boundary conditions	32
4.2.3	Validation	32
4.3	Walsoorden model grid	32
4.3.1	Domain	32
4.3.2	Resolution	32
4.4	Boundary conditions	33
4.5	Initial conditions	33
4.5.1	Bathymetry	33
4.5.2	Sediment layer thickness	34
4.5.3	Roughness	34
4.5.4	Salinity	35
4.6	Model parameters	36
4.6.1	Sediment transport formula	36
4.6.2	Numerical input	36
4.7	Simulation period	37
4.8	Discussion	37
<b>5</b>	<b>Hydrodynamic validation of the Walsoorden model</b>	<b>38</b>
5.1	MONEOS measurements	38
5.1.1	Water level	38
5.1.2	Velocity	39
5.2	Comparison with Delft3D NeVla model	40
5.2.1	Water level	40
5.2.2	Discharge	41
5.2.3	Velocity	42
5.3	Conclusion	43
<b>6</b>	<b>Modelling the morphological impact of the flow slide</b>	<b>45</b>
6.1	Initial conditions	45
6.1.1	Bathymetry	45
6.1.2	Sediment thickness	45
6.2	Effect of the flow slide on the hydrodynamics	46
6.2.1	Water level	46
6.2.2	Discharge	47
6.2.3	Velocity	48
6.3	Residual flow	49
6.4	Sediment transport	50
6.5	Morphological change	51
6.5.1	Erosion in the channel	51
6.5.2	Sedimentation in the gap	51
6.5.3	Conclusion	52

<b>7 Sensitivity of the model</b>	<b>54</b>
7.1 Sediment diameter	54
7.1.1 Sediment fractions	54
7.1.2 Sediment transport	54
7.2 Sediment transport formula	56
7.3 Tidal asymmetry	56
7.3.1 Vertical asymmetry	56
7.3.2 Horizontal asymmetry	57
7.4 3D effect	57
7.5 Mud	59
7.6 Discussion	60
7.7 Conclusion	61
<b>8 Conclusions and recommendations</b>	<b>62</b>
8.1 Conclusions	62
8.2 Recommendations	64
<b>9 References</b>	<b>65</b>
<b>Appendices</b>	
<b>A Bathymetry measurements</b>	<b>A-1</b>
A.1 Bathymetry	A-2
A.2 Erosion	A-5
A.2.1 With respect to June	A-5
A.2.2 With respect to August 2014	A-7
A.2.3 Monthly erosion	A-9
A.3 Cross sections	A-11
A.4 Longitudinal cross sections	A-14
A.5 Location of the sediment accumulation	A-16
<b>B Simulation period</b>	<b>B-1</b>
<b>C Validation domain decomposition</b>	<b>C-1</b>
<b>D Validation MONEOS measurements</b>	<b>D-1</b>
<b>E Modelled sediment transport</b>	<b>E-1</b>
<b>F Overview channels and shoals Western Scheldt (east)</b>	<b>F-1</b>

# 1 Introduction

## 1.1 Background

In July 2014 a large flow slide (*in Dutch: zettingsvloeiing, plaatval*) occurred on the tidal flat of Walsoorden (Figure 1.1). A flow slide is a underwater bed slope instability due to which a large amount of sediment flows from, for instance, a tidal flat or dike foreshore into deeper water in a relatively short time. It takes place when the slope is sufficiently steep and a trigger or instability occurs. Flow slides can give problems for the stability of dikes or other constructions. Ecologically it has an enormous impact on the benthos of a tidal flat. In the Eastern and Western Scheldt over 1000 flow slides were reported since 1800. More recently flow slides are observed on the tidal flat of Walsoorden periodically, about once every two years (Van den Ham et al., 2015).

The July 2014 flow slide was possibly initiated by low water levels in combination with large precipitation (Rijkswaterstaat, 2014). During the flow slide 800,000 m<sup>3</sup> of sediment flowed down the slope into the navigation channel, which was much more than during the average flow slides in the Western Scheldt (IMDC, 2014a).



Figure 1.1: Overview of the Western Scheldt (Schroevens, 2013) with a detail of the tidal flat of Walsoorden (Rijkswaterstaat, September 2014)

The Western Scheldt is important for the navigation towards the Antwerp harbour and other harbours along the estuary, as well as for nature conservation. To preserve the values of the Western Scheldt cooperation between the Dutch and Flemish government was set up, the Long-Term Vision (LTV, 2001). In this context three main objectives are considered 1) the safety against flooding, 2) accessibility of the ports and 3) nature development. To guarantee the accessibility of the ports a lot of dredging activities take place in the navigation channels. The dredged sediment is redistributed along the estuary.

## 1.2 Opportunities

Since the mechanism of a flow slide was not known in detail, and it was never observed real-time, *Stichting FloodControl IJkdijk* initiated the so-called *IJkdijkexperiment Zettingsvloeiing* in September-October 2014. During this experiment a flow slide was triggered by means of dredging and the morphological development was carefully monitored. The bathymetry development, soil pressures and sediment composition were measured. The initially chosen location to perform the test was exactly the location where the July 2014 flow slide took place. A new location was selected a few hundred meters to the east, with similar conditions.

On the northern tip of the tidal flat of Walsoorden dredged sediment is dumped. This is part of the *'Flexibel Storten'* strategy, related to the flexible dumping of sediment from maintenance dredging. To evaluate this strategy, the redistribution of the deposited sediment is being monitored. The bathymetry is measured monthly to observe erosion and sedimentation patterns. After the July 2014 flow slide, the measurement area was expanded to also include the flow.

These two campaigns provide a unique detailed, large scale dataset of measurements around the tidal flat. The development after the flow slide was extensively monitored, creating an opportunity to investigate the behaviour of the sediment in this area. The bathymetry was measured 1-2 times per month for a period of a year after the flow slide. After this the measuring frequency was bi-monthly.

The morphological development of the tidal flat of Walsoorden and the channel after the flow was uncertain. In the past only once the morphological development was investigated in the Western Scheldt after a flow slide, by Ebbens (1980). The investigation of the behaviour of the system after a flow slide would lead to a sufficiently grounded advice regarding dredging operations and nature preservation. In Figure 1.2 the situation directly after the flow is given, where a steep slope in the tidal flat is shown.

The provided datasets can be used to validate morphological models. With these models the effect of, for example, the deposition operation on the northern tip of the tidal flat of Walsoorden can be estimated. In the Long-Term Vision other dumping locations around the tidal flat of Walsoorden are tested, which all need to be calculated with a model. This model needs to be sufficiently validated, which can be done using the provided datasets.



Figure 1.2: Erosion of the tidal flat of Walsoorden directly after the flow slide, the 28<sup>th</sup> of July 2014 (photo: RWS)

### 1.3 Research objective and questions

The objective of this thesis is to determine, understand and model the fate of the sediment originating from the July 2014 flow slide on the tidal flat of Walsoorden.

The following research questions are formulated:

- 1 What is the fate of the deposited sediment in the channel and which processes are responsible for this morphological development?
- 2 How does the gap in the tidal flat develop after the flow slide and which processes drive this development?
- 3 How can we model the morphological evolution and the underlying processes?

This research is restricted to the recovery after the flow slide. The geotechnical processes that cause a flow slide are covered in various projects regarding dike safety, for instance in Rijkswaterstaat (2012).

### 1.4 Methodology and thesis outline

These research questions are answered through a combination of data-analysis and Delft3D numerical modelling. The available data is used to determine the processes around the tidal flat and this information is used to validate the model. The Delft3D NeVla model (2DH) is used since the accuracy is sufficient, it is validated for 2014 and it is available for usage in this research.

A literature study (Chapter 2) is performed on the relevant processes in the Western Scheldt, the tidal flat of Walsoorden and the mechanism of a flow slide. In Chapter 3 the available data around the site is investigated. The monthly bathymetry data from the measurements by Rijkswaterstaat and the Flemish government, velocity measurements, sediment transport data and the grain characteristics are used to determine the important processes. The sedimentation and erosion pattern is determined and a first estimation of the recovery time is made.

Hereafter, the model setup is described in Chapter 4. A part of the Delft3D-NeVla model is taken to setup a model for the area of interest. The hydrodynamics are validated using existing velocity observations and the validated Delft3D-NeVla model in Chapter 5. The effect of the flow slide on the hydrodynamic and morphological conditions is examined in 6. The morphologic sensitivity of the morphological changes in the model is given in Chapter 7. Finally, the conclusions and recommendations are given in Chapter 8.

## 2 Literature review

### 2.1 Western Scheldt

The Western Scheldt consists of a rather repetitive pattern of ebb and flood channels, called a multiple channel system. An overview is given in Figure 2.1. The ebb channels (grey, solid lines) are meandering while the flood channels (white, dotted lines) are relatively straight. The channels are separated by the intertidal flats (Tank, 1996). The ebb channels are generally deeper than the flood channels, which makes them more suitable for navigation purposes (Van der Werf and Briere, 2013).

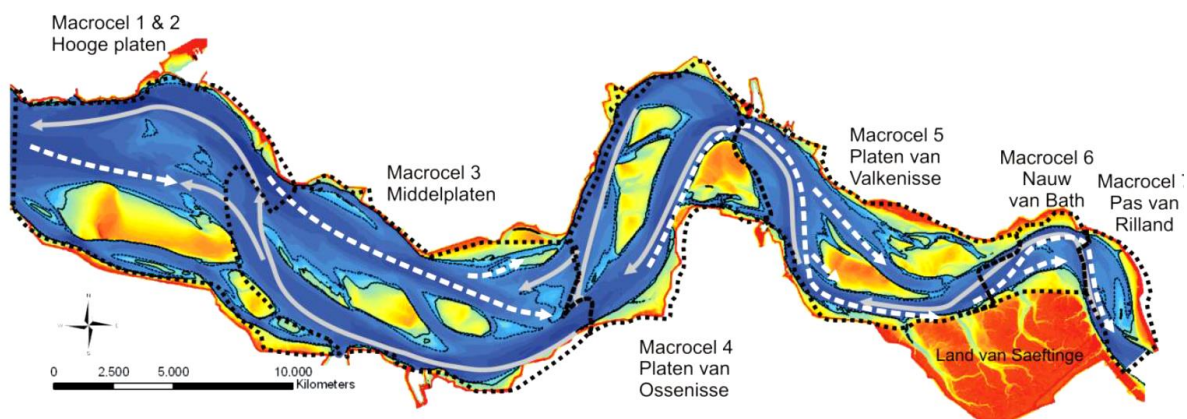


Figure 2.1: Schematization of the ebb and flood channels (Taal et al., 2013)

#### 2.1.1 Historical development

In the past the Western Scheldt estuary consisted of many islands. These islands were very sensitive to flooding due to storm surges. Since the 14<sup>th</sup> century the Western Scheldt became deeper and wider because of these storm surges. This created possibilities for navigation. However, since it was easier for the tidal wave to enter the estuary, the tidal amplitudes at the end of the estuary increased. From the 16<sup>th</sup> century on land was reclaimed from the sea on a larger scale. This forced the tidal wave to flow further into the estuary, which was fixed by dikes (de Kramer, 2002). The construction of dikes made the cross sectional area much smaller and the tidal amplitude increased even more. This caused larger flow velocities. Due to these velocities there was more erosion along the dikes and shoals causing flow slides to occur on regular base (Arends et al., 1999). From 1953 to 1987, in the framework of the Deltaworks, many foreshores and dikes were reinforced with stone protection and the yearly number of flow slides was reduced significantly.

In the 19<sup>th</sup> century the tidal flats in the estuary were smaller and more connecting channels existed compared to the current situation. This caused a more dynamic behaviour of these tidal flats. Half-way the 20<sup>th</sup> century these connecting channels partially disappeared and large shoals were formed (Kater, 2005).

In the 20<sup>th</sup> century the economic activity in the port of Antwerp increased. The ships became larger, requesting an increase in channel depth. Therefore, the channels were deepened three times, between 1971 and 1979, between 1997 and 1998 and the last one in 2010 (Taal et al., 2013). In between these large dredging operations there also had to be maintenance dredging to prevent the sills from silting up (Dam et al., 2013).

## 2.1.2 Hydrodynamics

In the Scheldt estuary the waves do not penetrate completely in the estuary. The influence of the river is far less than the influence of the tide. Therefore, the Scheldt estuary is characterized as a tide-dominated estuary. In this section some general information is given about the tidal forcing, as well as some information about the secondary circulations, the river influence and the human interventions in the estuary.

### Tide

The tide contains different components, where M2 (semi-diurnal with a period of 12h25m) and M4 (quarter-diurnal with a period of 6h21m) are the most important for the determination of the tidal behaviour (Bosboom and Stive, 2015). The ratio and the phase between these two are used to determine the tidal asymmetry (de Kramer, 2002). The tide can be represented in a vertical and horizontal component: the water levels respectively the discharge and flow velocity. The water levels and velocities are in phase for a propagating wave. When they are 90° out of phase a standing wave is occurring and the nodes stay on the same location. In the estuary the phase difference is small, suggesting a propagating wave. In the Sea Scheldt the phase difference is larger going almost to a standing wave (Van der Werf and Briere, 2013).

The tidal amplitude varies over time and space. The differences are caused by the spring-neap tidal cycle of 14.8 days (M2-S2-interaction) and the daily inequality. Spatially it varies due to four dominant processes: 1) inertia related to acceleration and deceleration effects, 2) the amplification due to the decrease of the width and depth in landward direction, 3) damping due to bottom friction and 4) partial reflection at the landward end of the estuary (Van Rijn, 2011). This causes a change in tidal range from 4.4 m at Vlissingen to 5.3 m near Antwerp and maximum channel velocities between 1.5 and 2 m/s.

### River discharge

The river discharge from the Scheldt is on average 100 m<sup>3</sup>/s (Portella and Neves, 1994). Since the Scheldt is a rain-fed river the discharges vary seasonally; in winter the discharges are higher than in summer. The discharged volume is rather low compared to the tidal volume, only 0.7% of the tidal volume at the seaward boundary. Therefore, the influence on the water motion due to the river discharge is almost negligible (Wang et al., 1999).

In the eastern part of the estuary the influence of the river discharge is larger. This leads to a horizontal density difference, which can create estuarine circulation. The Canter-Cremers number determines the rate of vertical mixing in an estuary and is equal to the ratio between the amount of fresh and saline water entering the estuary during a tidal period (Savenije, 2012). This number equals 149 at Vlissingen and 12 at Antwerpen, where a value over 10 indicates well mixed conditions (Baeyens et al., 1998; Thoolen and Wang, 1999). Horizontally the salinity differs from 7 ppt at the Dutch-Belgian border to 25 ppt near Vlissingen, over a distance of 60 km. The horizontal difference is sufficiently small to avoid circulation (Kranenburg, 1996).

### Circulation and residual flow

The Coriolis force is introduced due to the rotation of the earth, which acts on a fluid. This force is significant in large water bodies, like oceans, seas, wide estuaries and large lakes (Van Rijn, 2013). In estuaries this force cannot always be neglected. On the northern hemisphere the Coriolis force is directed to the right, perpendicular to the fluid motion (clockwise) (Bosboom and Stive, 2015). The Coriolis force is introducing ebb and flood chutes, which can eventually result in shortcutting channels through the shoals (Van den Berg et al., 1996). In large channels it can cause difference in direction across the channel.

Due to the centrifugal force the water levels in the outer side of the bend are larger than in the inner side of the ebb channel. The water body is pushed to the outside of the bend and the water levels are higher over there. When the difference in water level between the outer side and the flood channel is large enough the water will flow over the tidal flat and a connecting channel can be formed (Van den Berg et al., 1996).

During high water the propagation speed of the tide is larger than during low water. In combination with lower bottom friction during high water, this gives a higher velocity of the wave crest than the wave trough. This gives a net mass transport in the propagation direction, called the Stokes' drift.

### 2.1.3 Sediment transport

Once near the bed the critical velocity is exceeded the sediment will start to move, this is called the initiation of motion (Van Rijn, 1984). To determine the critical velocity the Shields criterion is used. Once the Shields parameter exceeds the critical value the sediment will start to move. The equation to determine the Shield parameter is given in 2.1.

$$\theta = \frac{(u_*)^2}{(s - 1)gD_{50}} \quad (2.1)$$

In this equation  $s$  is the specific density ( $\rho_s/\rho$ ),  $g$  is the gravitational constant,  $D_{50}$  is the median sediment diameter and  $u_*$  is the shear stress velocity. Below the critical value there is no sediment transport, above there is an initiation of motion.

When the sediment starts to move there are three transport modes, rolling and sliding, saltation and suspended particle motion. The first two modes are referred to as bed load transport. First they will start rolling and sliding, where they stay in continuous contact with the bed. With increasing velocity the particles will move along the bed with regular jumps (saltation mode). When the particle fall velocity is exceeded by turbulent diffusion and a higher Shield number is found, the particles will stay in suspension. In the Western Scheldt the ration between the magnitude of the suspended load transport and the bed load transport is 1:10 (Kuijper et al., 2006).

The amount of transported sediment is non-linearly related to the velocity. After flow reversal the particles need time to react, the relaxation time. After this time the particles will settle since the transport capacity is not sufficient any more. The direction of the sediment transport differs during ebb and flood. During ebb there is export and during flood there is import. These two sediment fluxes give a residual transport. In the Western Scheldt there is residual import of mud and residual export of sand (Jeuken and Wang, 2000).

#### Large-scale sediment transport patterns

In the Western Scheldt estuary there is a circulation of sediment, this is illustrated in Figure 2.2. The sediment is imported from the mouth of the estuary. The boxes represent respectively the west and east part of the estuary. The natural behaviour of the system is to transport sediment from the west towards the east of the estuary. In the eastern part the sediment settles on the sills, making them too shallow for navigation (Dam et al., 2013; IMDC, 2014b). To keep the estuary in equilibrium, the sediment, dredged in the eastern part, is deposited in the deep sections in the west (Port of Antwerp Expert Team, 2003). Besides the dredging for recirculation there is also a sand mining occurring in the east. This sediment is extracted from the system and cannot contribute to the equilibrium situation. From the eastern part there is also export towards the Land van Saeftinghe and the Sea Scheldt. All these export factors together cause a decrease of sediment volume in the eastern part of the Western Scheldt.

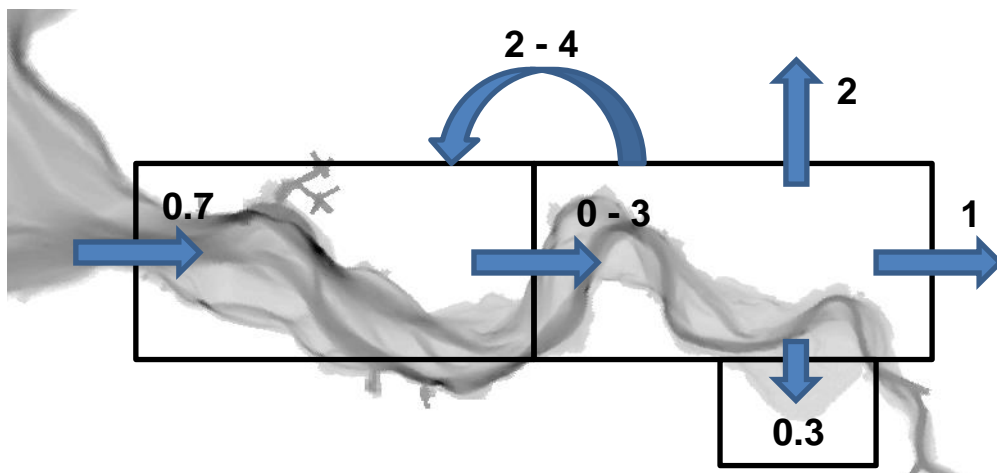


Figure 2.2: Circulation of sediment through the estuary in  $Mm^3/year$  for the period 1994-2010 (Cleveringa, 2013)

## 2.1.4 Morphology

A lot of the changes in morphology are made due to human interferences. In the past the building of dikes and reclaiming of land caused a permanent loss of intertidal area and lead to a fixation of the estuary. Later on dredging, sand mining and disposal became the main interferences that changed the morphology (Van der Werf and Briere, 2013). There has been three times a deepening of the channel by dredging. During the deepening the sediment was deposited in the deep parts of the estuary. After a while the sediment is redistributed along the estuary and eventually most of the sand is transported to the sills. The locations of these sills are given in Figure 2.3. To guarantee the navigation depth periodic maintenance dredging has to be carried out (Aantjes, 2014). Since the tips of the tidal flats are eroding, which reduces the ecological values, the idea came up to protect them by using the dredged material from the sills. This is done by disposing the sediment just before the shoals and let the currents take the sediment to the tidal flat, the 'Flexibel Storten' strategy (IMDC, 2014b). This is for instance done at the western side of the tidal flat of Walsoorden. If the sills are not dredged they would become too shallow and cause a problem for navigation in the end (Dam et al., 2013).

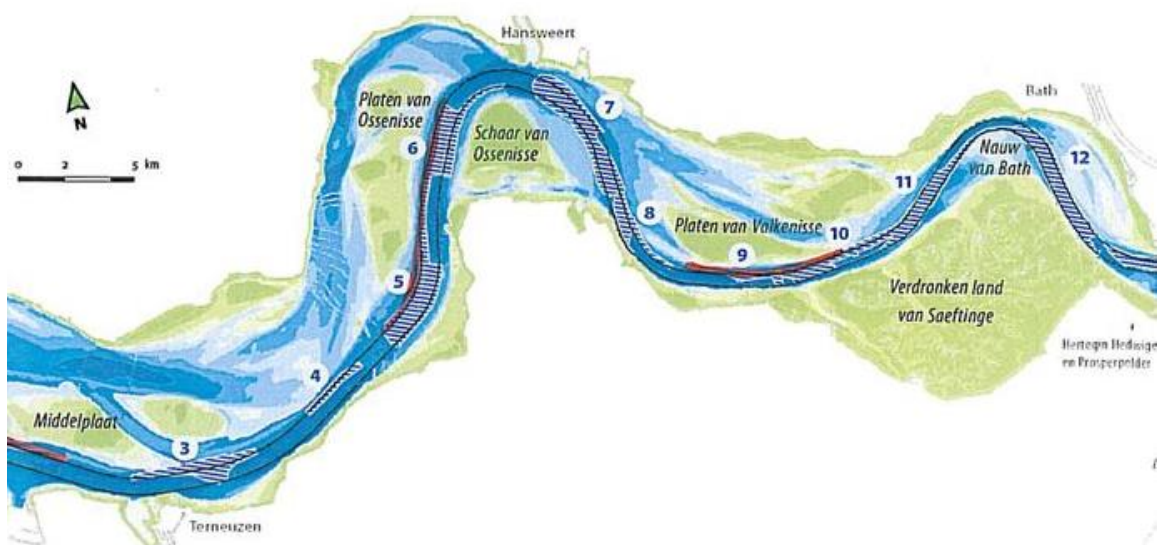


Figure 2.3: Locations sills (Departement Mobiliteit en Openbare Werken, 2015)

## 2.2 Tidal flat of Walsoorden

The tidal flat of Walsoorden is situated in the east of the Western Scheldt. In Figure 2.4 an overview of this part is given. The tidal flat of Walsoorden (1) is part of the Platen van Valkenisse and is the western tidal flat. The Zuidergat channel (2) is the channel on the west and south of the tidal flat and is the navigation channel. The Schaar van Waarde (3) is the channel on the north. The Zuidergat shows ebb dominant behaviour, the Schaar van Waarde shows flood dominant behaviour. A larger version of this figure can be found in Appendix E.

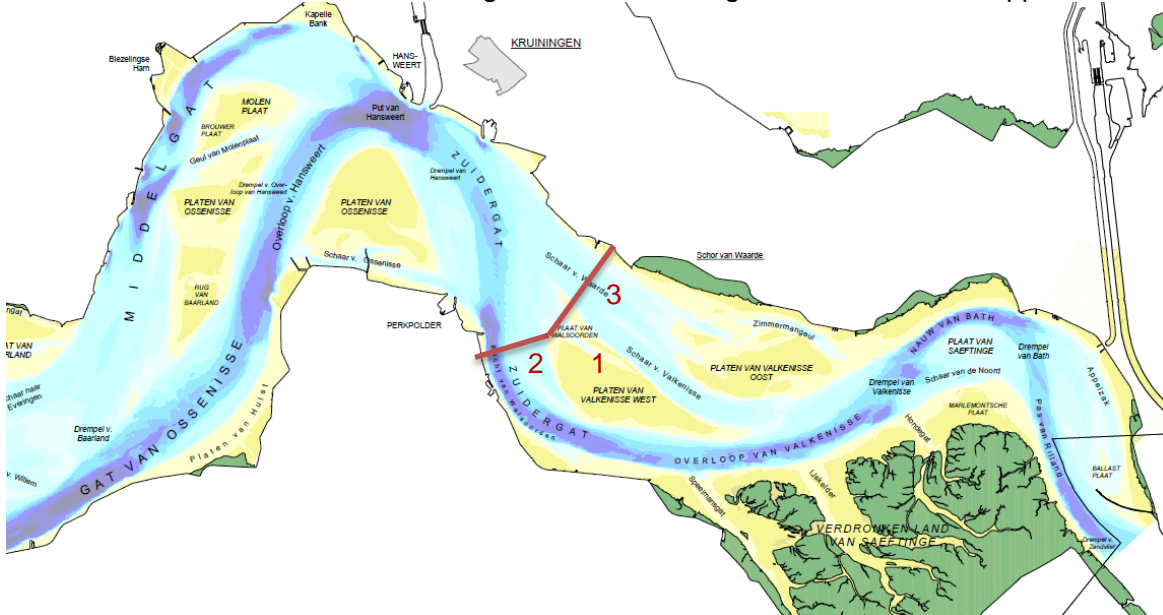


Figure 2.4: Overview channels and shoals in the study area (Cleveringa et al., 2014)

### 2.2.1 Historical development

The development in the last century of the tidal flat of Walsoorden can be observed using the 'vaklodingen', the yearly bathymetry measurements by Rijkswaterstaat (2015). For this area measurements are available since 1951 (Figure 2.5, left). At that moment the tidal flat was large and contained a lot of discontinuities. Several flood and ebb chutes existed around the tidal flat. The flood channel at the north of the tidal flat was not yet connected with the main ebb channel. After some time this flood channel is changing position and during the 1980's it almost disappeared. The channel is recovered after 2000 and is nowadays almost completely connected (Arcadis, 2013a).

The elevation map of 2013 is given in the right panel of Figure 2.5. In time the surface area of the tidal flat has reduced. At the same time, the height of the tidal flat has increased. This is due to sedimentation on top of the tidal flat after flood, and the lack of erosion during ebb due to the height of the tidal flat. This phenomenon is observed throughout the whole Western Scheldt. Together with the compacting of the tidal flat the number of chutes is reduced. This is also due to the increase of the height; more sediment needs to erode for the existence of a chute. The channel at the south of the tidal flat is gradually deepened in time, naturally and due to dredging. However, most of the dredging in this area occurred east of the shoal, at the Overloop van Valkenisse. Arcadis (2013a) did some further investigation on the development of the tidal flat of Walsoorden on meso-scale.

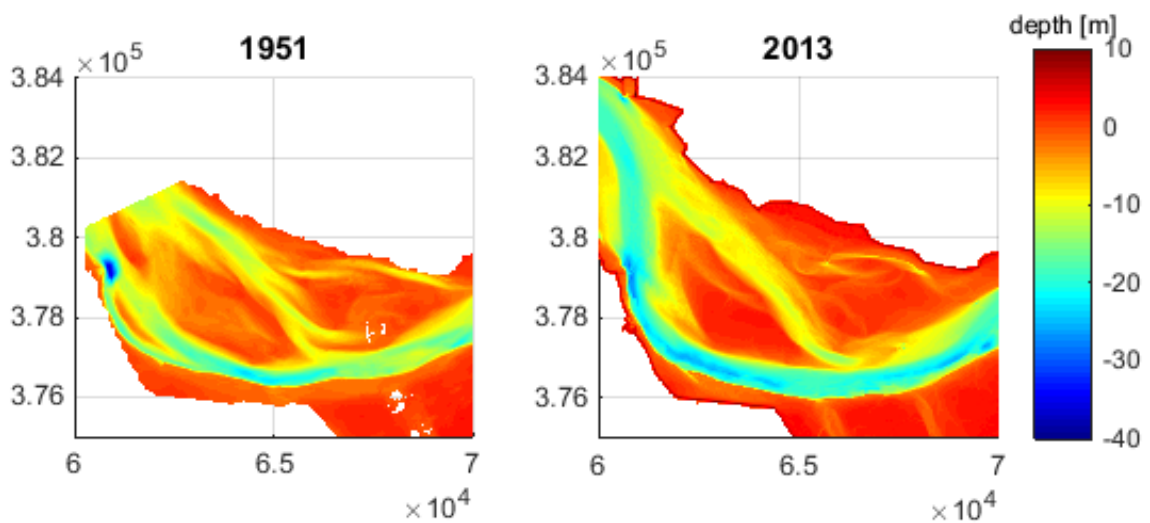


Figure 2.5: Elevation map of the tidal flat of Walsoorden for 1951 (left) and 2013 (right)

In the left panel of Figure 2.5 a large scour hole is visible at the western bank. This is due to the remains of an old sea dike, 'Het Oude Hoofd', that caused turbulent flow around it (Wilderom, 1973). In 1966 this dike was shortened and the ebb channel became straighter (Technische Scheldecommissie, 1984). To prevent the southern bank of the Zuidergat from bending out, the foreshores are defended.

Along the southern edge of the tidal flat of Walsoorden sand is dredged, which is partly extracted from the system and partly used for recirculation along the estuary. Annually around  $0.5 \text{ M m}^3$  is dredged in the Bocht van Walsoorden, south of the tidal flat. In the context of the 'Flexibel Storten' project the north-western tip of the tidal flat is reshaped and reinforced, using the dredged sediment (Port of Antwerp Expert Team, 2003).

## 2.2.2 Hydrodynamics

### Water level

The average high and low water level at Baalhoek, determined based on decades of data, are  $+2.8 \text{ m NAP}$  and  $-2.4 \text{ m NAP}$  respectively (Rijkswaterstaat, 2015). The average rising time is 6h01m and the falling time is 6h24m. Part of the tidal flat is above the high water level, this part is only flooded during exceptionally high water levels. At this part permanent vegetation is present. From the water level signal the tidal constituents are determined. From the measurements it is determined that the channel is ebb dominant, since the relative phase difference is approximately  $-5^\circ$  (Van der Werf and Briere, 2013).

### Velocity and discharged volume

Typical values for the maximum velocity in the channel are between 1.5 and 2 m/s. Rijkswaterstaat (2015) measures once every 3 to 5 years the velocity and discharge along several transects. During these measurements a boat with ADCP equipment is sailing along the transect. The most interesting transect around the tidal flat of Walsoorden is transect 5A, perpendicular to the Zuidergat channel. From these measurements it is found that the volume passing during ebb is larger than during flood. In Chapter 3 the hydrodynamics will be analysed in more detail.

## 2.3 Flow slides

A flow slide (*in Dutch: plaatval, zettingsvloeiing, dijk- of oevertal*) is a geotechnical phenomenon that occurs when a sandy submerged slope becomes unstable. Because of the steepness the sand starts to slide off and the slope becomes gentler. Currently two slope failure mechanisms are described that can cause a flow slide: static liquefaction (*verwekingsvloeiing*) and up-slope migrating breaches (*bresvloeiing*). A combination of these two can also occur. Both mechanisms result in a gentle slope, but the associated time scales are different (Mastbergen et al., 2015). In the next sections the different mechanisms will be elaborated in more detail.

For both mechanisms a relatively steep slope is a pre-requisite. This can be caused by erosion of the lower part of the slope whether or not combined with sedimentation of the upper part (Wilderom, 1979). Under the water surface high flow velocities cause erosion of the tidal flats and foreshores of dikes. During flood there is sedimentation on top of the tidal flats, which causes steeper slopes (Wilderom, 1972). This is observed on the tidal flat of Walsoorden. After a flow slide occurs the original profile is generally restored within some months or years. This gives a more or less periodic process, it repeats itself after the profile is recovered. Therefore a certain location has a certain return period for a flow slide (Van den Ham et al., 2013).

### 2.3.1 Static liquefaction

When static liquefaction occurs the slope will become more or less fluid and will slide down as a mass flow. This happens when loosely packed sand liquefies under water; it becomes quicksand. The shear stress between the particles decreases dramatically and they start to slide down the slope (Rijkswaterstaat, 2012). The time for this process is in the order of minutes. The profile of the flow slide due to liquefaction is shown in Figure 2.6.

The risk indicators for liquefaction are (Kleinhans, 2013):

- A sufficient steep and long slope, this causes sufficient high grain- and deviator stress;
- The minimal layer thickness of the loosely packed sand should be between 2 and 5 meter;
- The possibility for the sand to flow away, for example in an adjacent deep channel;
- There has to be a trigger to start the liquefaction, this can be for example an earthquake or an instantaneous water level decrease. Another possibility is a destabilization due to seepage water out of the bank

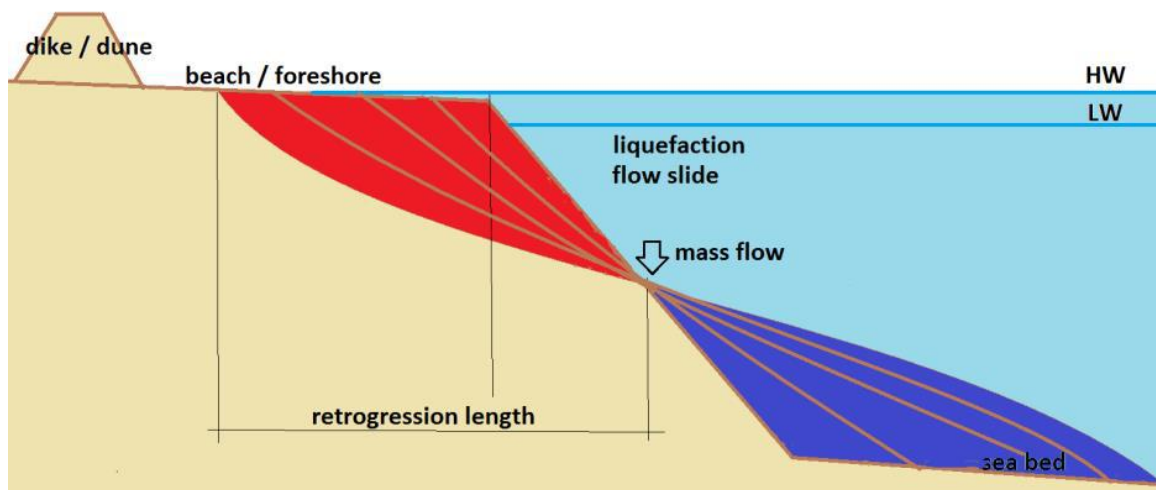


Figure 2.6: Static liquefaction (Mastbergen, 2014)

Actual liquefaction of the slope is only observed in lab tests. Several methods are possible to determine the sensitivity for a flow slide. Mostly this is done using cone penetration tests (CPT) or on basis of knowledge and experience (de Groot et al., 2007).

### 2.3.2 Up-slope migrating breach

In case of an up-slope migrating or retrogressive breach a sustained turbidity current is generated downslope of the location of initiation (Mastbergen and Van den Berg, 2003). This erosion process keeps continuing until a new equilibrium profile is formed. Local sliding initiates the breaching process after which the vertical breach slowly retrogrades and a turbidity current is flowing down the slope (de Groot et al., 2009). The turbidity current consists of a mixture of sand and water. This continues and the sand is 'falling' down the slope and is deposited at the toe of the breach. At the toe it needs to be possible for the sand to flow out and redistribute itself as a turbulent density current. When this is possible the erosive power of the turbidity current becomes stronger, causing a larger discharge (Delft Cluster, 2009). When this is impossible the breach will die out. The breaching is initiated under water, but after a while it may start to be visual above water, resulting in an amphitheatre shaped gap. Some of the risk indicators for an up-slope migrating breach flow slide are:

- The material should be sand or silt; the finer the material, the more sensitive it is for erosion and suspension;
- A continuous slope without any berms;
- There has to be enough space for the sand to flow out, once the sand cannot flow any further it will develop a gentle slope at the toe;
- The slope should be of sufficient height and steepness;
- There has to be an initial disturbance or trigger to start the breaching.

The slope failure mode by a breach flow slide only needs a minor trigger to start collapsing (Kleinhans, 2013). The development of a flow slide due to an up-slope migrating breach takes at least several hours. In Figure 2.7 the mechanism is shown. The breach remains quite steep while the sand is deposited under a gentle slope. This failure mechanism is used for sand mining, where dredgers generate controlled breaching by removing sand at the toe of the breach.

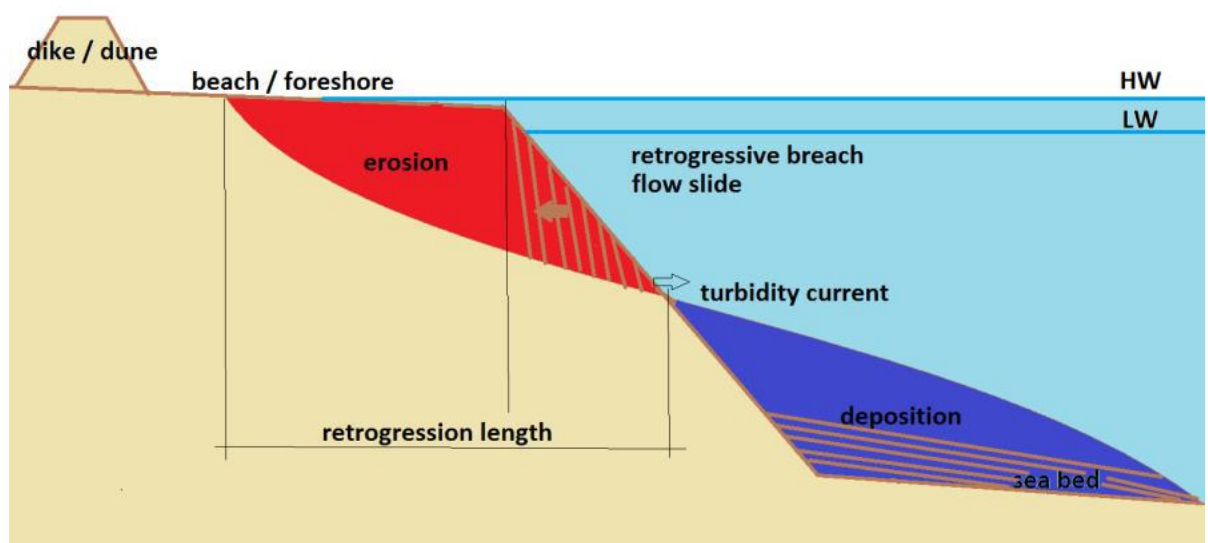


Figure 2.7: Up-slope migrating breaches (Mastbergen, 2014)

It is assumed that often a combination of both failure mechanisms occurs. However, during the IJkdijkexperiment it was proved that retrogressing breaches developed, being the start of a flow slide (Van den Ham et al., 2015; Mastbergen et al., 2015). The amount of transported sand due to flow slides can be up to 1,000,000 m<sup>3</sup> each time, like the 22<sup>nd</sup> July 2014 flow slide, but also in the Eastern Scheldt large flow slides were observed in the past (Wilderom, 1979).

### 2.3.3 Dike safety and flood defence

A flow slide can cause damage and flooding risk when it occurs next to a dike or foreshore (Van den Ham et al., 2015), or navigational problems when it happens near a navigational channel (Aantjes, 2014). Therefore, the dikes and foreshores in the Netherlands are regularly assessed (Rijkswaterstaat, 2012). The profiles after a flow slide are generally well known. However, the failure mechanism is still not fully understood. The retrogression length that can cause damage cannot be predicted very well, although the geometry is well known from a large number of historical observations (Wilderom, 1979). The IJkdijkexperiment at Walsoorden was initiated to define the failure mechanism of a flow slide and to test monitoring methods. In the experiment the development of a breach and turbidity current was observed several times after initial dredging in bathymetry measurements, but the flow slides stopped after some hours without becoming as large as the 22<sup>nd</sup> July flow slide (Van den Ham et al., 2015; Mastbergen et al., 2015).

### 2.3.4 Sensitive areas

Flow slides occur in other areas as well, they occur mostly in dynamic areas (Van den Ham et al., 2013). Along the Western Scheldt a lot of flow slides are known at the banks and the tidal flats. This makes the problem of deposition of sediment in the channel, loss of sand from the tidal flats and foreshores and damage to dikes due to flow slides is very relevant (Mol, 1995). Figure 2.8 shows the loss of tidal area due to flow slides in the tidal flat of Walsoorden in the last few years. In the Netherlands the phenomenon is also known in the Eastern Scheldt (Ligtenberg-Mak et al., 1990) and the Wadden Sea (Stichting FloodControl IJkdijk, 2014).

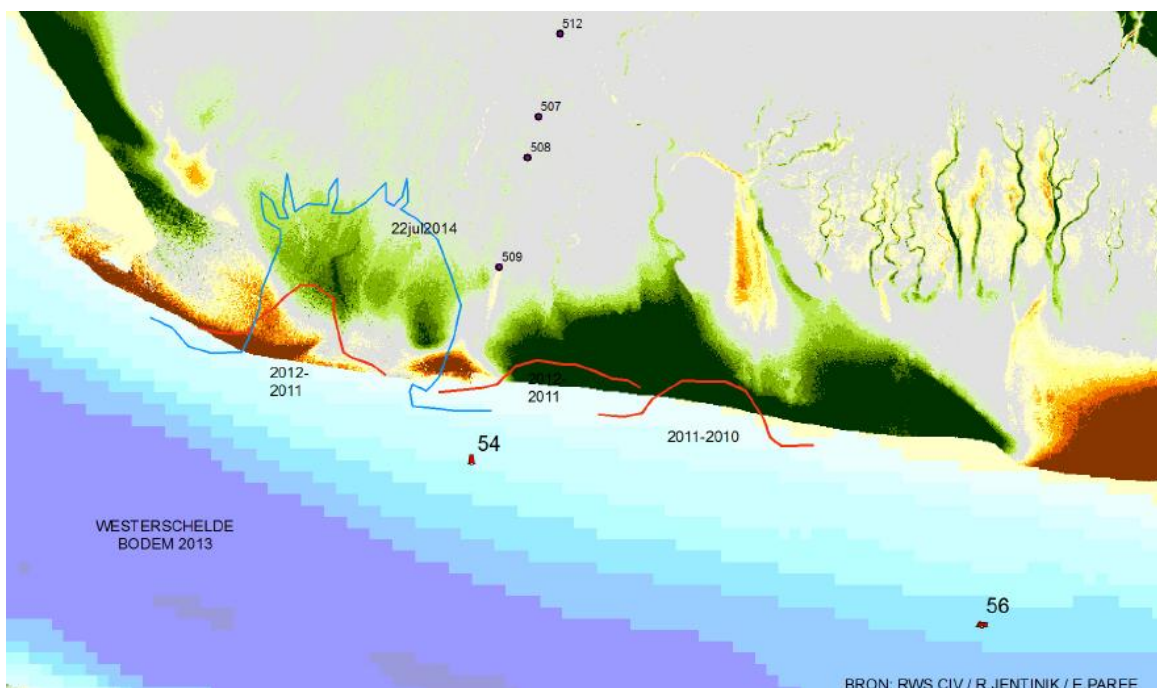


Figure 2.8: Flow slides on the tidal flat of Walsoorden in the last years (Rijkswaterstaat, 2014)

Also in other parts of the world flow slides occur. Numerous examples are available for the Mississippi river banks (US Army Corps of Engineers, 1988), British Columbia and Australia (Beinssen et al., 2014). In the Mississippi scour occurs near the river banks and this causes instability of the banks after some time. An example in Australia is the breaching along Inskip Beach. Probably there are more places where flow slides can be observed, but often it is addressed to shear slide or land slide failures. Most of the times it happens in sandy and morphological dynamic areas, with loosely packed sand and silt.

## 2.4 Conclusion

The behaviour of the complete Scheldt estuary is partially understood with its multichannel-system and ebb-tidal delta on the large scale. In time, human interventions made the estuary to what it is nowadays, a less dynamic estuary with fixed channels. However, as much is known of the Western Scheldt on large scale, less is known of a smaller area on meso-scale. The behaviour of the channels and shoal of the tidal flat of Walsoorden is observed over decades. However, a clear explanation is not found on why they behave the way they do. In the past several human interventions are obtained to keep the channel around the tidal flat of Walsoorden navigable. For example the dredging of the channel, fixing of the outer bend and removing the remains of an old dike. The edge of the tidal flat is sensitive to flow slides. The slope gets steeper due to accretion near the surface and erosion near the bottom. With an initial trigger a flow slide can possibly occur and part of the tidal flat flows into the channel.

The behaviour of the system after such a large event as the July 2014 flow slide has only been monitored once, in 1977 by Ebbens (1980). This flow slide took place at the tidal flat of Ossensisse. With bathymetry measurements the development after the flow slide was monitored. However, in this study only the filling of the gap was examined and there was no focus on the erosion of the channel in relation to the navigation in the channel.

### 3 Analysis of velocity, sediment transport and morphological data

To determine the relevant processes occurring in the Bocht van Walsoorden and the gap from the 22<sup>nd</sup> of July 2014 flow slide the available data is analysed. The velocity and discharge measurements are available to determine the ebb or flood dominance in the area. Next to this the sediment composition and sediment transport is analysed. The monthly bathymetry measurements are used to determine the redistribution of the sediment after the flow slide. With this gathered information the recovery time after the flow slide is estimated and the dominant direction (ebb or flood) is determined in the channel.

#### 3.1 Velocity

The velocity at Zuidergat and Schaar van Waarde is measured by Rijkswaterstaat (2015) on the 25<sup>th</sup> of April 2013. The locations of these transects is given in Figure 2.4. Along the transects the magnitude and angle of the depth-averaged velocity is measured. Using the angle of the transect and the angle of the flow velocity, the velocity perpendicular on the transect is determined. This velocity is given in Figure 3.1 with the blue dots, positive values are flood directed. Each dot represents the average velocity per minute along the transect. The spreading of these dots is caused by the boat that goes back and forth along the transect, while measuring the depth averaged velocity. The red line is the running 20 minute average of the blue dots.

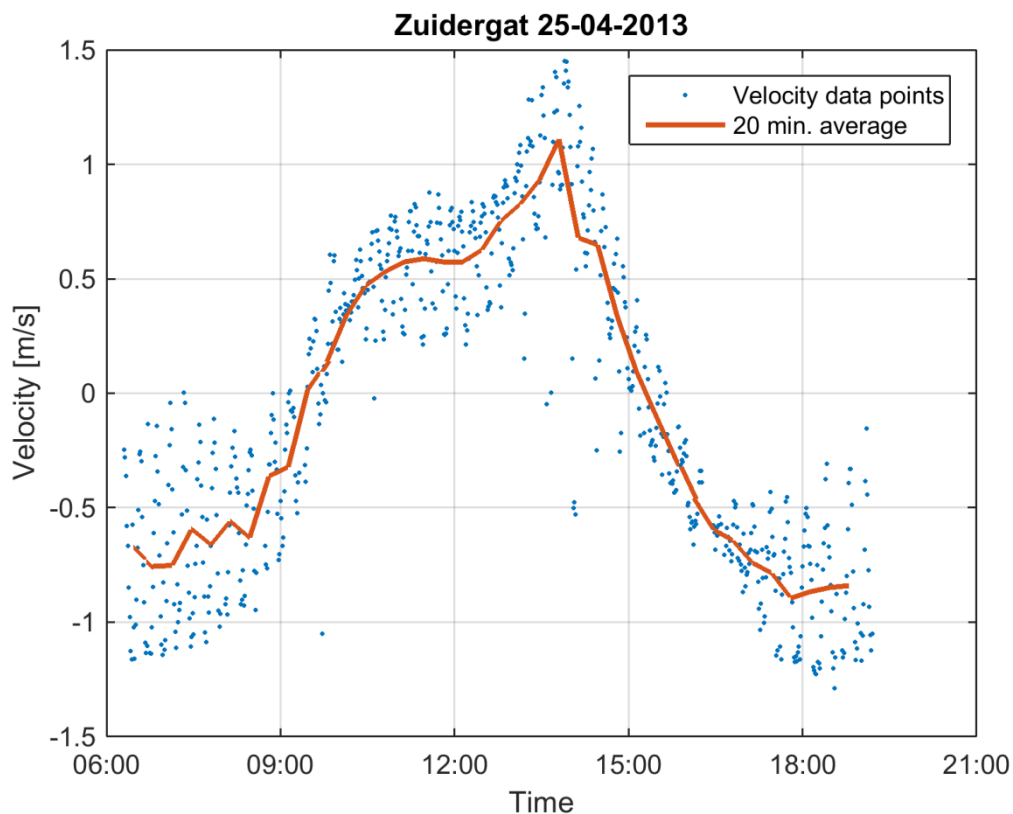


Figure 3.1: Measured velocity profile of the Zuidergat transect

From Figure 3.1 it is found that the maximum velocity in the Zuidergat during flood (1.1 m/s) is larger than during ebb (0.9 m/s). The third-order velocity moment  $\langle u^3 \rangle$  is a measure for the sand transport capacity.  $\langle u^3 \rangle$  equals  $-24,000 \text{ m}^3/\text{s}^3$ , indicating ebb dominance in this channel. Since the same amount of water is flowing through Zuidergat as through the Bocht van Walsoorden it seems logical that also the Bocht van Walsoorden is ebb dominant in terms of water volume.

### 3.1.1 Discharge

The discharge over the Zuidergat transect is given in Figure 3.2. The shape of the profile is similar to the shape of velocity profile. The water volume passing the transect during ebb (258  $\text{M m}^3$ ) is larger than the water volume passing during flood (239  $\text{M m}^3$ ). This indicated ebb dominance in the channel. Figure 3.3 gives the volume passing the transect per tide over time. The ebb volume is larger than the flood volume, but the volumes are getting closer to each other.

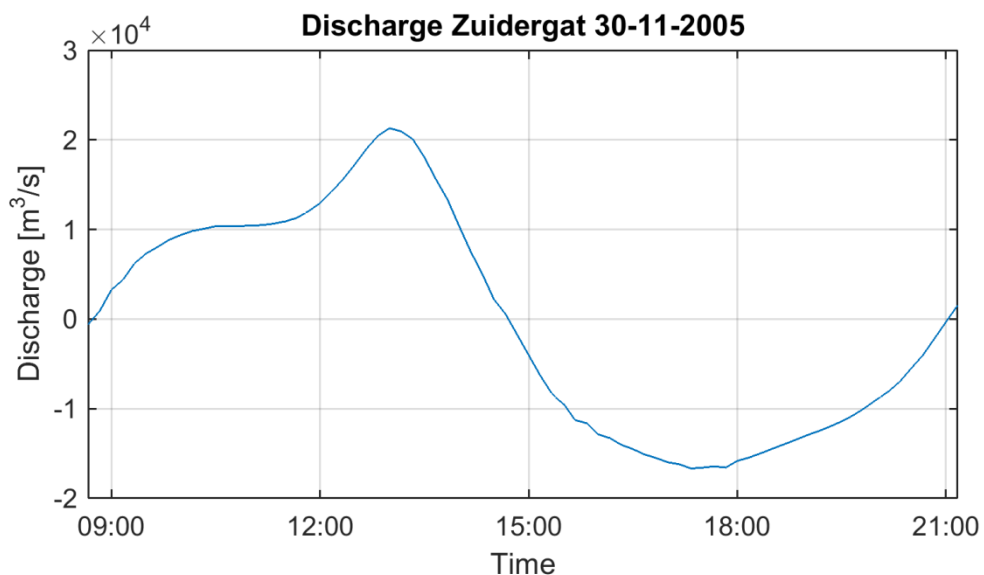


Figure 3.2: Discharge through the Zuidergat transect in  $\text{m}^3/\text{s}$

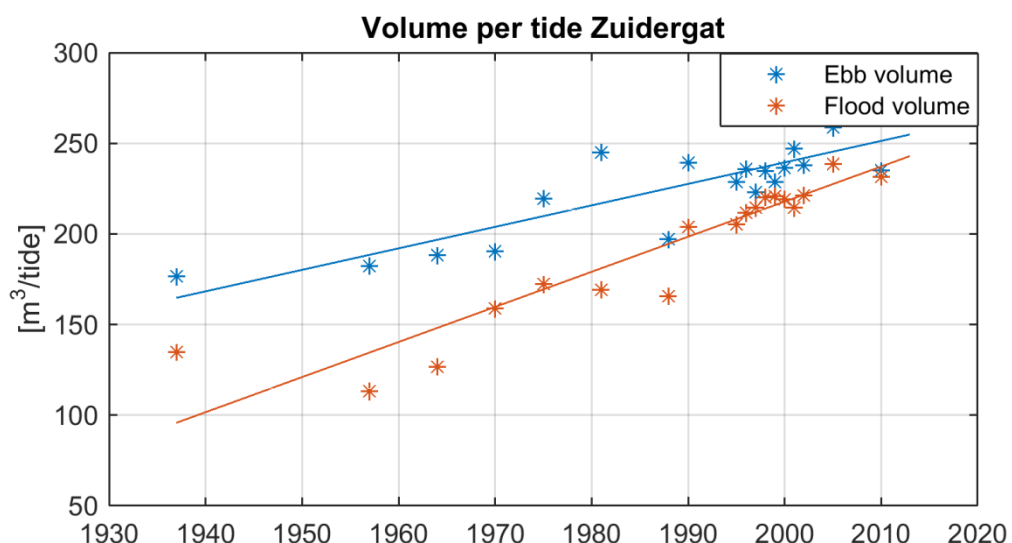


Figure 3.3: Discharged volume through the Zuidergat over time

### 3.2 Sediment composition

The sediment characteristics for a part of the Western Scheldt are measured by McLaren (1994). Near the tidal flat of Walsoorden some additional measurements were taken for the IJkdijkexperiment in 2014 (Van den Ham et al., 2015; Mastbergen, 2015).

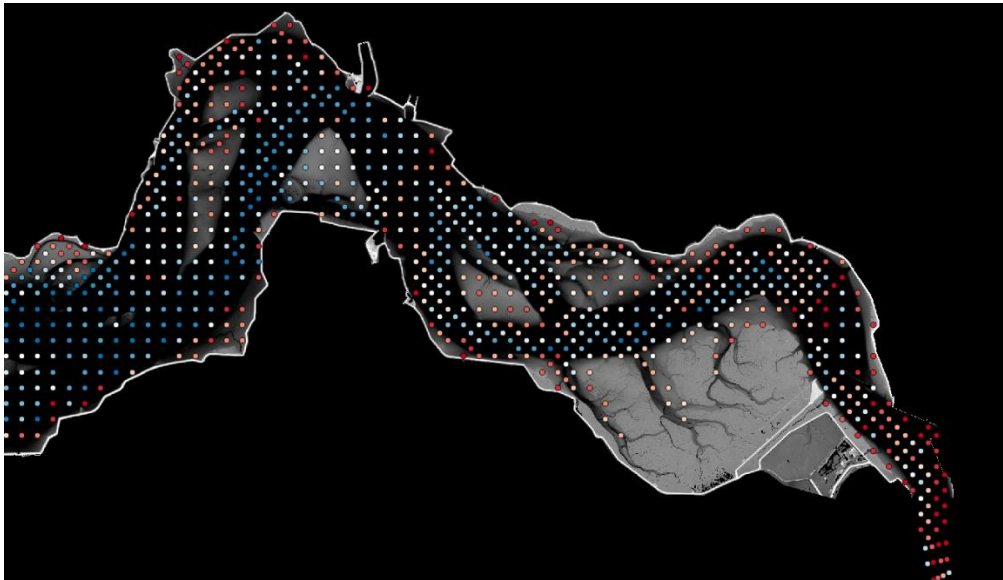


Figure 3.4: Sediment diameter from the McLaren dataset, red is a small diameter ( $<100 \mu\text{m}$ ) and blue is a large diameter ( $>170 \mu\text{m}$ ) (McLaren, 1994)

#### 3.2.1 McLaren

In 1994 the sediment diameter in a large part of the Western Scheldt is measured by McLaren. In Figure 3.4 the median sediment diameter is given ( $D_{50}$ ). In the channels the diameter is larger than on the tidal flats, indicated by a blue colour. This is due to the larger flow velocities in the channel, which makes it harder for sediment with a smaller diameter to settle. On the tidal flats the conditions are milder, making it possible for sediment with a smaller diameter (sand and mud) to settle.

#### 3.2.2 IJkdijk

Some of the measurements from the IJkdijk experiment regarding the sediment properties at the bed are given in Table 3.1. With a Van Veen bottom grab sampler samples are taken, the K1 till K4 measurements. These are taken during the experiment in the artificial flow slide (September 2014), on the east side of the natural flow slide (July 2014). The VB measurements are taken between the 12<sup>th</sup> and 15<sup>th</sup> October 2014 using vibrocores. Measurements VB8 till VB11 are taken in the gap of the flow slide of July 2014. These measurements show a stratified sediment composition, with layers of sand and mud. VB15 is taken in the IJkdijk experiment area, showing the sedimentation of the artificial flow slide (Wiertsema & Partners, 2014). The locations of the measurements are given in Figure 3.5.

On the fringes of the tidal flat (K-measurements, VB11 and VB15) the percentage of mud is very low. This suggests the absence of mud, sand is the main sediment source. However, in the gap of the flow slide the percentage of mud is high. Due to milder conditions it is possible for the finer sediment to settle. This suggests that relatively fine sediment settles in the sheltered area of the gap in the tidal flat.

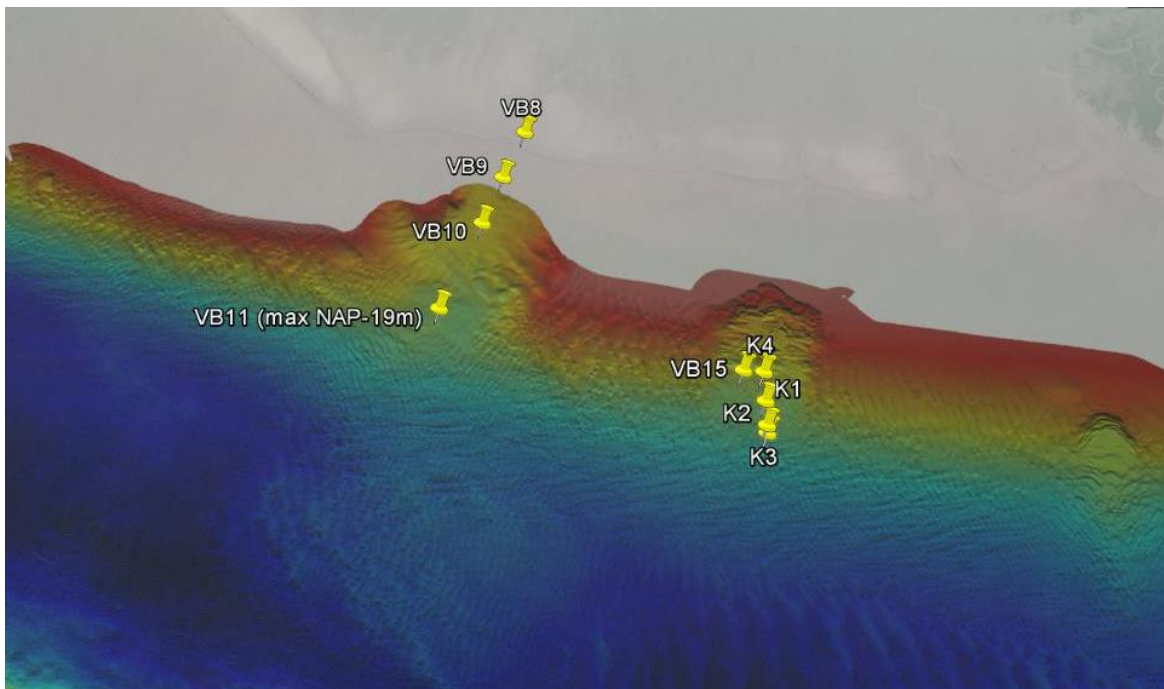


Figure 3.5: Locations of the sediment measurements

Table 3.1: Measurement locations and corresponding sediment diameter

Name	X-Cor	Y-Cor	Depth [m]	$D_{50}$ [ $\mu\text{m}$ ]	Mud [%]	Date
K1	63442	376931	12	150	0.1	23-09-2014
K2	63442	376899	14.3	180	0.1	24-09-2014
K3	63442	376889	15	185	0.1	28-09-2014
K4	63442	376970	11.5	145	0.2	30-09-2014
VB8	63162	377317	7.7	130	16.7	12-10-2014
VB9	63140	377261	8.0	110	43.8	12-10-2014
VB10	63112	377186	9.8	120	16.5	12-10-2014
VB11	63064	377054	12.7	150	1.2	12-10-2014
VB15	63418	376971	11.1	140	1.4	12-10-2014

### 3.3 Sediment transport measurement

The velocity and sediment transport along the Zuidergat is measured on the 30<sup>th</sup> of November 2005 (Rijkswaterstaat, 2006). The sand and mud concentration is measured at two points, at Zuidergat and Schaar van Waarde. The static monitoring point for the Zuidergat lies just next to the navigation channel, on the edge of the tidal flat. The sand concentration is measured at ten locations along the vertical using an AZTM, an acoustical sand transport water instrument. This instrument measures continuously the concentration based on a decrease of energy of the beam. The inaccuracy of this device is approximately 10%, which is sufficiently accurate. The silt concentration is measured with a MEX, an optical sensor, which is based on transmission. This device works sufficient for silt concentration measurements (Paridaens et al., 2001). The transport is calculated based on the concentration and is given in Figure 3.6. In this figure negative is ebb directed and positive is flood directed.

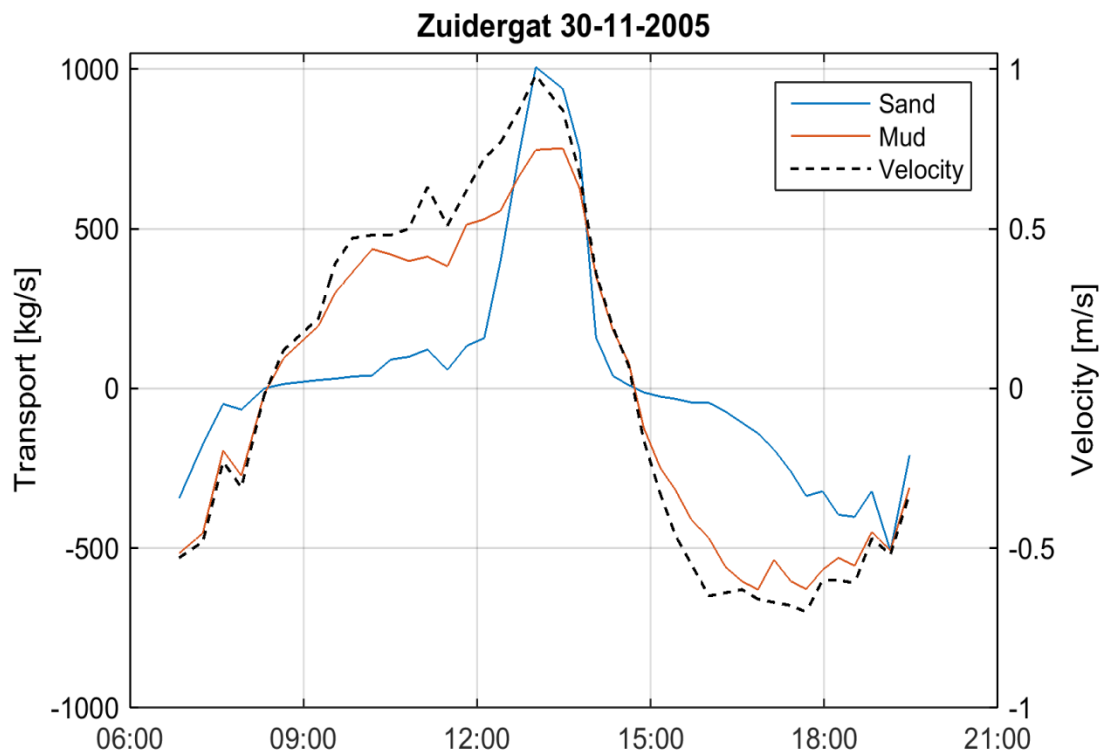


Figure 3.6: Sediment (sand and mud) transport and velocity on 30-11-2005 for Zuidergat (positive is flood directed)

The sand particles are transported after a critical velocity of 0.6 m/s is reached. The critical velocity for the Shields number with a particle size of 200  $\mu\text{m}$  is  $\sim 0.25$  m/s, which is rather smaller than the value found in this figure. When the total transport is calculated per tide the value is positive, indicating flood directed transport. The mud particles are mobile throughout the entire tidal cycle. Their magnitude is approximately the same for ebb and flood transport. If the total transport is calculated for mud the value is negative indicating ebb directed transport. A similar measurement is done in 2003, where the same results were found (Waterbouwkundig Laboratorium, 2007). For mud in the Schaar van Waarde a similar pattern is found as the mud pattern in the Zuidergat, both have residual transport is in ebb direction. Sand is almost only transported during flood, giving residual sand transport in flood direction.

### 3.4 Bathymetry

The bathymetry is obtained from multibeam echosounders and gives a complete overview of the area. The data covers the area from the northern tip of the tidal flat to the east of the flow slide. The accuracy is 1 meter in horizontal direction and 0.01 m in vertical direction. In Appendix A an overview is given of the dates and companies that measured the data. The data is supplied by Rijkswaterstaat, the Flemish government and Stichting FloodControl IJkdijk. The bathymetry of the different dates is given in Appendix A.1, the erosion with respect to the beginning of the 12<sup>th</sup> of June (before the flow slide) in Appendix A.2.1 and to the 21<sup>st</sup> of August (afterwards) in Appendix A.2.2. In the figures the RD coordinate system is used. The left panel of Figure 3.7 gives the bathymetry of the 21<sup>st</sup> of August 2014, which was the first complete measurement after the flow slide. The right panel gives the bathymetry for the 13<sup>th</sup> of August 2015, after somewhat more than one full year. The sediment accretion from the flow slide is eroded in the right panel. The gap in the tidal flat is in one year almost filled in to the original state.

The observed data (Appendix A.1) shows that the bathymetry from the 12<sup>th</sup> of June and the 8<sup>th</sup> and 9<sup>th</sup> of July are very similar. The situation of the 9<sup>th</sup> of July is chosen to be the reference situation. When the flow slide occurred the system starts to behave towards the original equilibrium. The sediment erodes from the channel and the gap fills in.

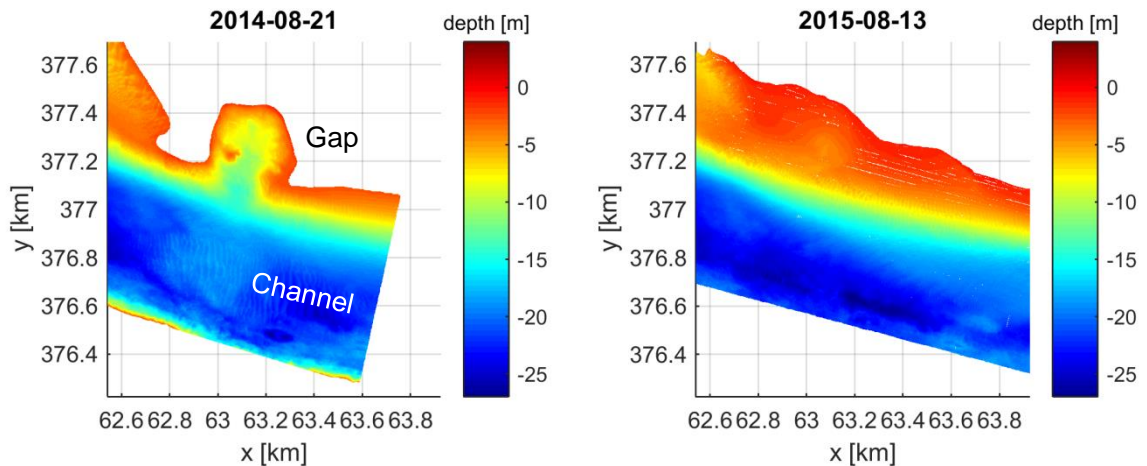


Figure 3.7: Measured bathymetry of August 2014 and August 2015 (Rijkswaterstaat, 2015)

### 3.4.1 Cross sections

The behaviour is examined using four cross sections and one longitudinal section. In Figure 3.8 the locations of cross sections A-A' till D-D' and the longitudinal section E-E' are given. The cross sections are taken in upstream direction. In Figure 3.9, and in more detail in Appendix A.3, the different cross sections are given. In the figures the MLW is the mean low water, which is -2.06 m NAP. The navigational depth is the required depth of -17.5 m NAP. The flow slide gives a reduction of the depth. In the figures the profile before the flow slide (the 12<sup>th</sup> of June 2014) is thickened. In all cross sections the profile returns more or less to this profile.

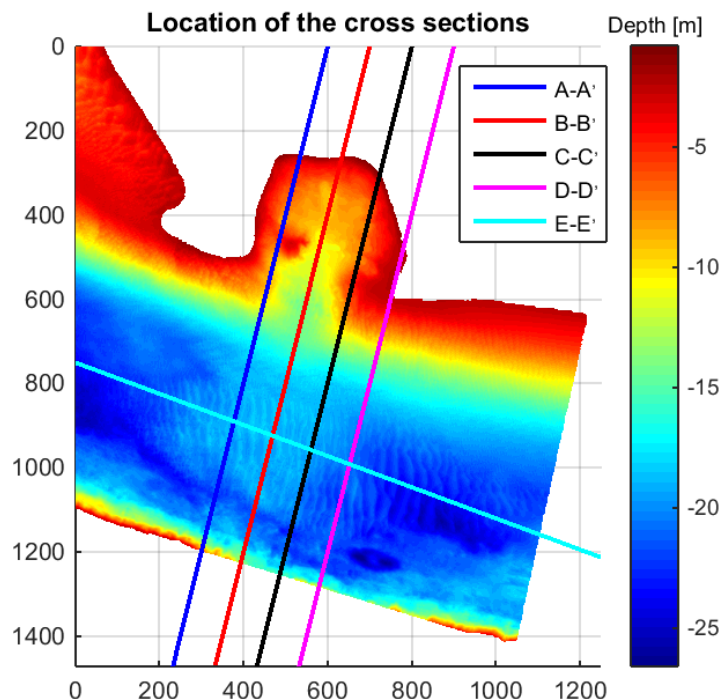


Figure 3.8: Location of the cross sections (background: bathymetry of August 2014)

Cross section A-A' shows fast recovery after the flow slide to the original situation. In this cross section the original situation (of the June 2014) has already recovered in November 2014. The more eastern-located cross sections need more time to restore to the original situation. In cross section B-B' the sediment in the channel erodes gradually, but the rate is smaller than in cross section A-A'. Here the system is almost recovered in January 2015. Going more to the east the recovery time increases. In cross section C-C' the amount of sediment is hardly changed in the first months. From October 2014 onwards gradual erosion can be observed. For cross section D-D' this effect is even larger, in the first months the sediment in the cross section is increasing and it stays at a constant level for a long time.

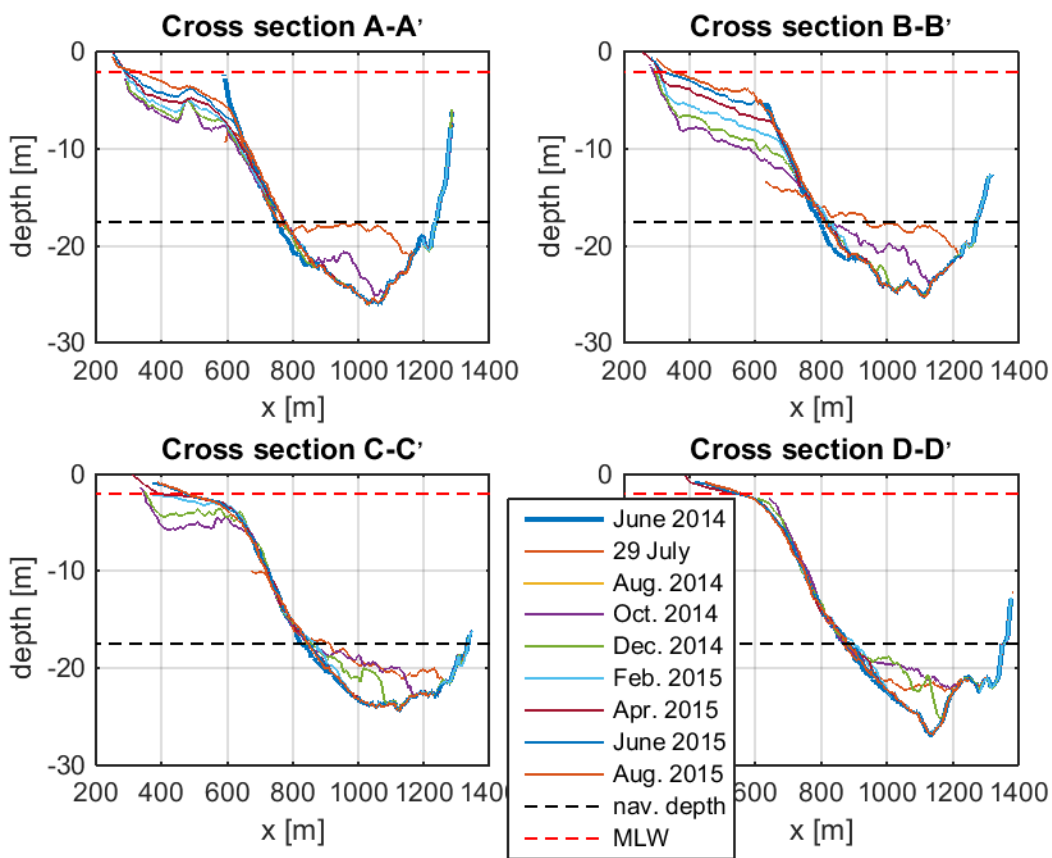


Figure 3.9: Morphological development along cross sections A-A', B-B', C-C' and D-D'

### 3.4.2 Longitudinal section

The bed level in the longitudinal cross section (Figure 3.10) displaces in flood (eastern) direction. The peak of the sediment accumulation lowers over time, together with the amount of sediment present in the channel. The sediment accretion is traveling towards the east, the slope of the accumulation remains approximately the same. After erosion, the original profile is restored, including the dunes that were present before July 2014. The exact recovery of the profile (from the western side on) indicates that the system was indeed in equilibrium in July (before the flow slide). However, it could also indicate a hard, immobile layer on the bottom, which could be armoured or consisting of coarser sand or cohesive sediment. More longitudinal cross sections along the channel are given in Appendix A.4. The section on the north of the channel, next to the edges of the tidal flat, shows slight ebb dominance in transport. This indicates some kind of circulation of bed load transport in the channel.

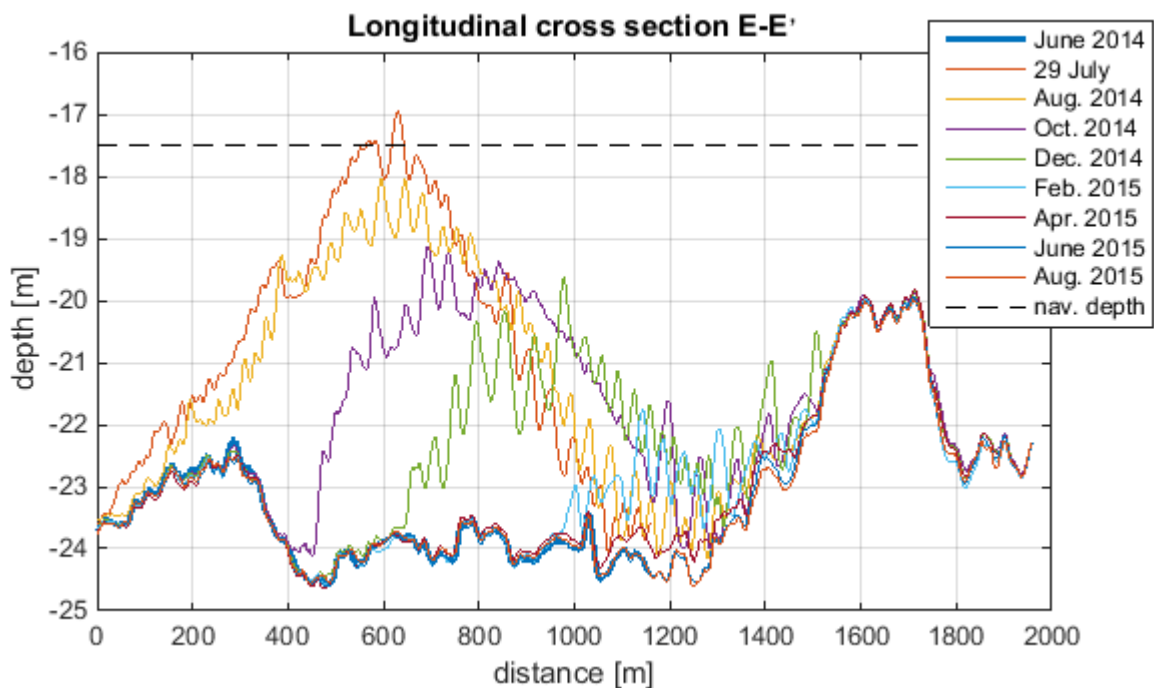


Figure 3.10: Morphological development along longitudinal section E-E'

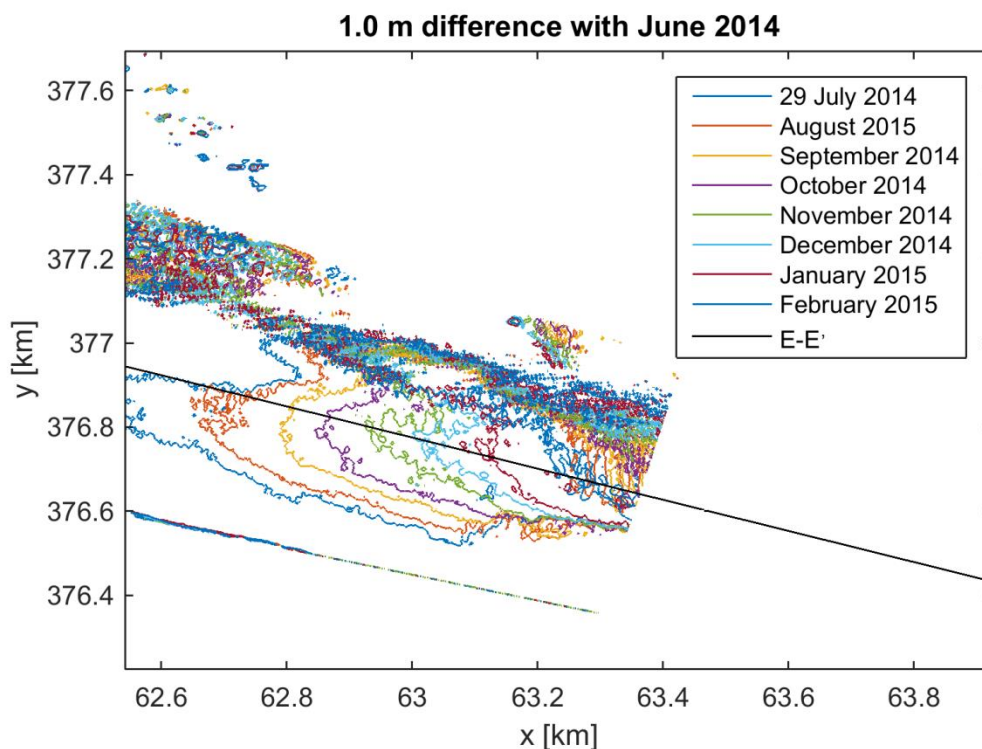


Figure 3.11: Contour lines indicating a difference of 1.0 m between June 2014 and the different months

### 3.4.3 Contour lines

Comparing the bathymetry data of June 2014 with the other months, the bed level changes can be determined. In order to get an idea on the sediment behaviour these changes are used to determine contour lines, given in Figure 3.11. The lines show the differences with the

June 2014 profile of 1.0 meter. It is observed that the area with a change of over 1.0 m moves towards the east. This was also already determined in the cross and longitudinal sections. The area over 1.0 m decreases in time. This indicates a flattening of the profile and a decrease of the sediment volume, suggesting part of the sediment gets into suspension and is transported out of the measurement domain. The lines indicate a propagation speed of this sediment accretion of approximately 100 m per month.

#### 3.4.4 Dune migration

In Figure 3.10 dunes on top of the sediment accumulation are visible. These dunes move back and forth with the tide (Waterbouwkundig Laboratorium, 2007). This causes asymmetry of the dunes over a tidal period. Since they do not travel the same distance during ebb and flood, there is a residual transport direction. The residual transport direction can be estimated from the observations taken one day after the other. The time of the measurement is not registered, so it cannot be determined if the measurement is taken during ebb or flood. Therefore the dune migration should be interpreted with some caution. However, for several months the same displacement is observed.

In the months August, September and October data is available with an interval of only one day. The data of October is visualised in Figure 3.12. For the different months a migration speed of the dunes is found of 0.9 m/day. As already suggested before, this velocity should be considered with some caution since the time between the measurements is not known. The shape of the dunes does not change significantly, making it possible to follow the dunes. The migration of individual dunes over a month cannot be estimated as the shape changes, making it impossible to track individual dunes.

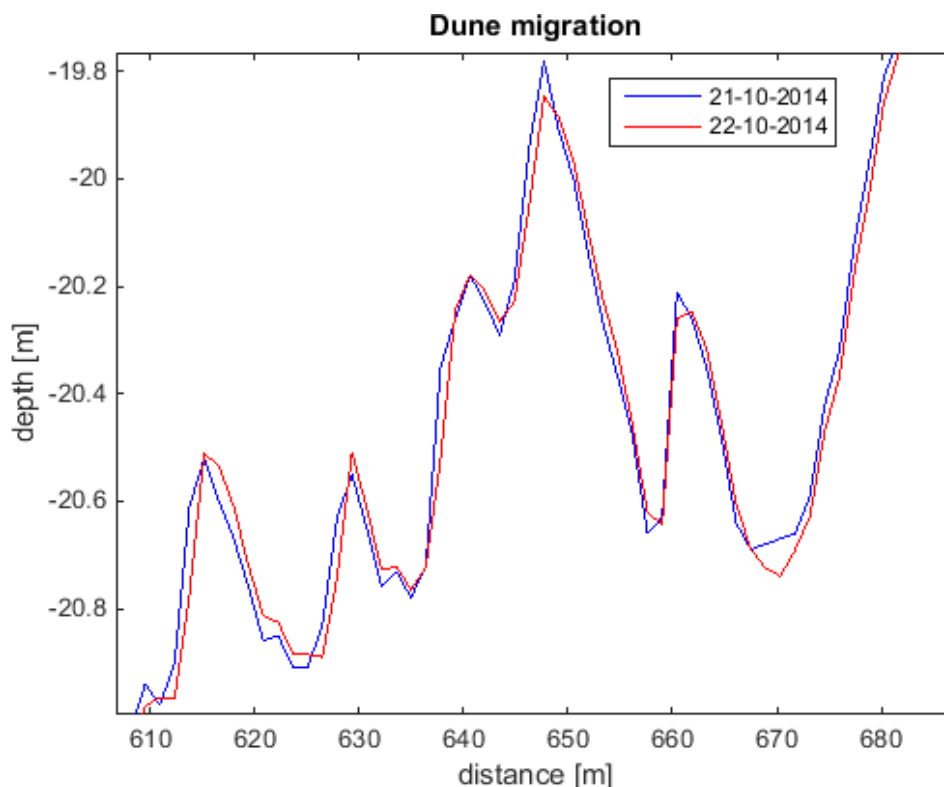


Figure 3.12: Dune migration on longitudinal transect E-E'

The geometry of the dunes differs along the cross section. On the western side the dunes are smaller than on the eastern side. Figure 3.12 shows the dunes on the western side of the cross section. The height is around 0.6 m with a length of 10 to 20 m, similar results are found in Vandenbruwaene et al. (2012). In this study only three measurements in the winter of 2006-2007 were available. During these observations ebb-dominated transport associated with bedform migration was found near the Zuidergat. The sediment transport found in this study is  $0.15 \text{ m}^3/\text{m/day}$  ( $0.07 \text{ m}^3/\text{m}$  per tidal cycle) in ebb direction. In the eastern part of the channel the height is up to 1.5 m and the length is approximately 40 m (Arcadis, 2014).

#### 3.4.5 Bed load transport

The difference in height and length between the ripples in the western part and in the eastern part could be explained by a different velocity along the channel. For a smaller velocity the height and length of the dunes are larger. The velocity along the channel is not measured, so this assumption cannot be confirmed. A rough estimation of the net sediment transport associated with dune migration can be made using equation 3.1 (Hoekstra et al., 2004):

$$\bar{q}_b = \alpha c H \quad (3.1)$$

In this formula  $\alpha$  is the bed load transport coefficient, which is used as a calibration factor. In literature this value is often between 0.5 and 0.6. The propagation speed of the dune,  $c$ , is given in m/day and  $H$  is the height of the dune. On the western side the height is 0.6 m and the propagation speed is 0.9 m/day. With these values the bed load transport lies between 0.27 and  $0.32 \text{ m}^3/\text{day}$  per m. On the eastern side the height is 1.5 m, giving a bed load transport between 0.68 and  $0.81 \text{ m}^3/\text{day}$  per m. These values are similar to the ones found by Vandenbruwaene (2012) near the tidal flat of Walsoorden.

### 3.5 Morphology

#### 3.5.1 Erosion and sedimentation pattern

The erosion/sedimentation pattern is determined using the bathymetrical change over time. Between July 2014 and August 2015 the original sediment accumulation in the channel is eroded. This is observed in Figure 3.13 in the bottom-right panel. The profile is for a large part recovered, the sediment is transported towards the Overloop van Valkenisse, upstream of the flow slide. In November 2014 the sill is dredged, but no significant increase in volume is found (IMDC, 2014c). In the top-right panel the change from July 2014 till January 2015 is shown. The sediment is already eroded for a large part, the difference between January 2015 and August 2015 is smaller than the difference between July 2014 and January 2015.

The erosion in the channel starts in the west and is continuing towards the east. The eroded area is increasing in time until all the sediment is transported (left-hand side panels in Figure 3.13 and Appendix A.2). In the gap most sedimentation occurs at the east side. This would imply that it is filled with sediment rich water during flood. Due to the water level difference between the gap and the channel water flows in, as the water level during flood is lower in the gap than in the channel. Due to the calmer conditions in the gap the transport capacity is lower than in the channel and the sediment will settle.

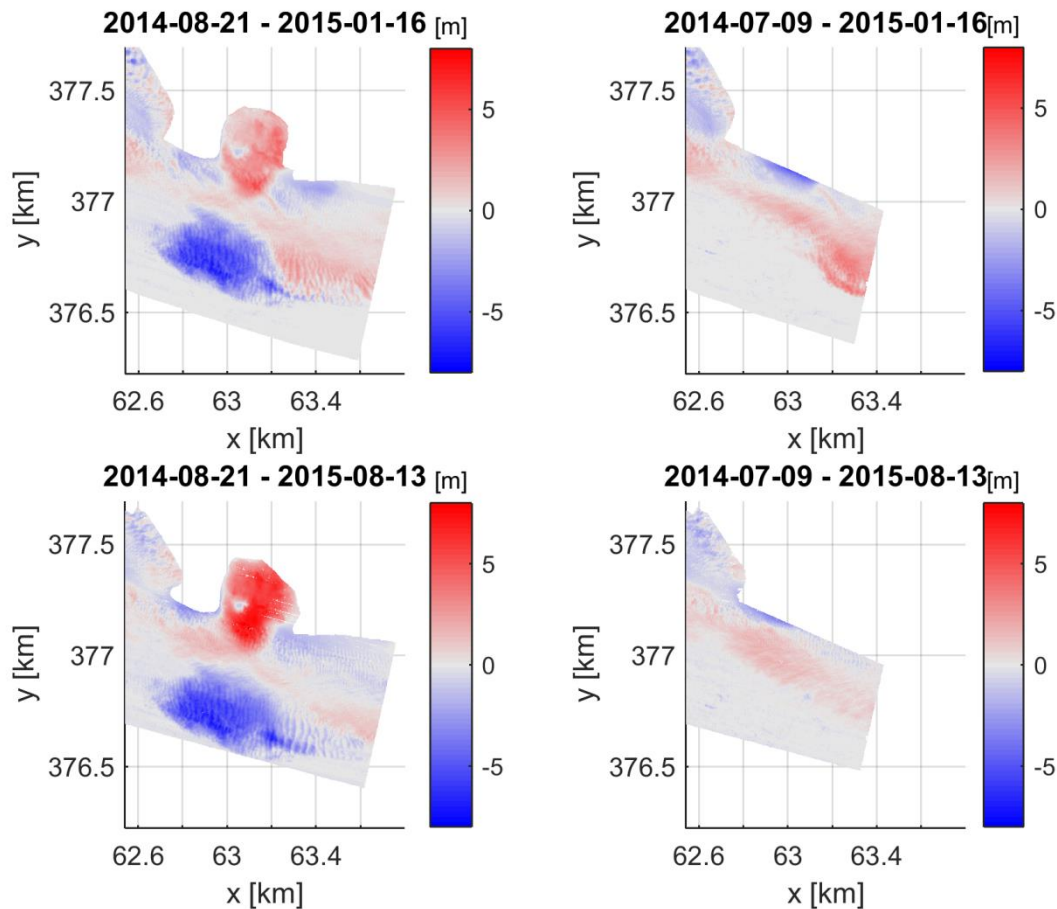


Figure 3.13: Erosion pattern, with on the left the erosion after the flow slide and on the right the difference with the original profile in January 2015 and August 2015

### 3.5.2 Volume

The erosion of the deposited sediment in the channel and the sedimentation in the gap are described using the volume of sediment in the system. To determine the volume, polygons are defined to describe the location of the gap and the location of the sediment accretion just after the flow slide. These polygons are given in Figure 3.14. The change in volume is used to estimate the recovery time and the sediment transport characteristics of the system. The volume of sediment in the system in June 2014 is considered as the equilibrium volume.

In the channel the measurement taken at 29-07-2014 (Flemish government, 2015) is the first measurement after the flow slide. In this measurement the bathymetry in the gap is not determined. The first available measurement of the gap is at the 21<sup>st</sup> of August 2014.

The change in sediment volume in the profile is given in Figure 3.15. The original volume of the gap is determined using the laser altimetry data of 2014 (Rijkswaterstaat, 2015). When the change in volume directly after the flow slide in the gap and the channel are compared, it is concluded that the volumes are approximately equal (~8 million m<sup>3</sup>). This means that almost no sediment is gone into suspension during the flow slide.

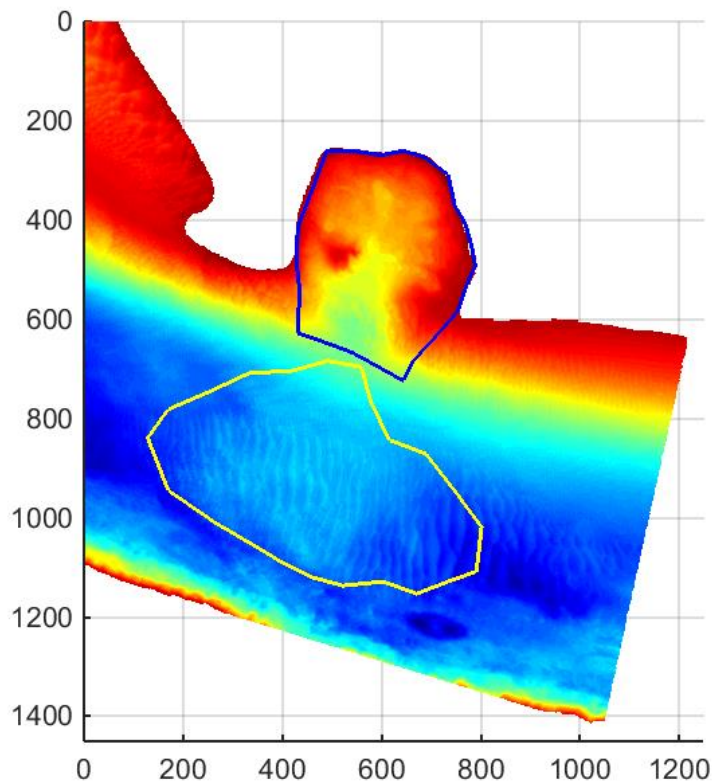


Figure 3.14: Polygons used to determine the sediment volume in the gap (blue) and the channel (yellow)

In Figure 3.9 and Figure 3.10 it can be found that the bed exceeded the required bed level of -17.5 m NAP. After the 29-07-2014 measurement a dredging operation was undertaken to guarantee the minimum navigation depth. From IMDC (2014a) it is found that 43,788 m<sup>3</sup> was dredged in situ in the beginning of August. Using the measurements the amount of sediment above NAP -17.5 m is determined, this equals 46,568 m<sup>3</sup>. The dredged volume is small (5%) compared to the total volume of the flow slide.

### 3.5.3 Volume change over time

Figure 3.15 shows that the sediment volume change in the channel is larger than in the gap, indicating faster erosion in the channel than sedimentation in the gap. The volumes are given in Table 3.2, as well as the rate of change. Due to the larger velocities in the channel the transport capacity is larger and more sediment is taken into suspension. In the gap this capacity is smaller since the hydrodynamic conditions are calmer, causing the import of fine sand and mud. The velocities should be very small for the fines to settle in the gap. The erosion in the channel shows an exponential decay. In March 2015 (after nine months) it is almost back to the original state. However, there is still some decay, but the rate of change is not very large any more.

The sedimentation rate in the gap is smaller than the erosion rate in the channel. The sedimentation in the gap follows approximately a linear pattern in the first half year. Hereafter an exponential trend can be visualised. Extrapolating the data, an assumption can be made on the recovery time. The original volume in the gap will be restored between November 2015 and June 2016, 1.5 to 2 years after the flow slide.

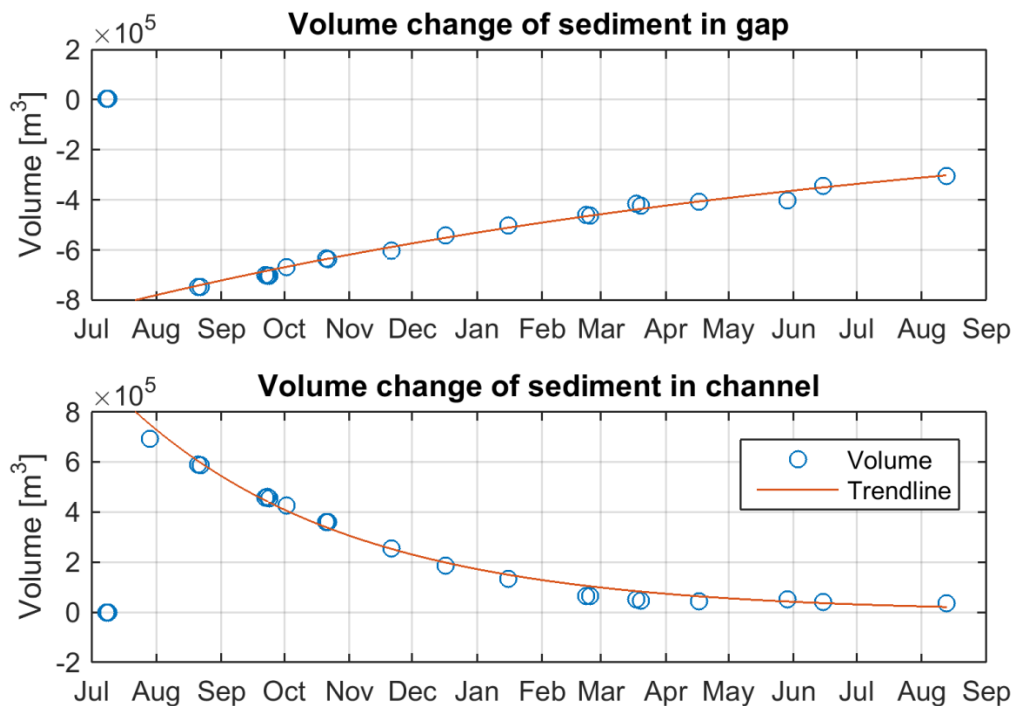


Figure 3.15: Sediment volume in the gap and channel relative to 12-06-2014

If uniform change over the area is assumed, the rate can be calculated in terms of vertical change per day. The used surface area of the gap is  $125 \times 10^3 \text{ m}^2$  and of the channel  $198 \times 10^3 \text{ m}^2$ . Consequently, the rate is in the order of a few centimetres per day. In the beginning there is erosion in the channel of approximately 2 cm/day. In the gap the sedimentation is around 1 cm/day.

Table 3.2: Volume difference with the situation of June 2014 (in  $\text{m}^3$ ) and rate of change in  $\text{m}^3/\text{day}$

Date	Gap [ $\times 10^3 \text{ m}^3$ ]	Change gap [ $\times 10^3 \text{ m}^3/\text{day}$ ]	Channel [ $\times 10^3 \text{ m}^3$ ]	Change channel [ $\times 10^3 \text{ m}^3/\text{day}$ ]
08-Jul-2014	-	-	-1	-
29-Jul-2014	-	-	692	-
21-Aug-2014	-747	-	588	4.5
22-Sep-2014	-699	-1.5	457	4.1
02-Oct-2014	-669	-3.0	425	3.3
22-Oct-2014	-638	-1.6	360	3.2
21-Nov-2014	-603	-1.2	254	3.5
17-Dec-2014	-542	-2.3	187	2.6
16-Jan-2015	-501	-1.4	134	1.8
22-Feb-2015	-461	-1.1	66	1.8
18-Mar-2015	-416	-1.9	53	0.6
17-Apr-2015	-409	-0.2	43	0.3
29-May-2015	-401	-0.2	51	-0.2
15-Jun-2015	-345	-3.3	41	0.6
13-Aug-2015	-304	-0.7	36	0.1

### 3.5.4 Suspended load transport from the deposited sediment in the channel

A rough estimation of the amount of suspended sediment transport can be made using the measurements. Tracking the sediment accretion in the channel, the volume difference with the original situation is determined. This volume difference is given in Figure 3.16. The used polygon to determine the volume is different for every month; it follows the deposited sediment in the channel. The locations of these polygons are given and elaborated in Appendix A.5. The polygons were determined manually, giving some inaccuracy of the volumes. This figure gives the actual volume of the sediment heap in the channel. The trend line gives an exponential decay in the channel. The difference between the months is the sediment that is disappeared, which is suggested to be gone into suspension. This percentage is approximately equal if exponential behaviour is estimated. From this data it is found that around 25 and 30% of the sediment in the channel has gone in suspension per month and is disappeared from the channel. The fall velocity of sand in the channel is smaller than the shear stress velocity, indicating the existence of suspended load transport.

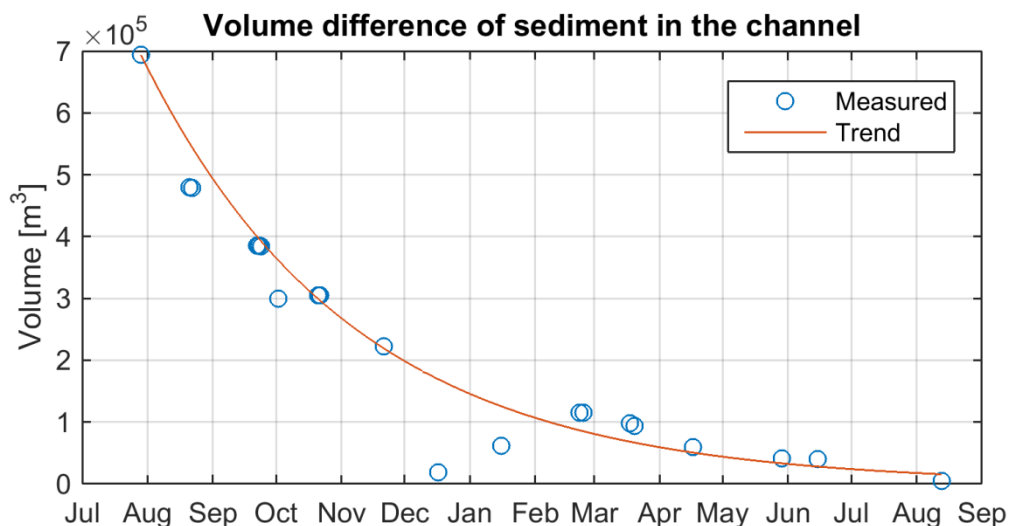


Figure 3.16: Volume difference of the sediment accretion in the channel

## 3.6 Dominant processes

### 3.6.1 Driving forces

The relevant processes occurring in the Bocht van Walsoorden are elaborated in Chapter 2. In the channel the main driving force is the tidal component. As the channel has a large bend the centrifugal force from the southwest possibly play a role. This causes erosion in the outer bend and sedimentation in the inner bend. The outer bend is reinforced with an armouring layer, fixing its position. The Coriolis force, directed to the right considering the flow direction, can be neglected over a tidal period. The main wind direction is from the southwest, so this causes small waves into the gap. The fetch is very small, so the set up due to the wind is negligible. Effects of waves in the channel are negligible, because of the large depth.

### 3.6.2 Estuarine circulation

The river run-off provides a longitudinal (horizontal) density gradient. The fresh water from the river mixes with the salt water from the sea. If the mixing capacity of the estuary is insufficient a strong stratification is present. This gives a difference in the flow direction over the vertical; the top layer has a dominant ebb direction, while the bottom layer has a dominant flood direction (Savenije, 2012). The Western Scheldt is classified as a well-mixed estuary, vertical density differences are negligible (Wang et al., 1999).

Since the estuarine circulation is controlled by the horizontal density gradient, this gradient needs to be determined. The annual mean density is  $1015 \text{ kg/m}^3$  at the Overloop van Hansweert and  $1010 \text{ kg/m}^3$  at Baalhoek in 2014. These values are based on observations by Rijkswaterstaat (2015) with an interval of 10 minutes. The distance between these two stations is 13 km. The horizontal density gradient modifies the logarithmic velocity profile, under the assumption of a non-stratified flow.

$$u(z) = -\frac{u_*}{\kappa} \ln \frac{z}{z_0} + \frac{1}{2} \frac{gh_0}{\kappa u_*} (z - z_0) \frac{1}{\rho} \frac{\partial \rho}{\partial x} \quad (3.2)$$

Equation 3.2 gives the velocity profile for the estuarine circulation. In this equation  $\rho$  is the density ( $\text{kg/m}^3$ ),  $g$  the gravitational constant ( $9.81 \text{ m/s}^2$ ),  $h_0$  is the water depth (22.5 m),  $x$  the horizontal coordinate,  $\kappa$  the Von Karman constant (0.41) and  $z_0$  the roughness height (m) (Kranenburg, 1996). The first part of the equation is the logarithmic velocity profile and the second part is the effect of the density gradient. The density gradient is positive directed towards the sea. For a vertical equilibrium the residual current in the profile should be close to zero, this is achieved with a  $u_*$  of 0.005 m/s. Figure 3.17 shows the velocity profile according to Eq. (3.2), which may be considered as the effect of the horizontal density gradient on the flow velocity profile. Near the surface there is seaward directed reinforcement, while near the bottom this reinforcement is landward directed. This causes during flood a higher velocity (than the logarithmic profile) near the bottom and a lower velocity near the surface. During ebb this is opposite, a lower velocity near the bottom and a higher velocity near the surface.

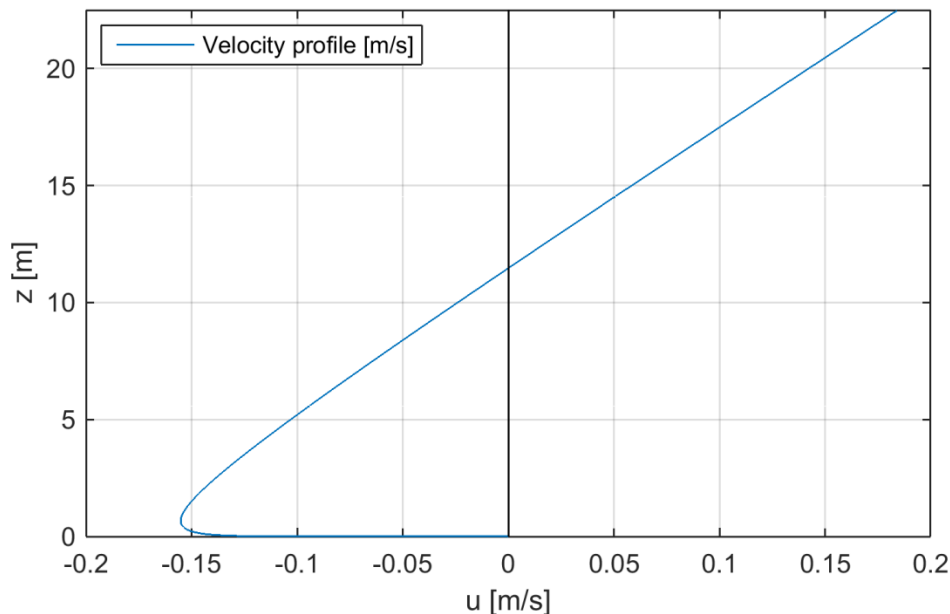


Figure 3.17: Estuarine circulation due to the horizontal density gradient

During the sediment transport measurement (Rijkswaterstaat, 2006), the velocity distribution over the vertical is measured. This profile is given in Figure 3.18. On the y-axis the depth is given (m), on the x-axis the velocity is given (m/s), positive is in flood direction. Near the bottom there is reinforcement during flood and weakening during ebb, indication the presence of estuarine circulation.

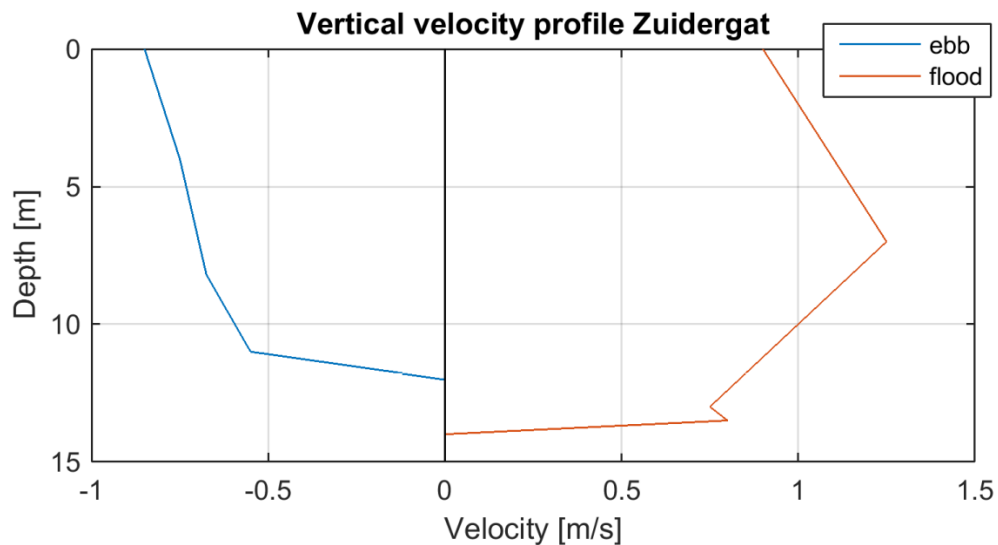


Figure 3.18: Vertical velocity profile at maximum ebb (blue) and maximum flood (red) (Rijkswaterstaat, 2006)

### 3.7 Discussion

The determination of the sediment transport is mainly done based on the bathymetry measurements. These give a good approximation of the bed load transport, but not of the suspended load transport. There are no suspended load measurements available in the period after the flow slide. Since most of the transport is suspended load transport in the Western Scheldt, this could influence the estimated transport direction significantly.

The sediment transport at the Zuidergat transect is measured once in 2005. This measurement was obtained at a static point, on the side of the channel, and over one tidal period. The behaviour on the side of the channel, near the tidal flat, is different than in the middle of the channel.

After the flow slide the sediment characteristics around and on the tidal flat are measured. This is done on the edges of the tidal flat and not in the channel or on the sediment accumulation. Measuring the sediment in the channel could give relevant information for the recovery of the system. In the model it is assumed that the characteristics are similar to those on the fringes of the tidal flat. This is reasonable, but actual measurements would cause smaller uncertainties.

### 3.8 Conclusion

#### 3.8.1 Ebb/Flood dominance

The ebb or flood dominance can be determined based on three characteristics: the water level, current speed, discharge, water volume and the net sediment transport (Bolle et al, 2010). These characteristics do not necessarily give the same dominance.

The water level signal, the vertical tide, is flood dominant if the rising time is shorter than the falling time. In the area of interest the rising time is 6h01m, while the falling time is 6h24 (Rijkswaterstaat, 2015). This suggests flood dominance based on the water levels. The asymmetry of the signal, the relative phase difference ( $2\varphi_{M2} - \varphi_{M4}$ ), gives a positive value, indicating also flood dominance.

The horizontal tide, the flow velocity, is flood dominant if the maximum flood velocity is higher than the maximum ebb velocity. In Figure 3.1 the velocity profile for the Zuidergat transect is given. From this measurement a maximum flood flow velocity is found of approximately 1.1 m/s, the maximum ebb flow velocity is approximately 0.8 m/s. The  $\langle u^3 \rangle$  is larger during ebb than during flood. The tidal constituents  $M_2$  and  $M_4$  give a negative relative phase difference. The volume passing the transect per tidal period is larger during ebb than during flood (Figure 3.3). The maximum velocity indicates flood dominance. However, the tidal asymmetry,  $\langle u^3 \rangle$  and the water volume indicate ebb dominance.

For the last characteristic sediment measurements are necessary. Due to lack of sediment transport measurements the monthly bathymetry measurements are used to determine the direction. The measurements show dune migration in flood direction. It is possible to have dune migration in a different direction than the residual sediment transport (Besio et al, 2004). The sediment transport measurement of 2005 shows residual sand transport in flood direction and residual mud transport in ebb direction (Rijkswaterstaat, 2006). The magnitude of the mud transport is larger than the sand transport (in kg/s). This would suggest residual sediment transport in ebb direction. This measurement contains only data for one tidal period. It is not necessarily representative for all tidal periods, causing a large uncertainty. To gain more insight in the sediment transport a numerical model is used, to determine the direction and magnitude of the transport.

### 3.8.2 Morphologic development

The monitoring of the development of the flow slide provides a unique dataset of the changes over one complete year. During the flow slide approximately 800,000 m<sup>3</sup> of sediment flowed into the channel. The appearance of this sediment in the channel indicates that only a very small part of the sediment directly went into suspension. From the observed data it can be concluded that the dunes in the channel migrate in flood direction. The sediment seems to be transported in upstream direction in the channel and in downstream direction near the fringes.

The gap is filling in mostly at the east side and the sediment in the channel is transported towards the east. The gap becomes filled in with a mixture of mud and sand. The particle size found in the gap is smaller than the particle size in the channel. The recovery time of the system depends on the location in the system. In the channel there is large erosion due to high flow velocities, the recovery time is approximately 9 months. The sedimentation rate in the gap is smaller than the erosion rate in the channel. The gap will take 1.5 to 2 years to recover. In the gap a mixture of sand and mud is found, deposited in layers. Based on the erosion/sedimentation rate of the different parts, the gap is determinative for the recovery time needed for the complete system. This suggests that the system is recovered after 1.5 to 2 years.

## 4 Walsoorden model setup

### 4.1 Delft3D

Delft3D is a numerical model developed by Deltares and is able to simulate the currents, wave propagation, sediment transport, morphological developments and water quality in coastal, riverine and estuarine areas (Hibma et al., 2003). The program solves the Navier Stokes equations for an incompressible fluid, under the assumptions of shallow water and Boussinesq (Deltares, 2014). For this study the FLOW module is used, which calculates the transport based on the hydrodynamic forcing.

### 4.2 NeVla model

The NeVla (Nederlands-Vlaams) model is a detailed 2DH model of the Scheldt estuary. The term 2DH means depth averaged, a homogeneous distribution over depth is assumed. This simplification is valid if the fluid is vertically homogeneous. It is developed from the SIMONA model and is transferred to Delft3D. The model includes a large part of the seaside, the Western Scheldt and the Flemish tidal rivers until the tide has no influence any more (at Gent). Several versions of this model are available, each with different boundary and initial conditions and bathymetry. Since the time of interest is July 2014 until the beginning of 2015 the model validated for 2014 is used (Vroom et al., 2015).

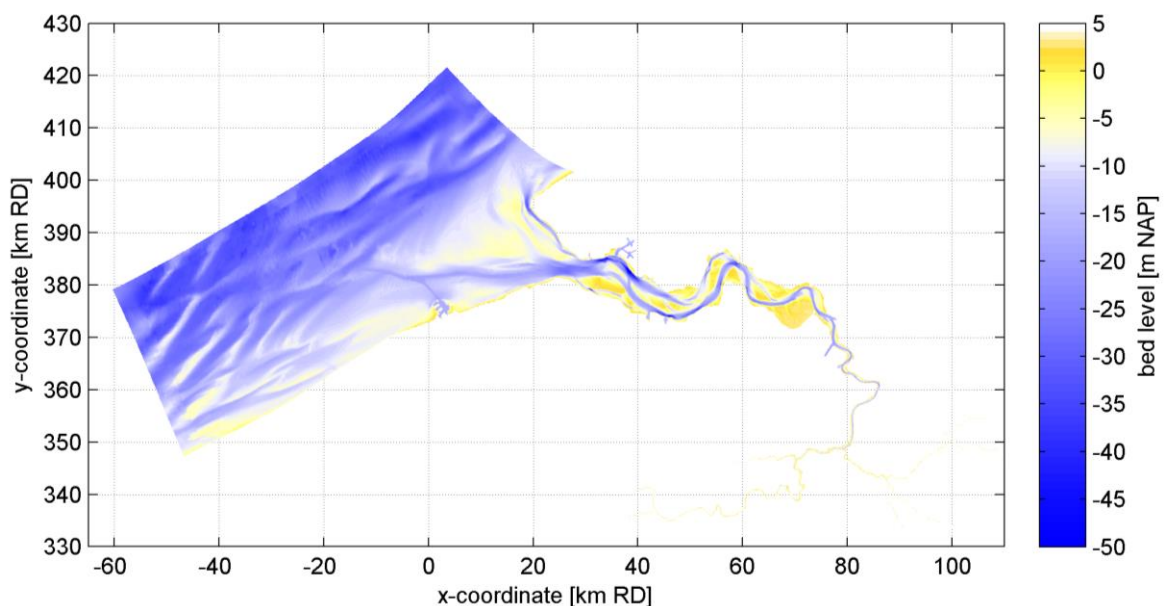


Figure 4.1: Bathymetry of the NeVla model (Vroom et al., 2015)

#### 4.2.1 Grid

Figure 4.1 gives an overview of the numerical domain. The grid size of the model ranges from coarse (200 m) at the sea to fine (10 m) in the river branches. In the Western Scheldt the size is between 50 and 100 m. The bathymetry is obtained from the Baseline-schematisation. In this program the characteristics of the bottom are saved and adjustments can be made. The bathymetry used in the NeVla 2014 model is merged from the 2011 measurement of the mouth, the 2008-2010 measurements for the Sea Scheldt and upstream of Rupelmonde from 1965-2001. For the more upstream river branches the bathymetry of the 2006 NeVla model is used. The bathymetry used in this model is thus after the third deepening.

#### 4.2.2 Boundary conditions

The seaward boundary conditions are generated from the ZuNo (Southern North Sea) SIMONA model. The boundaries perpendicular to the coast make use of Riemann invariants. The boundary parallel to the coast uses water level as a boundary condition. At the upstream sides of the river branches the measured discharges are used. The boundary conditions for salt are constructed using MWTL measurements; this gives a more accurate result than in previous studies. These measurements are taken with a large interval, which is not disturbing in this case, since the seasonal variation is larger than the tidal variation on the seaward boundary. The wind is spatially uniform; it consists of a corrected time series by the KNMI from measured wind characteristics. It is corrected using a value for the friction of the wind over sea and over land, giving the potential value for wind.

#### 4.2.3 Validation

The model is validated using water level measurements, currents and discharges (Vroom et al., 2015). The area of interest for this model is the mouth of the Western Scheldt. This gives high accuracy in the mouth and a little less accuracy in the river branches. Further upstream of Schoonaarde the error is considerable. However, in the area near Walsoorden the model behaves very well. The currents in the measurement station of Hansweert show the same pattern and order of magnitude as the computed values. This makes the model trustworthy in this area. The measured discharges of the Zuidergat and Schaar van Waarde are compared with the computed discharges using the boundary conditions of 2013. These values are approximately the same. This makes the model suitable for the use in the area near the tidal flat of Walsoorden.

### 4.3 Walsoorden model grid

#### 4.3.1 Domain

The computational grid is based on the original NeVla grid. Figure 4.1 gives an overview of the NeVla grid. At the boundaries there must be as little intertidal area as possible. Intertidal area gives problems when boundary conditions are imposed. At the boundary the velocities can only be imposed perpendicular. Therefore it is important to have the boundary at a location where the currents are almost perpendicular to the grid. Next to this the boundaries should be sufficiently far from the area of interest to be able to neglect boundary effects.

Therefore, it is chosen to start the domain at the Drempel van Baarland, where the least intertidal area is present from the locations on the west of the tidal flat of Walsoorden. On the east there is the Saeftinge salt marsh, which is a very large intertidal area. Chosen is to impose the boundary at the Drempel van Zandvliet, to include Saeftinge, but exclude intertidal area at the boundary. At this location the velocity is almost perpendicular to the grid, making it possible to impose a velocity boundary condition at this location.

#### 4.3.2 Resolution

The resolution of the NeVla grid is too coarse in the area of interest; it differs from 30 m to 150 m. Therefore, the grid has to be refined. Instead of using a refinement for the complete area, domain decomposition (DD) is used in order to save calculation time. With domain decomposition the model is divided into smaller domains, which can communicate with each other along internal DD-boundaries. In this way one domain can be more refined than the other. However, the time step must be the same for both domains and the grid lines need to continue in the different domains. This means that only an integer refinement number can be used.

The developed grid for the Walsoorden model thus includes two domains: a large overall domain, with the same resolution as the NeVla model and a smaller domain around the area of interest with a smaller resolution. The division of the different domains is given in Figure 4.2. The resolution of the larger grid varies from 30 m till 100 m near the tidal flat to 150 m at the edges of the domain. For the smaller domain local refinement is applied. This local refinement results in more grid cells and more accuracy. The refinement in the x-direction is 1:6 and in the y-direction 1:3. These refinement numbers are not equal, because the grid cells are rectangular in this area. With the different refinement values the grid cells become more squared. The refined grid has a resolution of 20 m to 30 m. This is sufficient to visualize the flow slide since the gap is around 300 m wide.

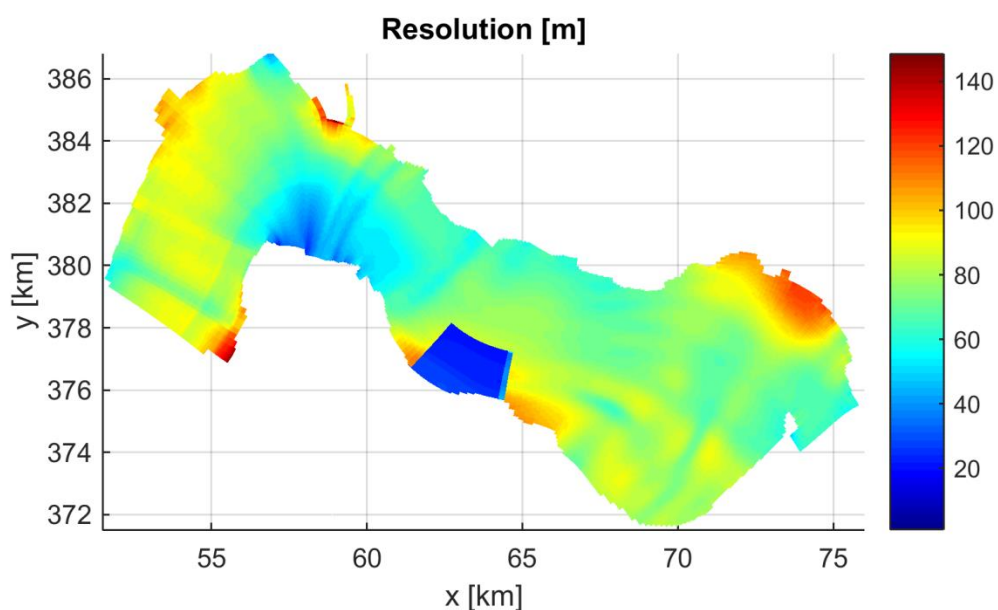


Figure 4.2: Resolution of the Walsoorden model, with in blue the smaller domain with a higher resolution

#### 4.4 Boundary conditions

The boundary conditions of the Walsoorden model are generated with the NeVla model. On the west, downstream side of the model water levels are used. On the east, upstream side the velocities are imposed on the boundary. At the intertidal areas on the sides of the boundaries the conditions gave some problems. Therefore, no boundary conditions are imposed at the grid cells that are located in the intertidal areas. This can be justified by the fact that these areas are dry most of the time, having almost no velocity and water level change. The boundary conditions for the sediment and salinity flux are also generated by the NeVla model.

#### 4.5 Initial conditions

##### 4.5.1 Bathymetry

The bathymetry measurements by Rijkswaterstaat and the Flemish government are used to determine an accurate bathymetry for the situation before the flow slide. The bathymetry is completed with the bathymetry of the 2013 NeVla model. Figure 4.3 gives the initial bed level before the flow slide. The bathymetry measurement of the 8<sup>th</sup> of July 2014 is used to construct this bathymetry, completed with the 'vaklodingen' of 2013 (Rijkswaterstaat, 2015) and the NeVla bathymetry.

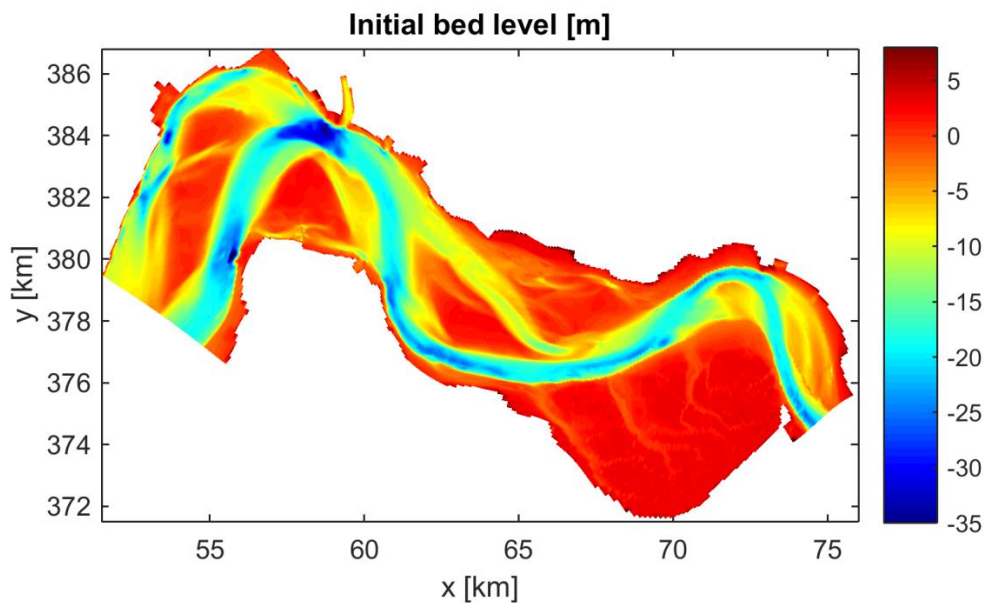


Figure 4.3: Initial bed level

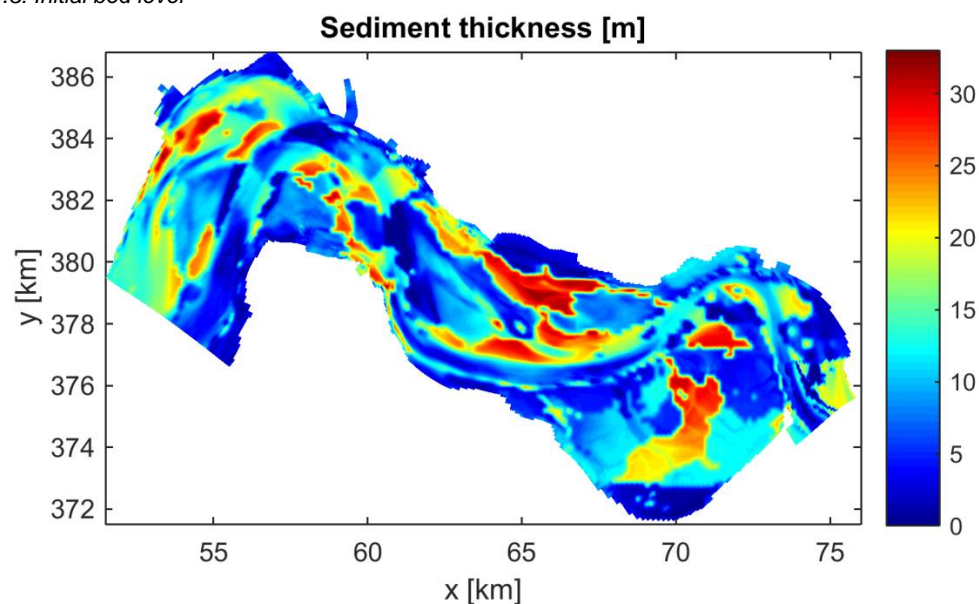


Figure 4.4: Initial sediment thickness

#### 4.5.2 Sediment layer thickness

The sediment layer thickness (Figure 4.4) is the available sediment for erosion. This layer is adopted from the NeVla model. The height is based on the largest depth ever measured; this is seen as the hard layer. The difference between this point and the actual depth is the available height of sediment (Dam, 2013). In the ebb channel there is less sediment available to erode than on the tidal flats. The flood channel has some sediment to erode.

#### 4.5.3 Roughness

The roughness of the area is determined from the NeVla model, given in Figure 4.5. In the Land van Saeftinge the roughness is higher than in the rest of the domain. This difference is caused by vegetation in the intertidal area. The vegetation gives a higher roughness, which gradually damps the currents. The rest of the domain has a constant value of  $0.022 \text{ s/m}^{1/3}$ . At

the edges of the domain the roughness is slightly higher. This is based on the NeVla model, where a higher roughness was obtained in the areas upstream and downstream of the domain.

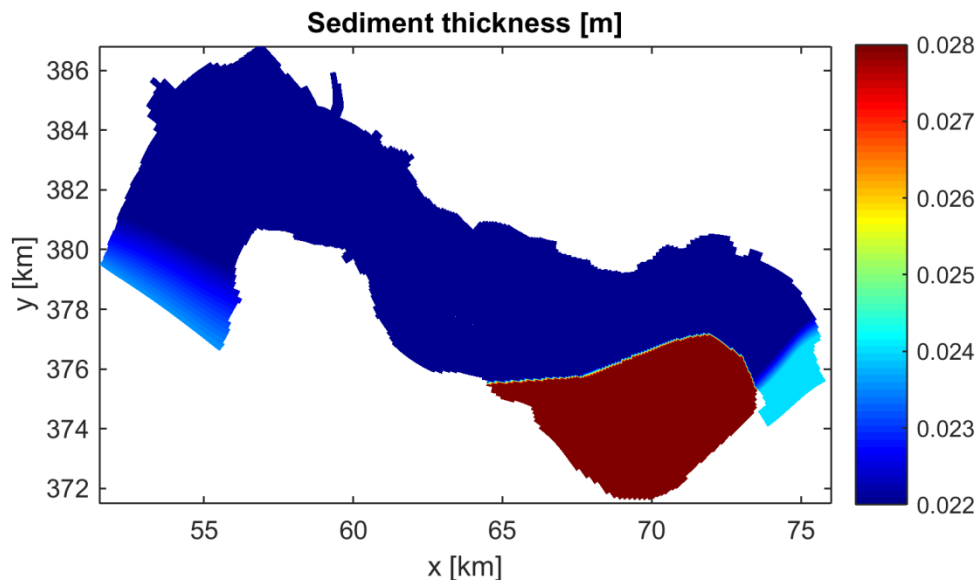


Figure 4.5: Imposed Manning roughness

#### 4.5.4 Salinity

The environment near the tidal flat is brackish. The salinity varies spatially from 17 ppt at the seaward end to 5 ppt at the river end. The domain decomposition seems to be sensitive to large changes in the salinity, especially when uniform values are imposed. Therefore it is chosen to give the model a 'hot start' using spatially varying values. The information of the restart file from the NeVla model is extracted and used for the different domains. When this file is used the correct initial conditions are generated for the velocity, water level and salinity. This minimalizes the initial disturbances and decreases the spin up time.

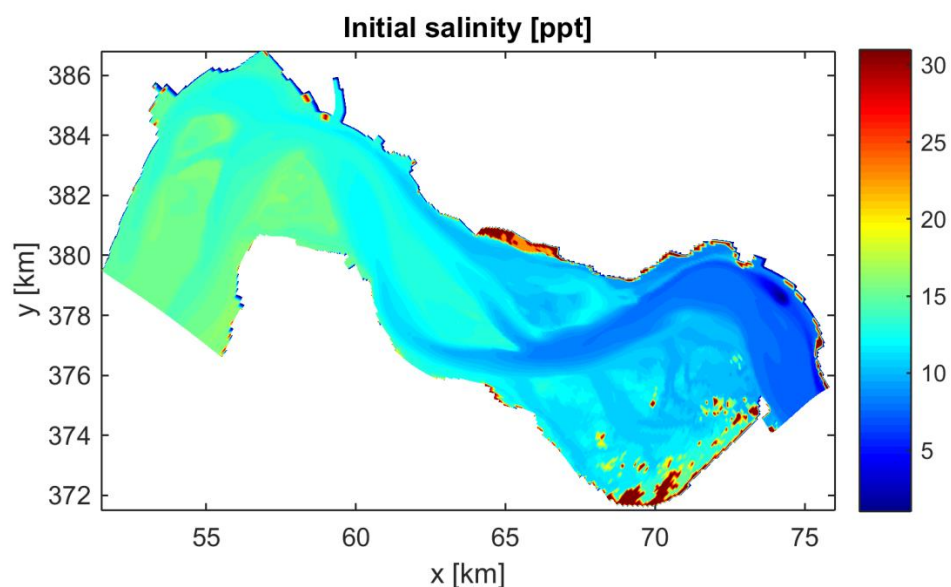


Figure 4.6: Initial salinity

At the land boundaries of the domain a higher salinity is calculated, this is because of the drying and flooding of these cells. If they dry out the amount of salt inside the cell cannot decrease fast enough, causing these higher values. Although the values are larger than in the rest of the domain, they are still acceptable.

## 4.6 Model parameters

### 4.6.1 Sediment transport formula

Different from the NeVla model the Engelund-Hansen transport formula (1967) is used in the Walsoorden model. This formula imposes the transport rate as bed load transport, which gives better result with the domain decomposition. The domain decomposition gives problems in calculating the suspended load transport. More information about this is given in Appendix C, together with the verification of the domain decomposition boundaries.

The Engelund-Hansen transport formula reads (Deltares, 2014):

$$S = S_b + S_{s,eq} = \frac{0.05 * \alpha * q^5}{\sqrt{g} * C^3 * \Delta^2 * D_{50}} \quad (4.1)$$

In this formula  $q$  is the magnitude of the flow velocity,  $\Delta$  the relative density of the sand particles (=1.65),  $C$  the Chézy friction coefficient,  $D_{50}$  the median sand grain size and  $\alpha$  is the calibration coefficient. The calibration coefficient is set to the default value of 1. In the entire domain a  $D_{50}$  of 200  $\mu\text{m}$  is chosen. The major difference between Van Rijn (2004) and Engelund-Hansen is the power of the flow velocity. Van Rijn uses a power 3, whereas Engelund-Hansen uses a power of 5. Van Rijn also makes the distinction between bed load and suspended load transport, with a critical velocity from where the particles start to move.

The value of the Chézy friction coefficient is determined from the roughness of the bed. The imposed Manning values are translated to the Chézy values, using formula (4.2). Afterwards these values are used in the transport formula.

$$C = \frac{H^{1/6}}{n} \quad (4.2)$$

The Engelund-Hansen transport formula calculates the total transport. The relation between bed load and suspended load transport in the Western Scheldt is approximately 1:10. This means that the magnitude of the suspended load is 10 times larger than the bed load transport. The used factor for transverse bed load is 10 times smaller than when Van Rijn is used, giving a value of 10 (Kuijper et al, 2006).

### 4.6.2 Numerical input

The behaviour of the model does not only depend on the initial and boundary conditions. The influence of the model parameters should not be ignored. To optimise the model several modelling parameters are used.

Inside the modelling domain by default only perpendicular flow velocities are allowed. Using the command *Cstbnd* this can be changed. The command allows flow velocities inside the domain to approach on a different angle.

On the boundaries some erosion and sedimentation can occur. To prevent this, a Neumann boundary condition, a zero concentration gradient, is implemented at the boundary. This means an equal concentration at the boundary and just inside the domain. The transport conditions on the boundaries are determined with the Neumann boundary condition. By using the command *NeuBcSand* this feature is implemented in the model.

The morphological factor (*MorFac*) is used to reduce the computation time of the morphological change. In this model a morphological factor of 13 is used. The morphological change of one spring-neap cycle in the model corresponds thus with half a year in reality.

#### 4.7 Simulation period

In order to save calculation time a representative simulation period is chosen for the year 2014. This period consists of one spring-neap tidal cycle that is representative for the entire year. Using the measured water level at Baalhoek the different spring-neap cycles are determined (Rijkswaterstaat, 2015). The annual water level and wind are determined to find a representative period. For the salinity only the second half year is used since there is a large seasonal variability. A more extensive elaboration of the simulation period is given in Appendix B.

Based on the water level, wind and salinity, the period 22-Jul-2014 08:20:00 till 06-Aug-2014 03:20:00 is chosen as the representative spring-neap tidal cycle. This period gives a representation of the period after the flow slide for the water level and salinity. For the wind it also gives sufficient, steady results. The only disadvantage of this period is the absence of a storm condition. However, since waves are not imposed in the model this effect will be very small.

#### 4.8 Discussion

For this study a depth averaged model is used, which is very accurate in case of an almost logarithmic velocity profile. In the model the velocity profile is assumed to be logarithmic, as was found in the data analysis. However, in the data analysis there is also a small influence of the estuarine circulation found. This effect is simplified in the 2DH model, making the implementation of it not very clear.

The usage of domain decomposition gave some difficulties. First the communication through the boundary for suspended load transport was not accurate. Second the secondary circulations could not be implemented in the 2DH model with domain decomposition. These two difficulties lead to simplifications of the model. Nevertheless, the model was accurate enough and was suitable for the purpose of this research.

During the simulation period storms are absent. This could give a distorted image of the sediment transport. However, the model represents half a year and during this longer period the moderate conditions are more important than the extreme conditions. If the wind characteristics for the complete year are compared with the characteristics for this period they are very similar. This gives confidence in the selected simulation period.

## 5 Hydrodynamic validation of the Walsoorden model

For the validation of the model the hydrodynamics are compared with the existing data measurements and the NeVla model. The MONEOS measurements around the tidal flat of Walsoorden are used. The water level and velocity is compared with the model outcomes. Hereafter, the water level, velocity and discharge of the Walsoorden model are compared with the NeVla model. The NeVla model is validated using other measurement stations (Vroom et al., 2015). By comparing with the NeVla model the nesting process is verified.

### 5.1 MONEOS measurements

For the period between 08-10-2014 and 17-11-2014 point measurements are available around the tidal flat of Walsoorden. These measurements are made in the context of the MONEOS campaign (Meire and Maris, 2008). At the observation stations the water level, velocity magnitude and direction were determined. In 2014 fourteen points were measured around the tidal flat of Walsoorden. The locations of these points are given in Figure 5.1. For the validation of the model the bathymetry of November 2014 is used together with the 'vakdodingen' of 2013. This gives the most recent bathymetry for the comparison with the measurements. Especially in a smaller area it is important to use matching bathymetry with the measurements. In this section the results are graphically given for the points MP0101, MP0309 and MP0622. These points are representative for different parts around the tidal flat and have short exposure duration. An overview of the results for the other points is given in Appendix D, where a further comparison between the measurements and the model results is given.

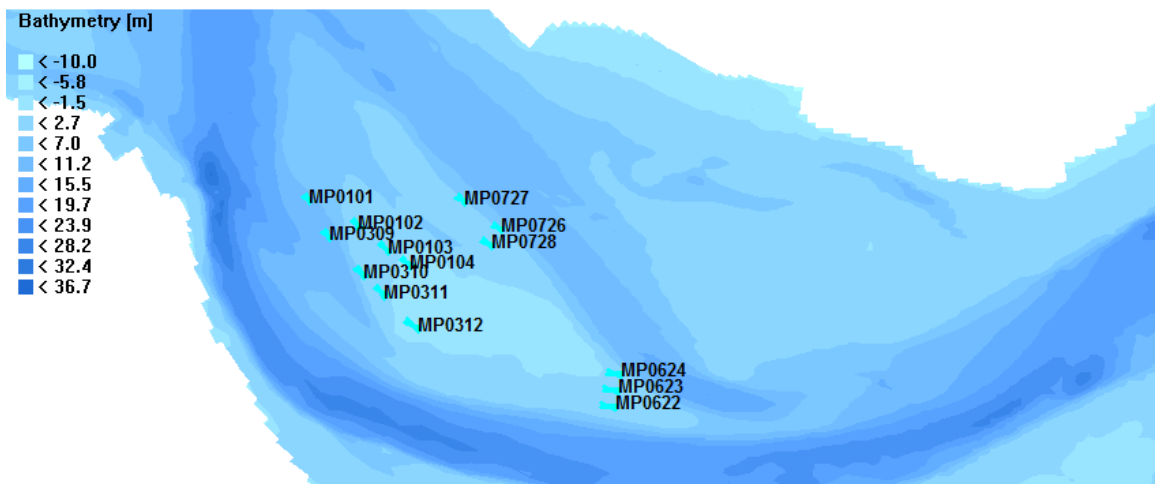


Figure 5.1: Locations MONEOS measurements 2014

#### 5.1.1 Water level

The water level from the measurements shows the same pattern as the water level calculated by the model. In Figure 5.2 the results of some representative stations along the tidal flat are given. During low water the water level is predicted sufficient, the error is at most 0.1 m. The differences during low water are mostly because of the bed level. In the model the bed level is showed if the water level is beneath the bed level, the cell is dry at that moment. In the measurements the water level is interpolated without using the dry points. This gives a complete water level signal, but it is not showing the dry falling of the tidal flat. This is for example the case in station MP0623.

The high water is overestimated with 0.1 – 0.4 m in the model. The underestimation of the low water level together with the overestimation of the high water level gives an overestimation of the tidal range. The high water in the measurements is somewhat earlier than in the model. This leads to a longer rising period in the model than in reality, which makes the model more ebb-dominant in these points. The shift of the peak is in the order of minutes, causing a very small difference. In section 2.2.2 it was found that the rising time is 6h01m and the falling time is 6h24m (Rijkswaterstaat, 2015). A difference of a few minutes would not cause a shift in dominant direction.

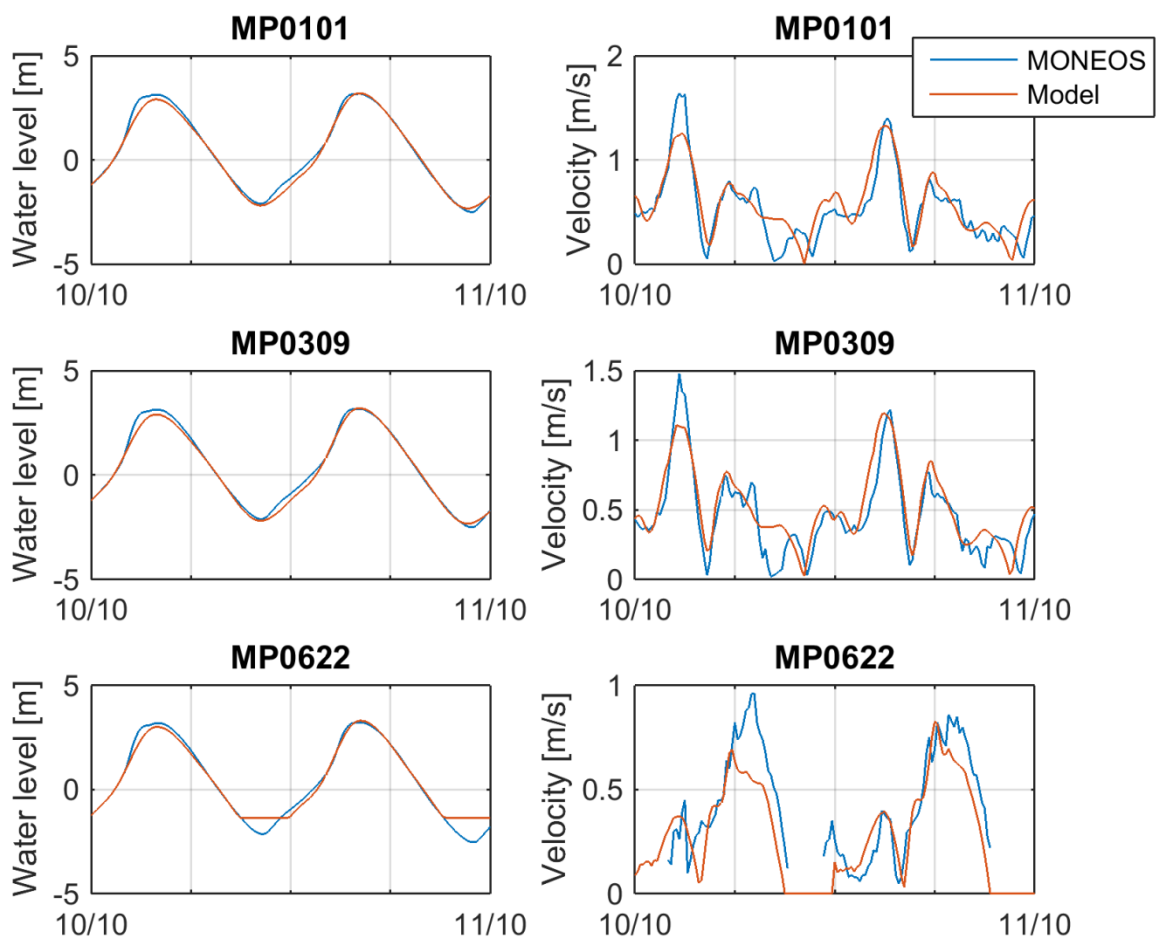


Figure 5.2: MONEOS measurements compared with the model results, with on the left the water level signal and on the right the velocity signal

## 5.1.2 Velocity

The points closest to the channel give the best approximation of the flow velocities. A larger water depth gives fewer disturbances in the velocities. The model is depth-averaged, so a minor error in the bathymetry could cause a large error in the depth-averaged flow velocities on the tidal flat. With this in mind, the velocities should be interpreted with some precaution. In Figure 5.2 the measured velocity is compared with the modelled velocity. The measurements show small disturbances, since it is measured every 10 minutes. These small disturbances are not visible in the model, because the model spreads these disturbances. Due to the drying of the tidal flat the velocity signal is not complete. When the water level is below a certain level the velocity cannot be measured any more. This is seen at point MP0622.

The velocity at the locations MP0101, MP0103, MP0309, MP0311 and MP0622 are well reproduced. These points are located on the southern part of the tidal flat, so they are important in the area of interest.

The points on the north of the tidal flat, MP0726, MP0727 and MP0728, show an overestimation of the velocity. This could indicate an overestimation of the water volume that is transported through the northern channel (Schaar van Valkenisse). Especially since the overestimation is during flood, this could lead to more flood directed transport in the Schaar van Valkenisse. This gives less flood directed transport through the Zuidergat, which leads to lower velocities in this area. The points MP0102 and MP0104 show a minor overestimation of the flow velocity.

Lower velocities than in the measurements are found in the points MP0310 (only during spring tide), MP0312, MP0623 and MP0624. This supports the suggestion that the water distribution between the two channels in the model is not completely equal to reality.

## 5.2 Comparison with Delft3D NeVla model

The model is not only validated using real-time measurements, but is also compared with the results of the NeVla model. The Walsoorden model is nested in the NeVla model and this nesting procedure needs to be validated. Since the NeVla model is already validated by Vroom et al. (2015), the results of this model are compared with the Walsoorden model. The NeVla model is validated using water level data from the stations showed in Figure 5.3. For Hansweert the model is also validated with velocity data. The stations in the figure are used to compare the outcome of the Walsoorden model with the NeVla model.

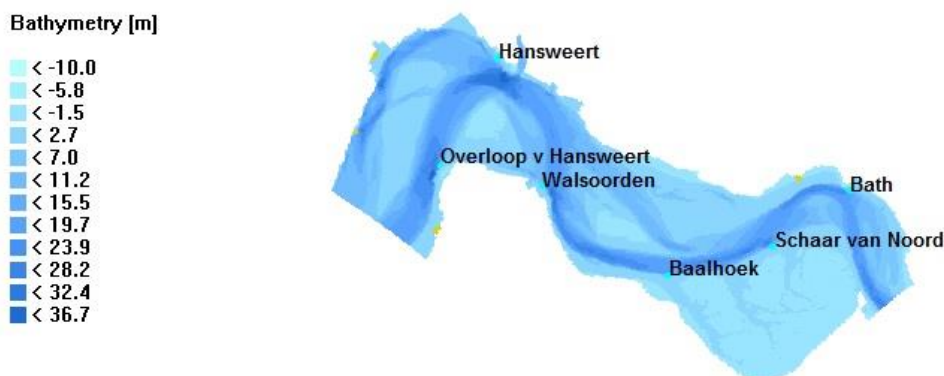


Figure 5.3: Locations of the stations

### 5.2.1 Water level

For the comparison with the NeVla model several monitoring stations are used. These stations are located at the actual measuring stations, given in Figure 5.3.

In Figure 5.4 the water levels for the stations are given for the NeVla and Walsoorden model. The difference between the two models is small, at the peaks the difference is at most 0.1 m, on average the peak difference is around 0.05 m. This difference is mainly due to the updated bathymetry in the Walsoorden model. The values of the root-mean-square error between the two models are given in Table 5.1. All values are below 0.03 m, which is acceptable for the purpose of this model. The two stations closest by the area of interest are Walsoorden and Baalhoek. Both perform very acceptable for the water levels, compared to the NeVla model.

Table 5.1: Root-mean-square error for water level and velocity

Station	Water level [m]	Velocity [m/s]
Baalhoek	0.0214	0.0299
Bath	0.0261	0.0242
Hansweert	0.0156	0.0445
Overloop Hansweert	0.0125	0.0799
Schaar van de Noord	0.0255	0.0327
Walsoorden	0.0169	0.0520

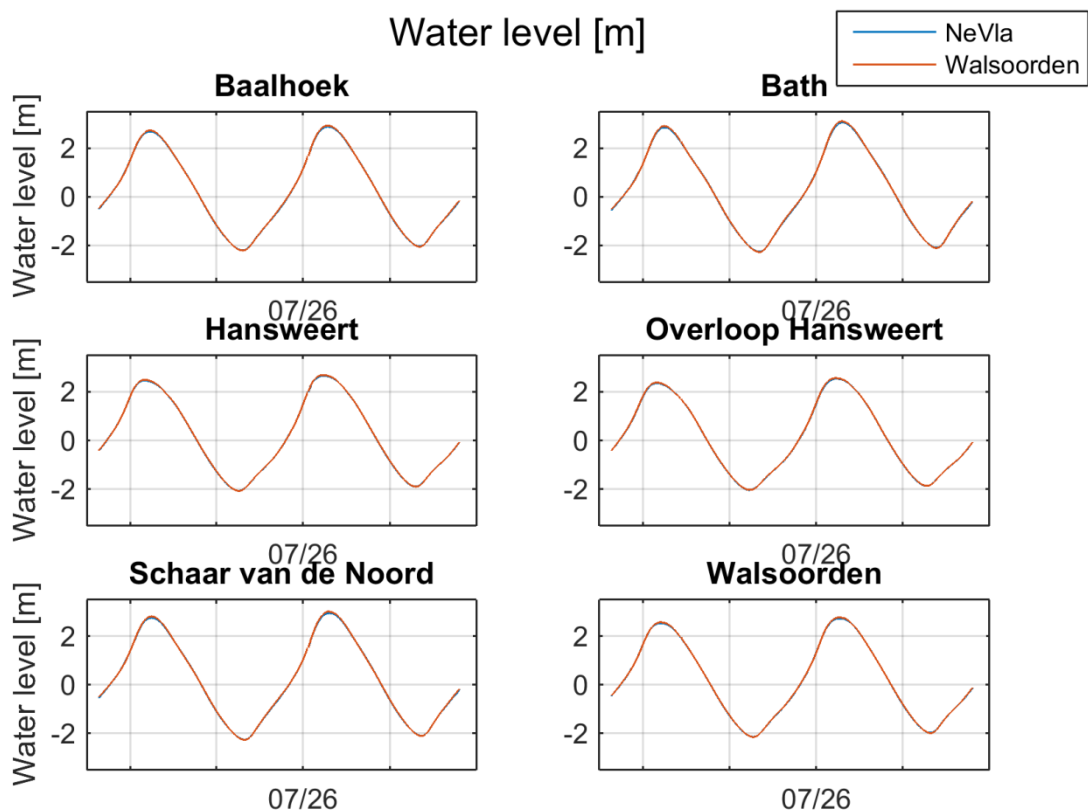


Figure 5.4: Water levels for the measurement stations along the domain

## 5.2.2 Discharge

Bathymetry [m]

- < -10.0
- < -5.8
- < -1.5
- < 2.7
- < 7.0
- < 11.2
- < 15.5
- < 19.7
- < 23.9
- < 28.2
- < 32.4
- < 36.7



Figure 5.5: Locations transects

The discharge of the Walsoorden model is compared with the NeVla model. The transects for which this is done are given in Figure 5.5. For the area of interest the Zuidergat is most important, as it is representative for the Bocht van Walsoorden, the channel in front of the flow slide. Zuidergat is the southern part of the transect, while the Schaar van Waarde the northern part is. The results of both models for Zuidergat are given in Figure 5.6. In this figure positive is flood directed. The discharge for the Zuidergat is validated in the NeVla model. Therefore it is not necessary to validate the values of the Walsoorden model again with the data, as they are similar to the values of the NeVla model. For the other transects the same validation is done, the Walsoorden and NeVla model give the same result for all transects.

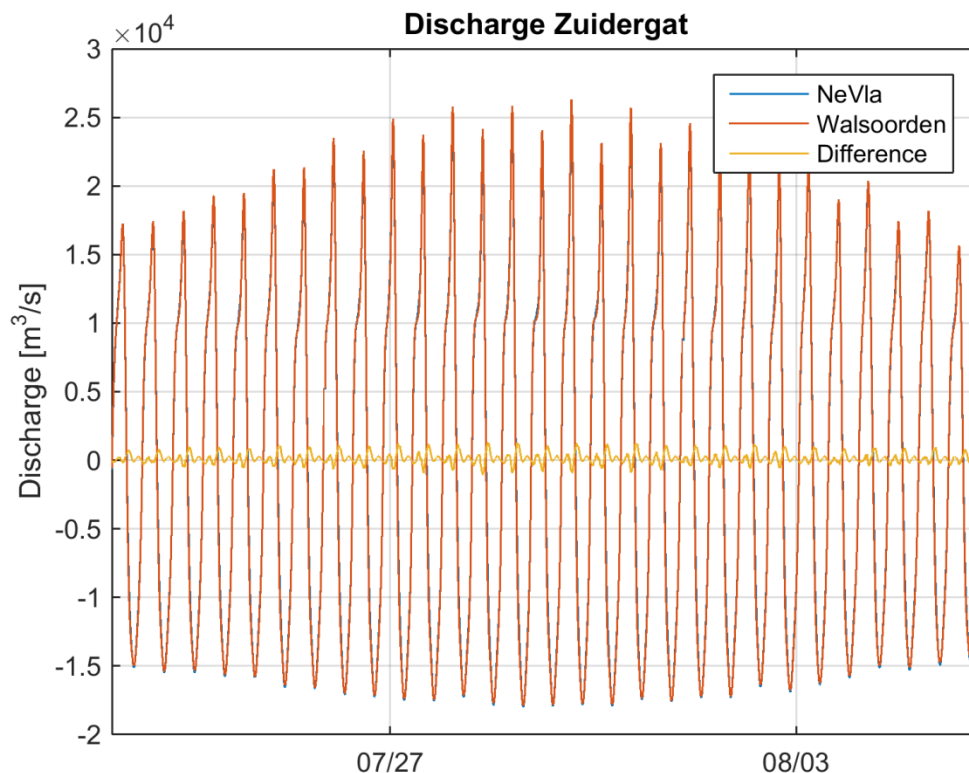


Figure 5.6: Discharge through the Zuidergat transect for the NeVla and Walsoorden model

### 5.2.3 Velocity

For the same stations the velocities are compared. The velocities perform a little bit worse than the water levels. However, the order of magnitude and the shape is generally the same. The Walsoorden model shows a smoother behaviour than the NeVla model. In Figure 5.7 the velocities for the stations are given for both models. The root-mean-square error for the velocity is given in Table 5.1. It varies between 0.024 m/s for Bath and 0.08 m/s for the Overloop van Hansweert. The stations closest to the flow slide have an error around 0.045 m/s. This error is considered small enough to give sufficient accurate results in the area of interest. The difference between the models is mostly because of the difference in bathymetry. For the Walsoorden model the bathymetry is updated using the measured values in July 2014.

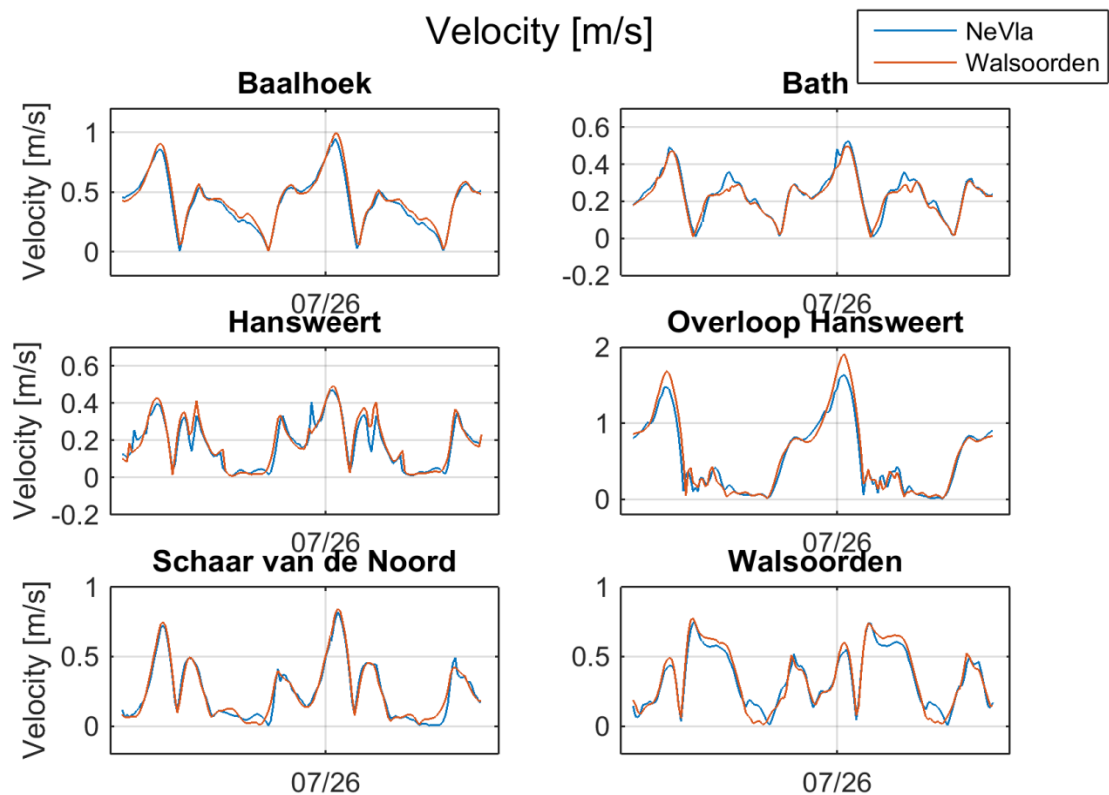


Figure 5.7: Velocity for the measurement stations along the domain (maximum flood velocity occurs around 26-Jul-2014 0:00)

### 5.3 Conclusion

On the hydrodynamic signal from the model a same analysis is done as in section 3.7 for the water level, velocity and discharge. The water level in the model gives a rising time of approximately 6 hours; the time for the water level to drop is around 6h20m. These values correspond with the values found in literature (see section 3.8.1). The relative phase difference in the middle of the channel is slightly ebb dominant (negative).

The velocity signal in the middle of the channel gives higher flood velocities than ebb velocities during spring tide and vice versa during neap tide. The period with higher flood velocities is shorter, indicating ebb dominance. The relative phase difference for this signal gives a negative value, suggesting ebb dominant behaviour. The spatial distribution of the maximum ebb and flood velocity is given in Figure 5.8 and Figure 5.9 respectively. The ebb velocity is concentrated in the channel, while the flood velocity also is located on the tidal flat. This part of the tidal flat is drowned during high water. The flood chute makes the area complex, especially during the first phase of flood. The water needs to flow through a narrower channel, causing higher velocities. When the water level is elevated and the tidal flat is partially drowned a turbulent eddy is created on the edge of the tidal flat (Figure 5.9).

The discharge through Zuidergat (Figure 5.6) is combined with the cross sectional surface to determine the transect averaged velocity. This velocity is representative for the Zuidergat and it is used to determine the dominant direction in the channel. The velocity through the transect,  $u$  and  $\langle u^3 \rangle$ , are both negative. Based on these three characteristics, the Zuidergat turns out to be ebb dominant. The same analysis is made for Schaar van Waarde, this transect gives flood dominant behaviour. However, the strong asymmetry as found in the measurements is not found in the transect averaged velocity.

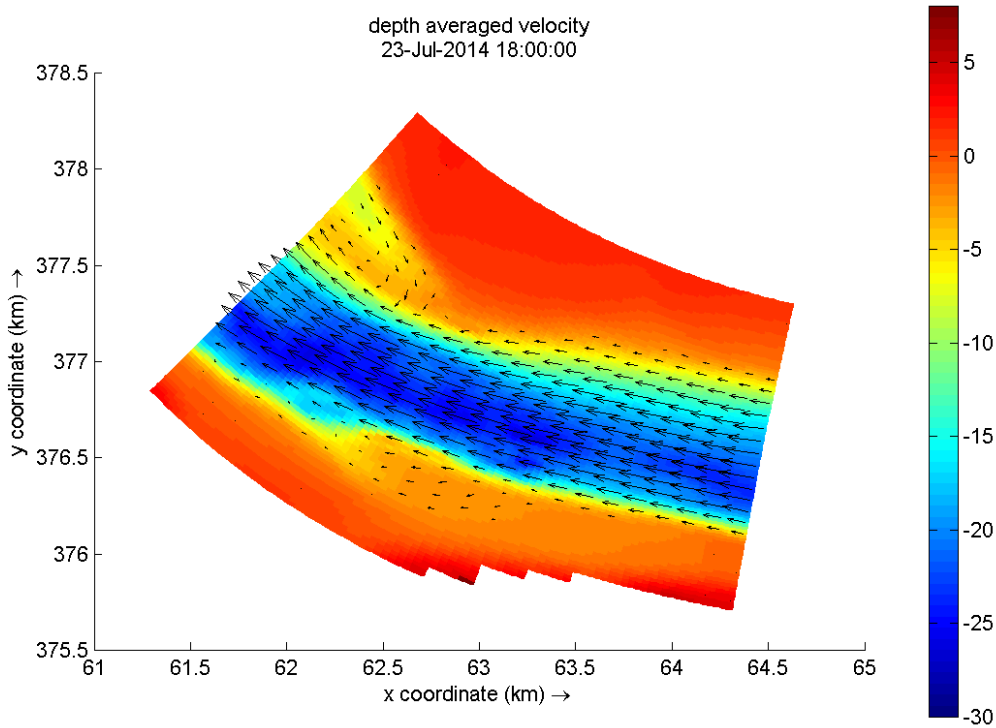


Figure 5.8: Maximum depth averaged velocity during ebb (arrows) (background: initial bed level)

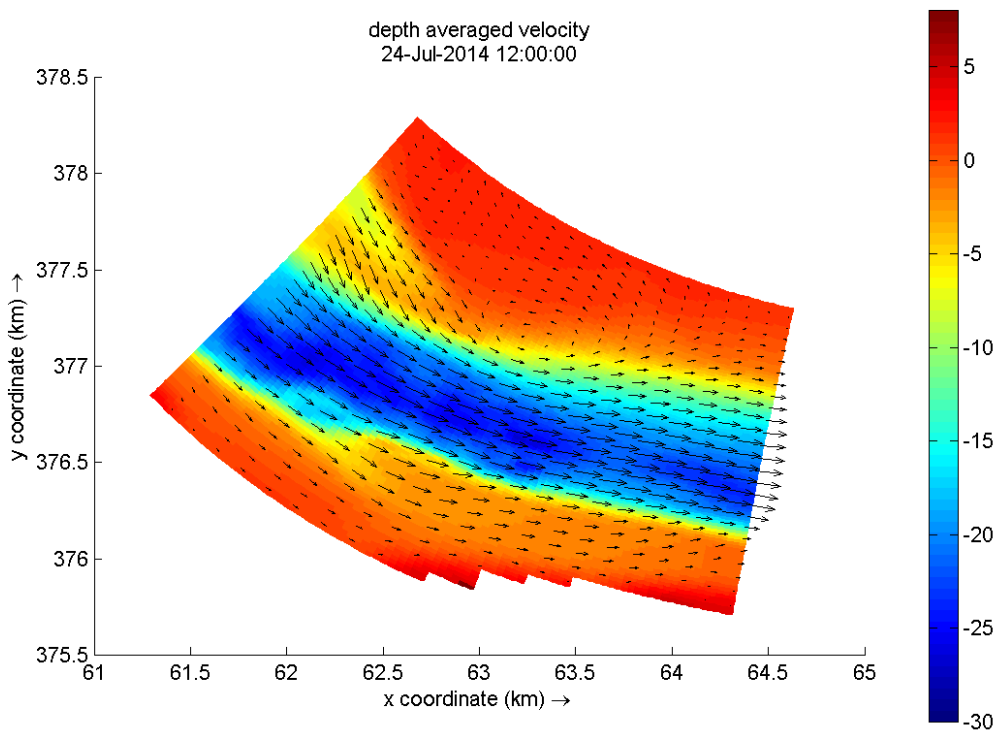


Figure 5.9: Maximum depth averaged velocity during flood (arrows) (background: initial bed level)

## 6 Modelling the morphological impact of the flow slide

In order to make the comparison between the situation before and after the flow slide, the flow slide is implemented in the model. This is done by comparing the hydrodynamics and morphological development before and after the flow slide. The original settings of the model are used as described in Chapter 4. The main difference of this run compared to the original situation is in the initial conditions, these are described in section 6.1. Since the hydrodynamics of the model are already validated in Chapter 5; the situations before and after the flow slide can be compared. In this way the effect of the flow slide on the hydrodynamics and the morphology is determined.

### 6.1 Initial conditions

#### 6.1.1 Bathymetry

The bathymetry of the original Walsoorden model is updated using the bathymetry measurement of 22<sup>nd</sup> August 2014, which is the first complete bathymetric dataset that includes the flow slide. The largest differences are found in the smaller domain. The influence in the large domain is small, therefore only the small domain is given in Figure 6.1. On the tidal flat the bed level is lowered, because during the flow slide the sediment was flown down from the tidal flat into the channel. The bed level is increased in the channel.

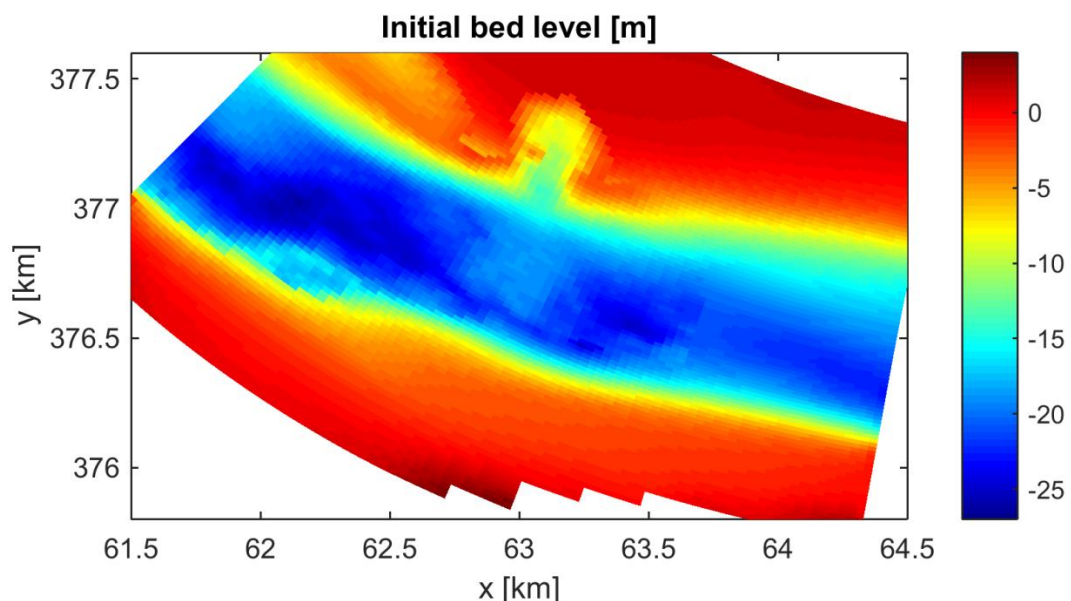


Figure 6.1: Initial bed level after the flow slide

#### 6.1.2 Sediment thickness

The sediment thickness after the flow slide is determined using the difference in bathymetry before and after the flow slide. This is added to the original sediment thickness. On the tidal flat this leads to a decrease of available sediment. In the channel the availability is increased, more sediment can be eroded here. The initial sediment thickness is shown in Figure 6.2.

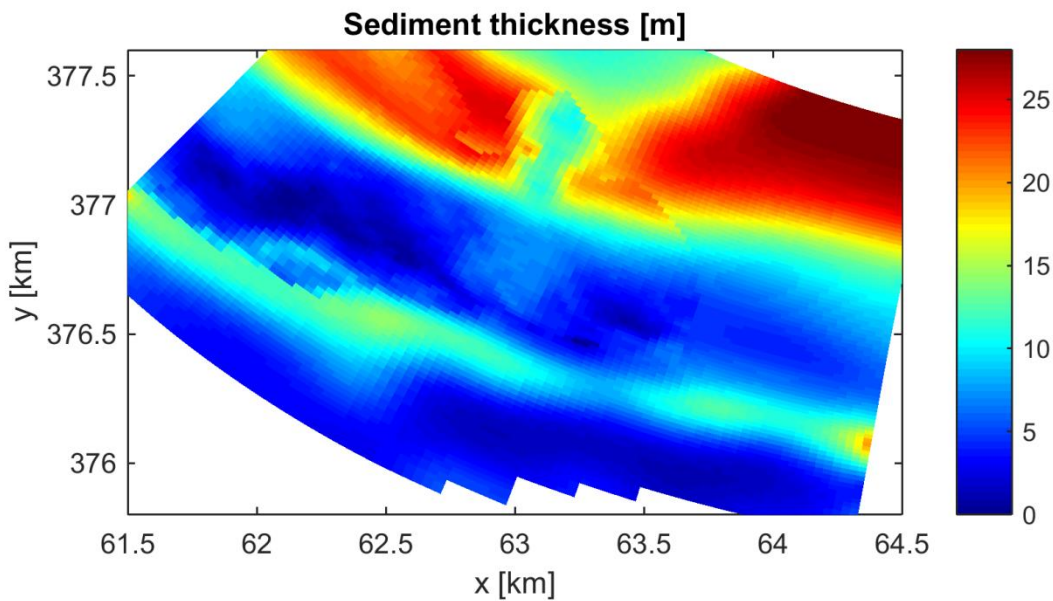


Figure 6.2: Initial sediment thickness after the flow slide (m)

## 6.2 Effect of the flow slide on the hydrodynamics

With the updated initial conditions the model is run for the situation after the flow slide. Since the effect of the flow slide is very local, this is done for stations near the flow slide, located within the domain of the local model. For these stations, given in Figure 6.3, the computed water levels and velocities before and after the flow slide are compared.

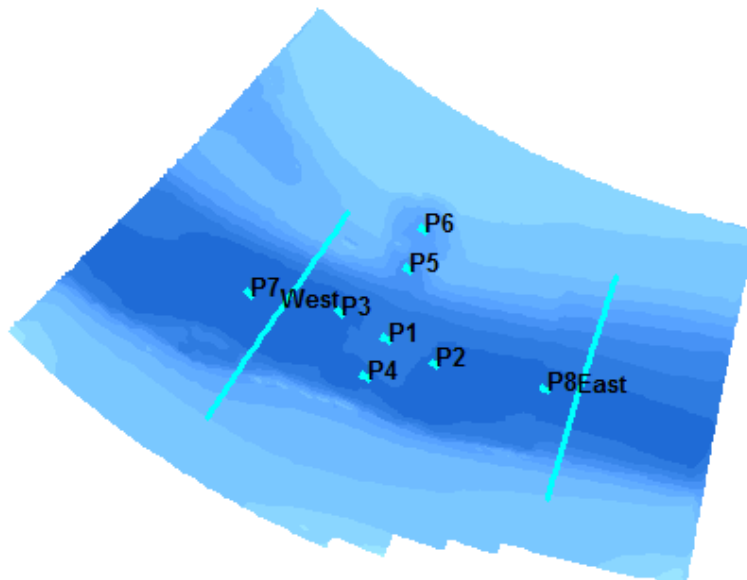


Figure 6.3: Stations and cross sections around the flow slide

### 6.2.1 Water level

The water level before and after the flow slide is very similar. A large change was not expected since the water volume over the estuary was not changed significantly. This makes the effect negligible. The tidal range shows a minor increase, in the order of a few

centimetres. The high water peak after the flow slide is a few centimetres (around 2 cm) higher than before the flow slide. This is shown both on the tidal flat and in the channel. The low water peak is a few centimetres lower for the situation after the flow slide. These both peaks contribute to a small increase of the tidal range. However, this effect is very small and the influence on the water level can be considered negligible. Location P6 was exposed during low water before the flow slide occurred. This is visualised by the blue line in the figure. After the flow slide this point is always beneath the low water level.

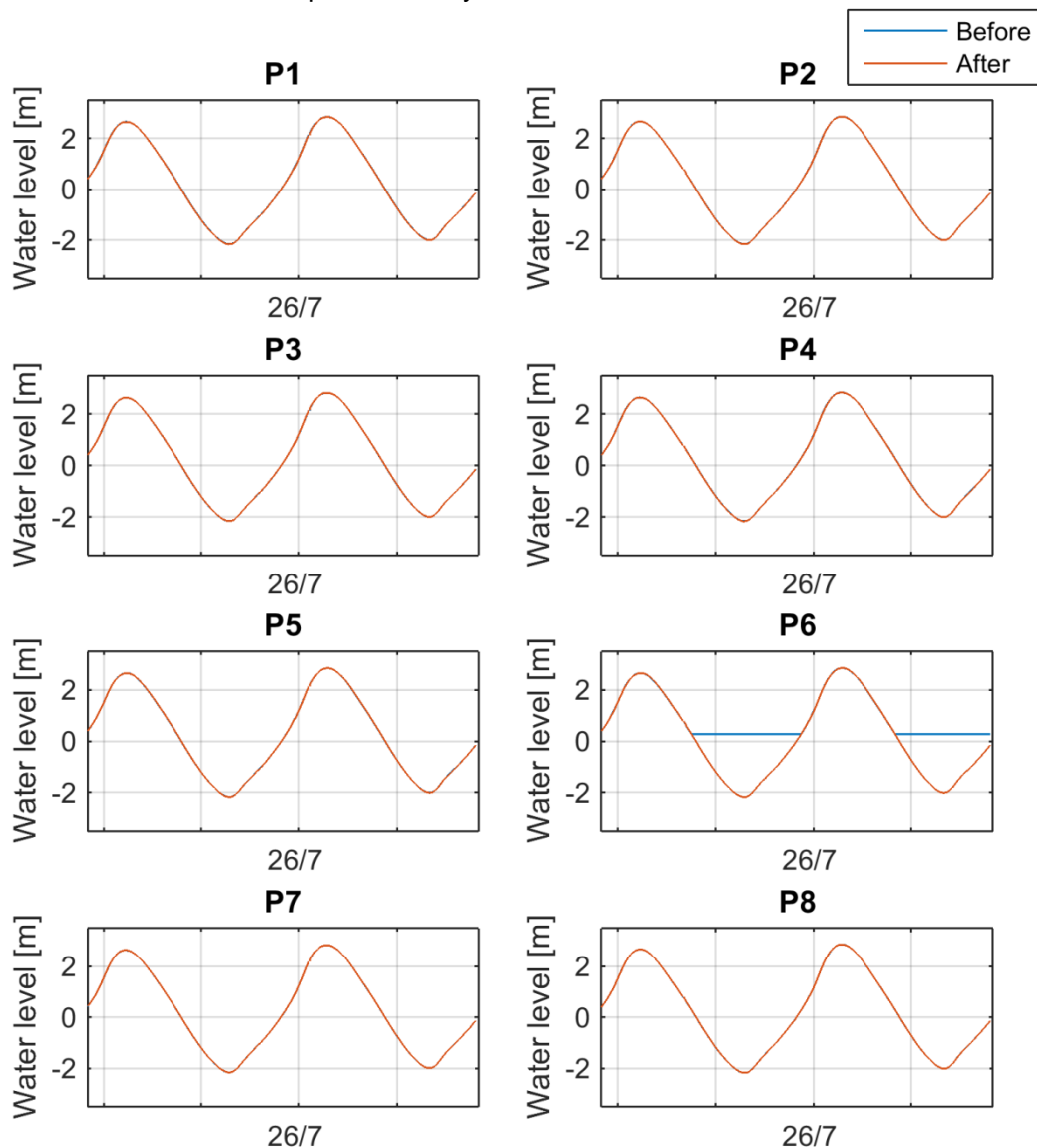


Figure 6.4: Water level before (blue) and after (red) the flow slide

## 6.2.2 Discharge

The discharge in the channel before and after the flow slide is given in Figure 6.5, in this figure positive is flood directed. The locations of these transects are given in Figure 6.3. The discharges show a very similar pattern before and after the flow slide. There is slightly less water flowing through the transects during ebb and flood after the flow slide. However, this difference is small ( $100 \text{ m}^3/\text{s}$ ) with respect to the total discharge. The flow slide did not result in a significant change in distribution of water between the Schaar van Waarde and the Zuidergat, according to the model.

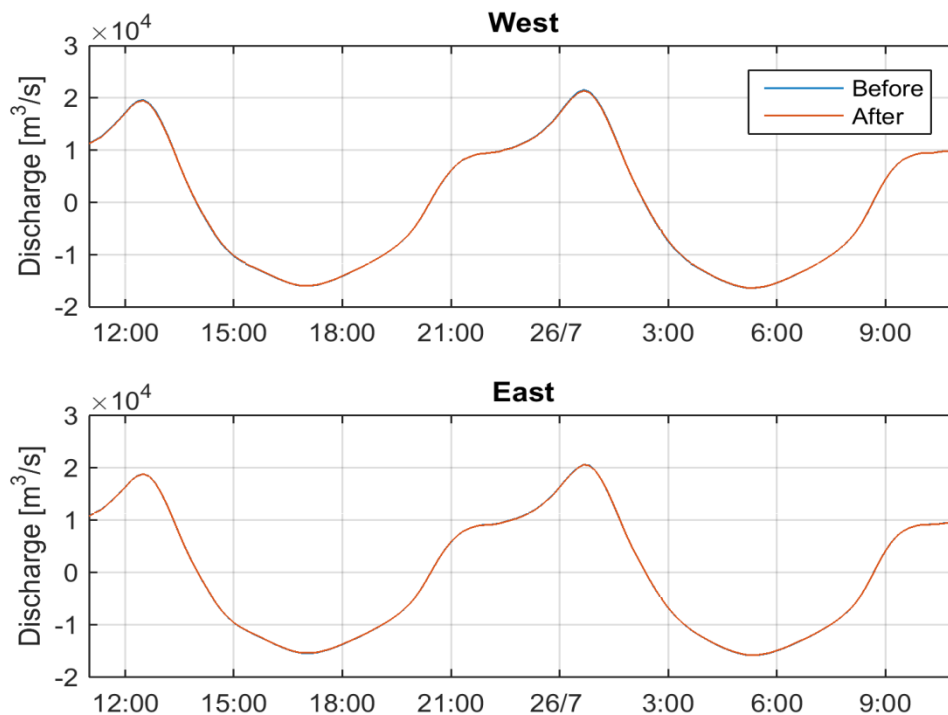


Figure 6.5: Discharge in the channel before and after the flow slide

### 6.2.3 Velocity

The depth-averaged velocity is given in Figure 6.6. In the channel the points closest to the flow slide (P1 till P4) show the largest observed differences. On top of the sediment accumulation (P1) the velocities are higher for the situation after the flow slide. Almost the same amount of water flows through this point, but the water depth is smaller. This causes higher flow velocities; the model gives slightly higher peaks for the ebb and flood velocities after the flow slide.

On the sides of the flow slide (P2, P3 and P4) this effect is also visible. For point P2 both the flood and ebb velocity increased. For point P3 and P4 the ebb velocity increased. The increase in all cases is around 0.2 m/s. The difference in increase along the tidal cycle is probably due to the bathymetry change before and after the flow slide. The fact that the ebb velocity changes, indicates that this velocity is more sensitive to bathymetry changes than the flood velocity. For point P2 this change is approximately 3 m, while for P3 and P4 this change was respectively 0.7 and 1.2 m. It can be concluded that a small change in bathymetry causes small changes in the velocity.

For the points in the gap created by the flow slide (P5 and P6) large velocity differences are found. The depth increased after the flow slide. This leads to a decrease in flow velocity, found in points P5 and P6. The velocities in ebb and flood direction decreased after the flow slide. If a closer look is taken to the direction of the flow velocity this is not changed after the flow slide. This is remarkable, since also velocity, and thus, transport should be expected inside the gap of the tidal flat.

The velocities in the channel away from the sedimentation area (P7 and P8) show little changes. This indicates that the effect of the flow slide on the hydrodynamic conditions is only very locally.

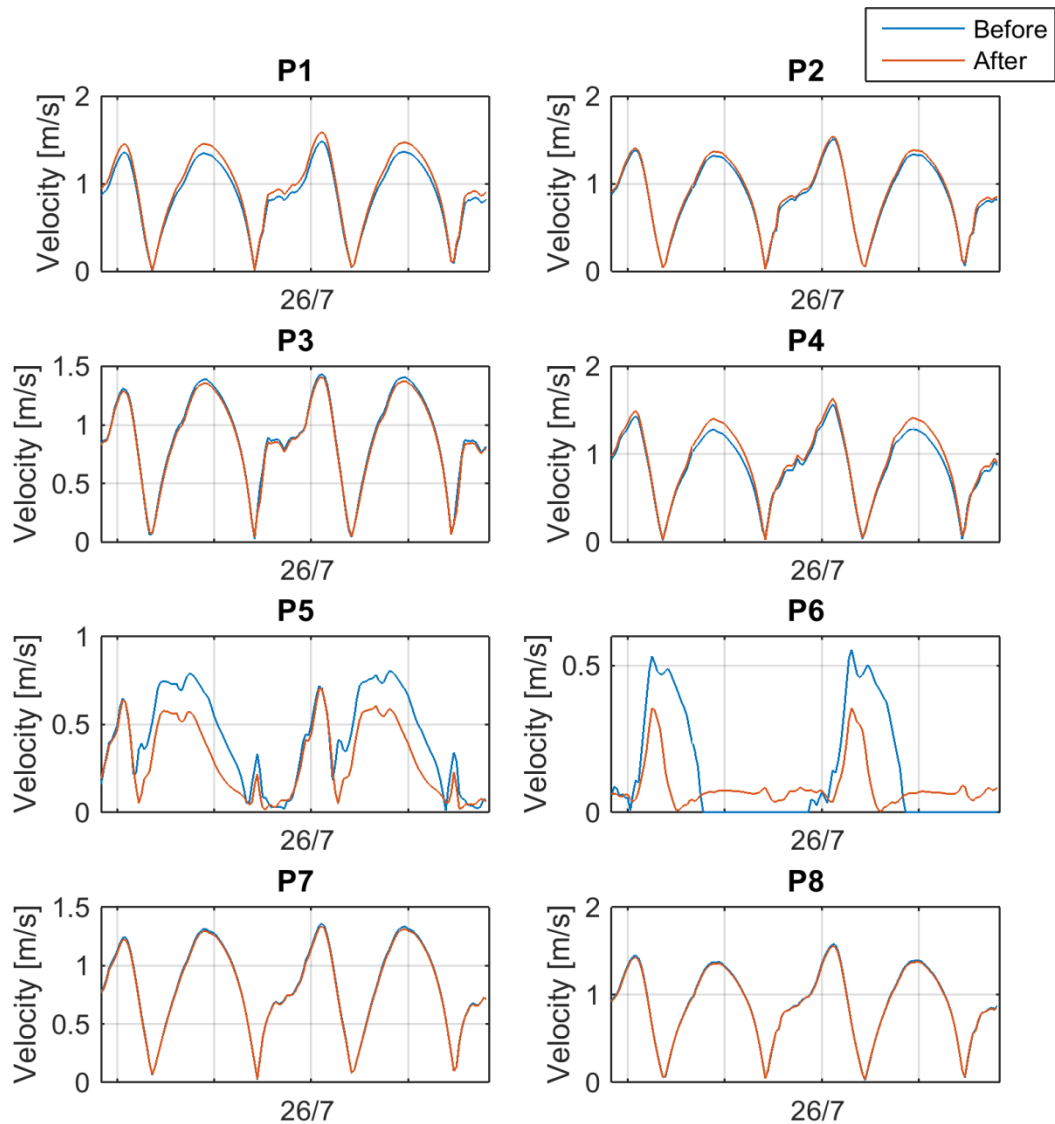


Figure 6.6: Depth-averaged velocity before and after the flow slide; around 0:00 26.07.2014 maximum flood occurs

### 6.3 Residual flow

The residual flow direction is given in Figure 6.7. In the channel the residual direction is in ebb direction. This fits the expectation of an ebb channel. Also on a large part of the tidal flat the residual flow is in ebb direction. On the northwest of the channel there is a flood chute, which is also visible in the residual flow pattern. The residual flow is in flood direction and a circulation is created when this flood directed current meets the ebb directed channel flow. On the south of the channel the residual current is in flood direction. The order of magnitude is around 0.02 m/s.

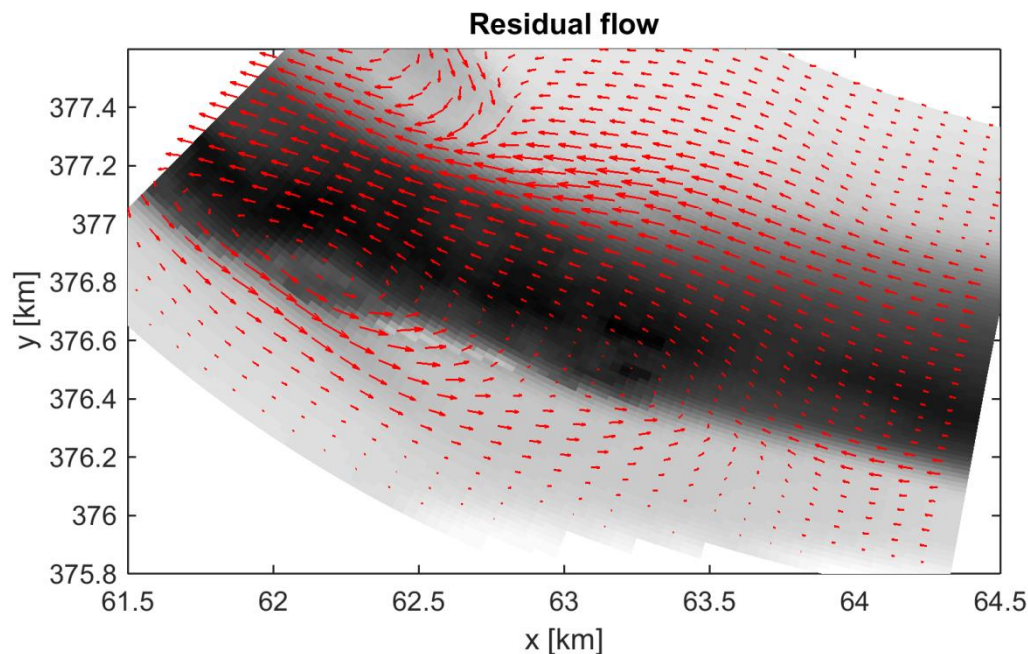


Figure 6.7: Residual flow (arrows) in the area of interest after the flow slide (background: initial bed level before the flow slide)

#### 6.4 Sediment transport

Figure 6.8 gives the mean sediment transport before the flow slide, with the direction indicated with arrows and the magnitude in the background. In the channel there is a clear distinction in ebb and flood directed transport. The north of the channel is mainly ebb directed, while the south is flood directed. This distinction is due to the bend in the channel and is also observed in Waterbouwkundig Laboratorium (2007) based on the bed form asymmetry. In Appendix E the sediment transport is given for the situation after the flow and the total transport with the Van Rijn equation. The mean sediment transport calculated with the Van Rijn equation gives a similar pattern as given by Engelund-Hansen.

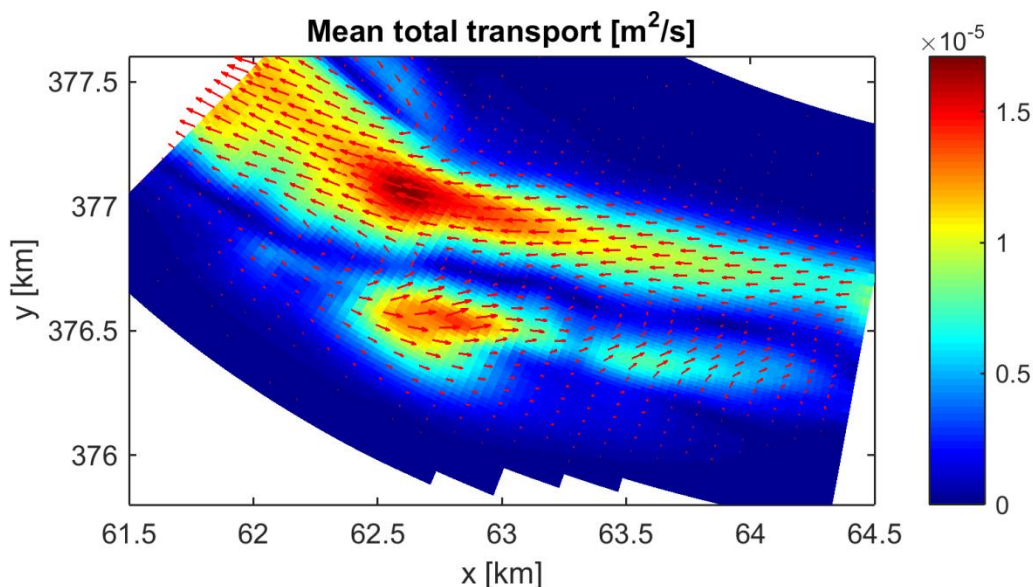


Figure 6.8: Mean sediment transport for the small domain with Engelund-Hansen

## 6.5 Morphological change

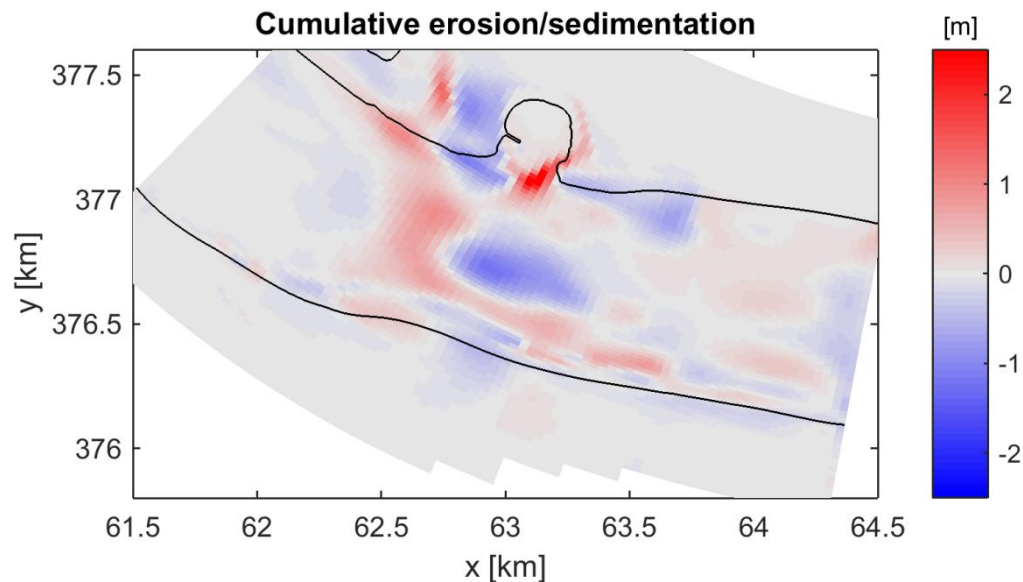


Figure 6.9: Cumulative erosion and sedimentation in the smaller domain after half a year, with the line indicating a depth of -6 m NAP

Based on the flow velocity signal and sediment transport, the morphological change is calculated. Using the representative simulation period and a morphological acceleration factor of 13 the change over half a year is calculated. The effect of the flow slide is determined by extracting the original situation from the situation after the flow slide. This effect is given in Figure 6.9. Sedimentation is positive and indicated in red, while erosion is negative and indicated in blue. In the next sections the change in the channel and in the gap is discussed.

### 6.5.1 Erosion in the channel

A large part of the sediment in the channel is eroded after half a year. However, still there is some sediment from the flow slide situated in the middle of the channel. As can be observed from Figure 6.9 the eroded sediment is for a large part settled on the sides of the sediment accretion. This suggests smoothing of the profile after the flow slide. On the west side of the flow slide there is only sedimentation directly next to the accumulation, further on in the channel there is no effect visible from the flow slide. On the east side of the flow slide there is a whimsical pattern visible of sedimentation and erosion.

### 6.5.2 Sedimentation in the gap

The sedimentation in the gap is clearly visible in the measurements (Figure 3.13). Most of the sediment is deposited on the east side of the gap, driven by the flood current. The edges of the tidal flat are eroding; this sediment is partly deposited in the gap. This pattern is also showed in the model. In Figure 6.9 the erosion of the tips can be found. Also the sedimentation of the eastside of the gap is described well by the model. However, the infilling of the gap is not described by the model. This could be caused by too high velocities in the gap; the water enters and circulates in the gap. This makes it very hard for the sediment to settle, but observations show a sediment deposition.

### 6.5.3 Conclusion

Based on the above, the effect of the flow slide is especially visible in the area directly next to it. There is sedimentation around the sediment accretion. In the measurements a transport of the complete bulb was found in upstream direction. This transport is not found in the model results. Further in downstream direction there is no effect visible, this is also found in the measurements. In the gap there is no infilling found over the whole surface, only in the eastern part sediment is deposited. This deposition on the east is also found in the measurements.

To determine where the sediment from the flow slide is directed to, two sediment fractions are used in the model. The fractions are called SedimentSand and SedimentPlaat. In this SedimentSand is the original fraction in the model, SedimentPlaat is the sediment from the flow slide. Both the sediment characteristics are supposed to be the same. Figure 6.10 gives the distribution of the sediment from the flow slide over the domain. Large part is deposited at the sides of the original accretion; which was already found in the erosion/sedimentation plot. The suspended sediment is supposed to travel a longer distance and is mainly transported in downstream direction. This sediment is spread over a large area, making it less visible on the erosion/sedimentation plot.

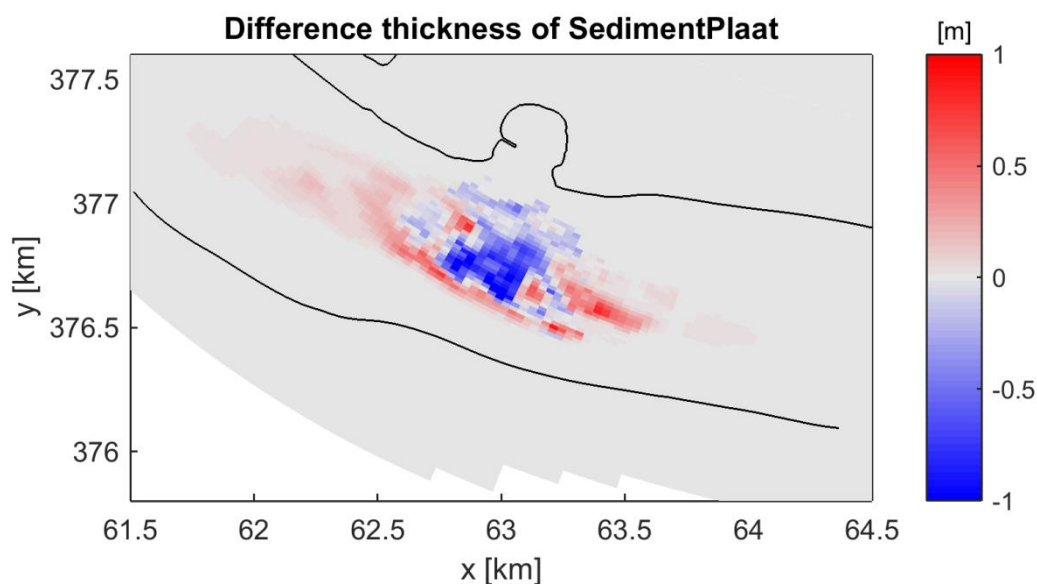


Figure 6.10: Difference thickness SedimentPlaat after half a year, with the line indicating a depth of -6 m NAP

Despite the transport in both directions there is a strong dominant transport direction for the sediment from the flow slide. In Figure 6.11 the total transport is given for SedimentPlaat, the sediment fraction of the original sediment accretion after the flow slide. The arrows show the mean total transport direction and the magnitude. Most of the sediment is transported towards the west, in ebb direction. Only a smaller part is transported towards the east.

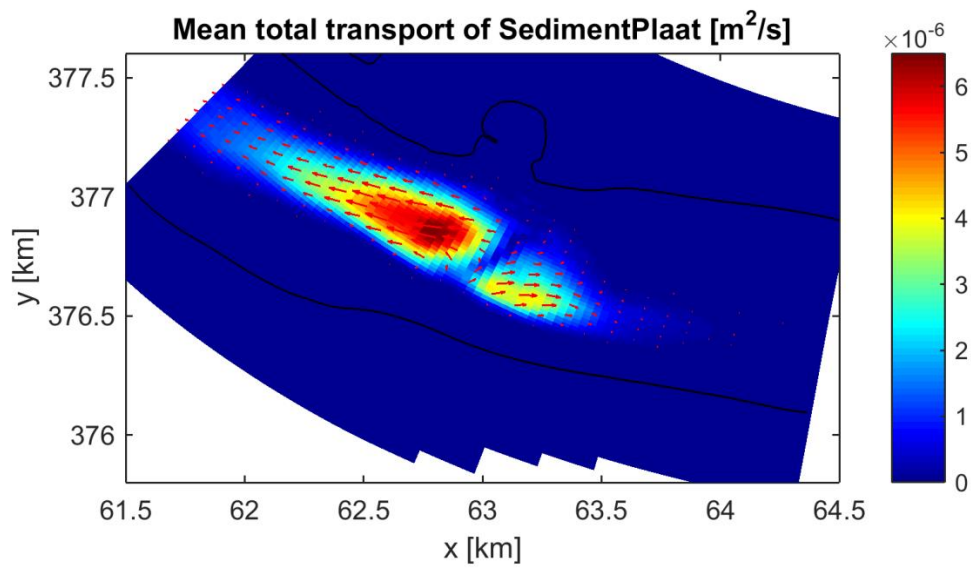


Figure 6.11: Total transport SedimentPlaat; Arrows show the direction, superimposed on the transport magnitude; the contour line corresponds to an initial bathymetry of -6 m NAP

## 7 Sensitivity of the model

The morphological change given by the model did not completely correspond with the observations. The sensitivity of the model is tested based on several characteristics. The effect of the sediment diameter and sediment transport formulation is tested. The effect of a change in the tidal asymmetry, both horizontal and vertical, is examined. The results of the 2DH model are compared with a 3D model to find out what the influence of the secondary circulations is on the sediment transport. Finally, the effect of mud on the morphological change is examined.

### 7.1 Sediment diameter

The measured sediment diameter on the tidal flat is  $140\ \mu\text{m}$  (Mastbergen, 2015). The profile of the grain size distribution shows a steep slope. This suggests minor variation of sediment diameter in the sample. In the bathymetry measurements bed forms are showed (dunes and ripples), which is not usual for sediment with a small diameter (below  $200\ \mu\text{m}$ ). For the sand in the channel no samples are available. It is possible that during or after the flow slide fine sediment is washed away by the current, while the coarser sediment remained at the bed.

#### 7.1.1 Sediment fractions

The effect of the grain size on the morphological change is tested by the model. This is done with the fractions described in section 6.5.3. SedimentSand has a constant diameter of  $200\ \mu\text{m}$ , while the diameter of the SedimentPlaat fraction is variable. The thickness of this layer is determined using the bathymetry difference before and after the flow slide, after which it is placed on top of the SedimentSand layer. The thickness of this layer is given in Figure 7.1. Only where the sediment was deposited in the channel the SedimentPlaat layer is defined, on all the other locations the thickness of this layer is zero.

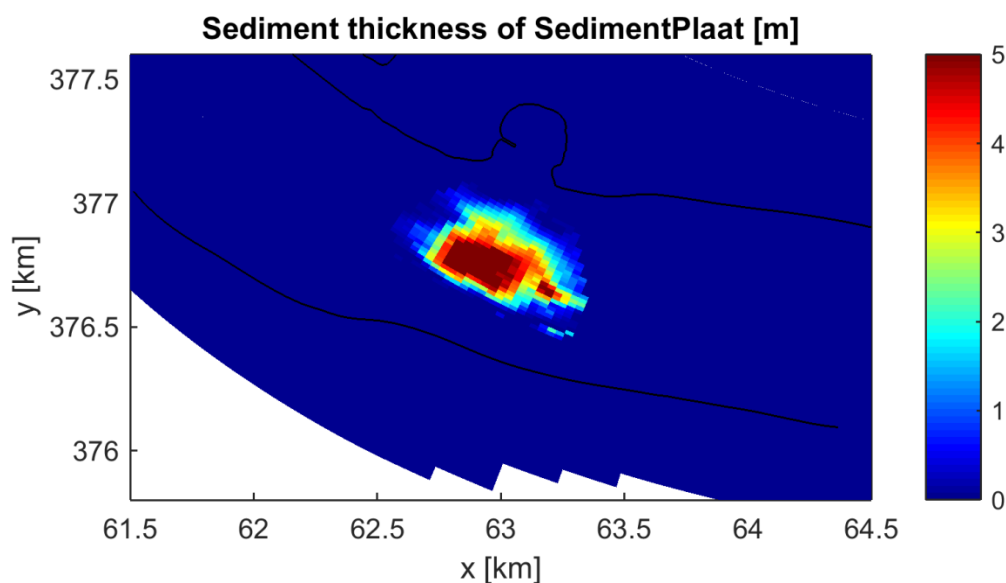


Figure 7.1: Sediment thickness of SedimentPlaat in m

#### 7.1.2 Sediment transport

The used sediment diameters are:  $140\ \mu\text{m}$ ,  $160\ \mu\text{m}$ ,  $180\ \mu\text{m}$ ,  $200\ \mu\text{m}$ ,  $220\ \mu\text{m}$  and  $240\ \mu\text{m}$ . The sediment diameter affects the magnitude of the transport, as can be expected from

equation 4.1. If the sediment diameter is small the sediment will be more easily entrained from the bottom and will be transported further away. To determine the transport rate of the sediment, different transects are determined (Figure 7.2). The transport is given for one spring-neap cycle. A positive transport is flood directed (east), a negative transport is ebb directed (west).

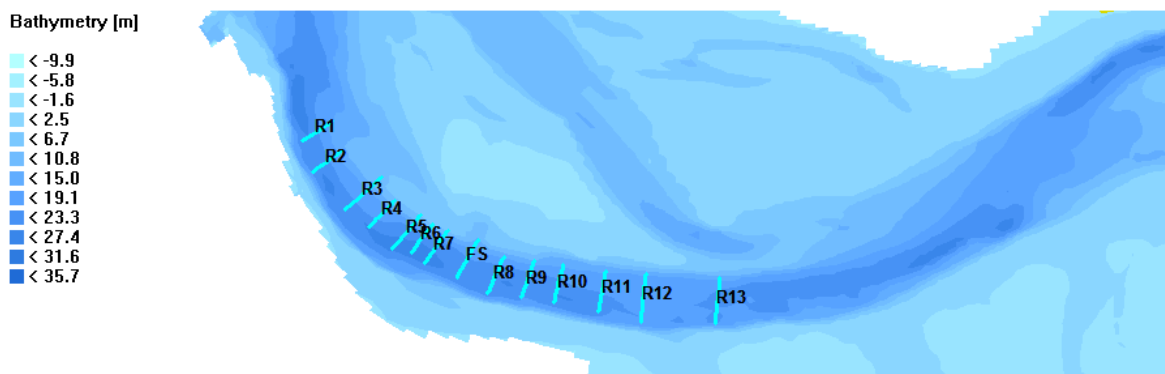


Figure 7.2: Transects for sediment transport

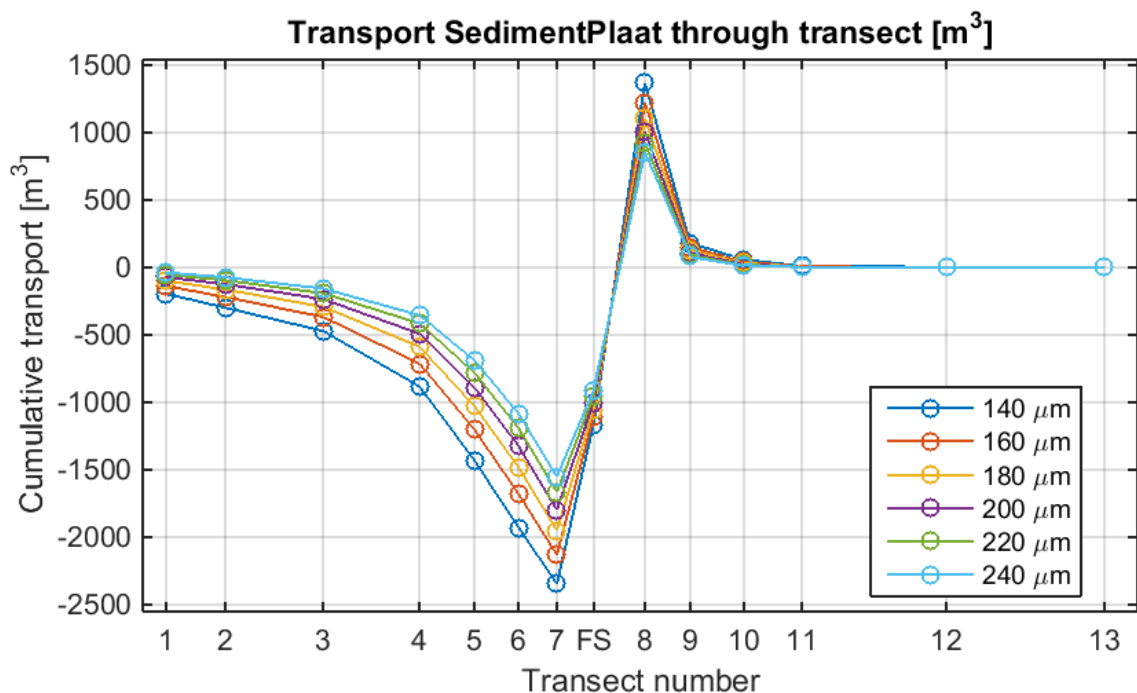


Figure 7.3: Cumulative transport of SedimentPlaat through the transects after half a year

The transport through the transects is given in Figure 7.3. The transport magnitude and distance in upstream direction is much lower than in downstream direction. The residual direction of the sediment transport is in downstream direction, since most of the sediment is transported towards the west.

The sediment diameter has effect on the amount of transported sediment. When the diameter is small the sediment is easily picked up and transported. For the smallest diameter the travelled distance is larger than for a larger diameter. With a large diameter it is harder to pick up the sediment and this is also seen in the figure.

The residual transport direction stays the same with a changing sediment diameter. It could be expected that due to the higher flood velocities the sediment would be transported only in flood direction, if the sediment is really coarse. However, this is not seen with 'realistic' sediment diameters. Even with sediment diameters over 400  $\mu\text{m}$  the residual transport is in ebb direction. If another sediment transport formulation would be used, for example Van Rijn, there is possibly a change in direction.

## 7.2 Sediment transport formula

The used sediment transport formula in the model is Engelund-Hansen (1967). Different transport formula can give different transport rates and transport directions. To test this, the transport found by Engelund-Hansen is compared with Van Rijn (1993), Van Rijn (2004) and Meyer-Peter-Muller (1948). The disadvantage of Van Rijn is the discrepancy of suspended sediment transport through the domain decomposition boundaries, which is described in Appendix C.

The largest difference between these formulations is the transport mode. Engelund-Hansen calculates everything in once as bed load transport. The Van Rijn formulations calculate bed load and suspended load transport as two different modes. This gives a very small bed load transport compared to the suspended load transport. The Meyer-Peter-Muller also calculates is a bed load formula. The magnitude of the sediment transport is to the third power of the velocity for Van Rijn and Meyer-Peter-Muller. This suggests less importance of the peak velocities over the average velocity. Engelund-Hansen uses the fifth power of the velocity, which makes the peak velocities more important.

All the formulations show the same pattern; in Appendix E the sediment transport for Van Rijn (2004) is given. The ratio between bed load and suspended load is 1:10 for Van Rijn (2004). The sediment is transported in both directions, but the majority is transported in ebb direction. There is a small difference in magnitude of the transport between the transport formulations. Since Engelund-Hansen and Meyer-Peter-Muller only calculate the total transport they show a different magnitude. The residual transport direction is the same as for the other formulations. This suggests that the sediment transport formulation does not have a large influence on the direction of the transport.

## 7.3 Tidal asymmetry

For the validation of the NeVla model, the vertical tidal asymmetry is checked against measurements (Vroom et al., 2015). These results show a good correlation of the model with reality. The tidal asymmetry has influence on the dominant direction of the channel.

To determine the tidal asymmetry the amplitude and phase of the  $M_2$  and  $M_4$  tidal components needs to be determined. The ratio between  $\zeta_{M_4}/\zeta_{M_2}$  determines the strength of the tidal asymmetry. The relative phase difference,  $2\varphi_{M_2} - \varphi_{M_4}$ , gives the dominant direction. If the relative phase difference is positive (between  $0^\circ$  and  $180^\circ$ ) there is flood dominance (Wang et al., 1999). A relative phase difference between  $-180^\circ$  and  $0^\circ$  indicates ebb dominance. The asymmetry can be determined for the vertical tide (the water level) and the horizontal tide (the velocities).

### 7.3.1 Vertical asymmetry

For the vertical asymmetry the water level from the stations in the NeVla model are compared with the observed data. This is done for the same period in the model and the measurements. For the Walsoorden station the information of the measurements is neglected, because too much information was missing in the measured dataset. The relative amplitude is in the same

order of magnitude for the data and the model results. For the measurements the relative phases are all positive, which indicates flood dominance. The model shows negative results, indicating ebb dominance.

To examine the effect of the tidal asymmetry the boundary conditions are converted to astronomic constituents. This gives the possibility of changing the boundary conditions to fit the measurements. The phases of the  $M_2$  and  $M_4$  components are changed to give a positive phase difference in the area of interest. However, this gives no change in the transport direction. The sediment from the flow slide is still transported to the west. This is mainly due to the effect of the vertical asymmetry that can influence the horizontal asymmetry, but does not necessarily change the sediment transport.

### 7.3.2 Horizontal asymmetry

For the velocity there are no measurements available in the channels to compare with the model results. Therefore only an analysis is done on the model results. The asymmetry of the horizontal tide is determined in the same way as the vertical tide. All the above mentioned stations indicate ebb dominance based on the relative phase difference ( $2\varphi_{M_2} - \varphi_{M_4}$ ). To determine the effect of the flow slide, observation points were located at the flow slide location (Figure 6.3). This gives an indication of the local dominance in the area of interest. In the middle of the channel (P1) there is ebb dominance, as expected since this is an ebb channel. From the fringes towards the middle of the tidal flat the ebb dominance decreases. According to the model, the transition point between ebb and flood dominance is located at the north of the flow slide (P6).

To test the sensitivity of the model for the horizontal asymmetry the astronomical components  $M_2$  and  $M_4$  are corrected for the phase on the velocity boundary condition. When the horizontal asymmetry in the channel is changed from ebb to flood dominance the residual sediment transport is still in ebb direction. Due to the velocity correction this does not give a realistic situation compared to the MONEOS measurements. Since the transport is still in ebb direction the horizontal asymmetry gives no solution for the difference in transport direction.

## 7.4 3D effect

The secondary circulations are not yet supported for domain decomposition. Therefore the results with domain decomposition and secondary circulations are under consideration. In the 2DH model the secondary forces are not implemented. The secondary circulations, for instance due to the bend or the density effects could have a significant effect on the results, which are neglected in the 2DH model.

To get an idea on the effect of the secondary circulations in the model, a 3D run is executed. This model is run with 10 vertical sigma-layers. The thickness of these layers is, from bottom to top: 2%, 3%, 4%, 6%, 8%, 10%, 12%, 15%, 20% and 20%. From the erosion/sedimentation plot, Figure 7.4, it is found that the sediment in the channel erodes. The sediment is transported in both directions, but most of the sediment is transported to the west, in ebb direction. In the channel a distinction is visible. The sediment on the southern part of the channel is transported towards the east, while the northern part is transported towards the west. The transport directions are given in Figure 7.5. When both graphs are combined it is found that the sedimentation on the east of the flow slide is not from the sediment from the flow slide itself. This sediment has to come from another part of the domain since only a very small part of the flow slide propagates into this area. The flow accelerates on top of the sediment accumulation; consequently the sediment transport capacity is increased. After this the flow decelerates again to the normal velocity, with a lower

transport capacity. This leads to sedimentation just after the flow slide with sediment that was taken into suspension in another part of the domain.

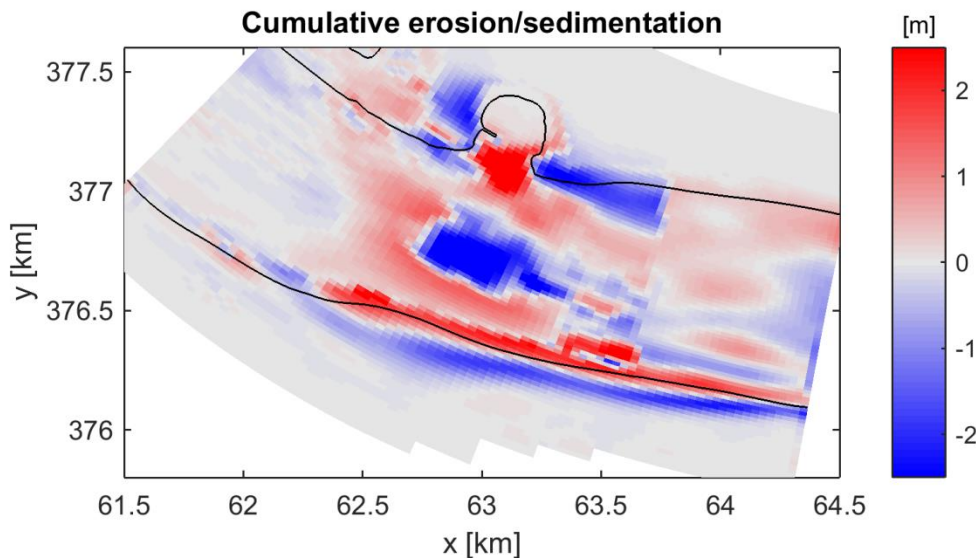


Figure 7.4: Cumulative erosion/sedimentation for the period of half a year in case of 3D model

The sedimentation in the gap shows a similar pattern as the 2DH model. On the eastside of the gap there is sedimentation, caused by the flood directed flow. The tips of the tidal flat along the flow slide show erosion. Inside the gap there is no sign of complete, linear infilling, which is seen in the measurements.

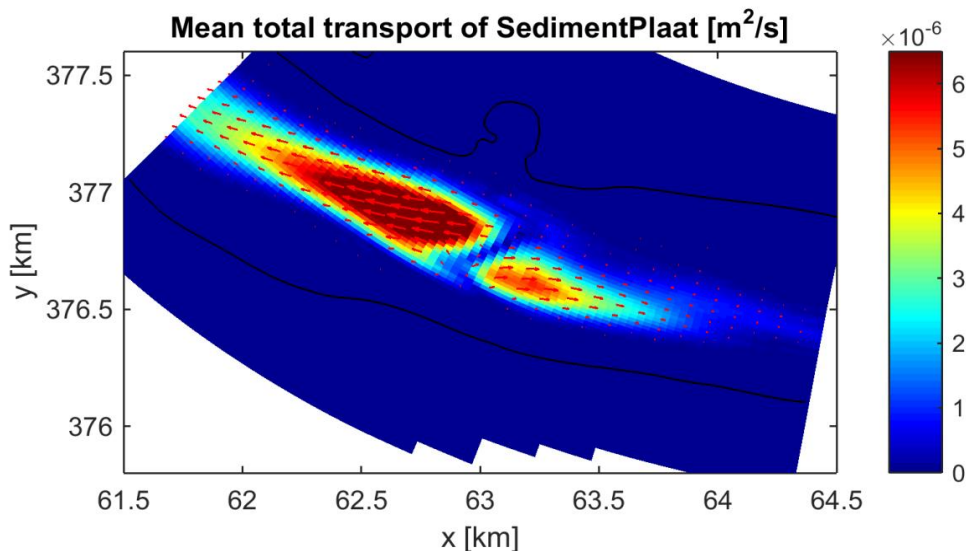


Figure 7.5: Transport direction and magnitude using the 3D approach

In section 3.6.2 the effect of the estuarine circulation is found in the observations. This effect should also be visible in the 3D model. The velocity in the channel is given in Figure 7.6, where the magnitude of the maximum ebb and flood velocity is given. The effect of the estuarine circulation is not visible in this figure. This implies the estuarine circulation is not correctly implemented in the model.

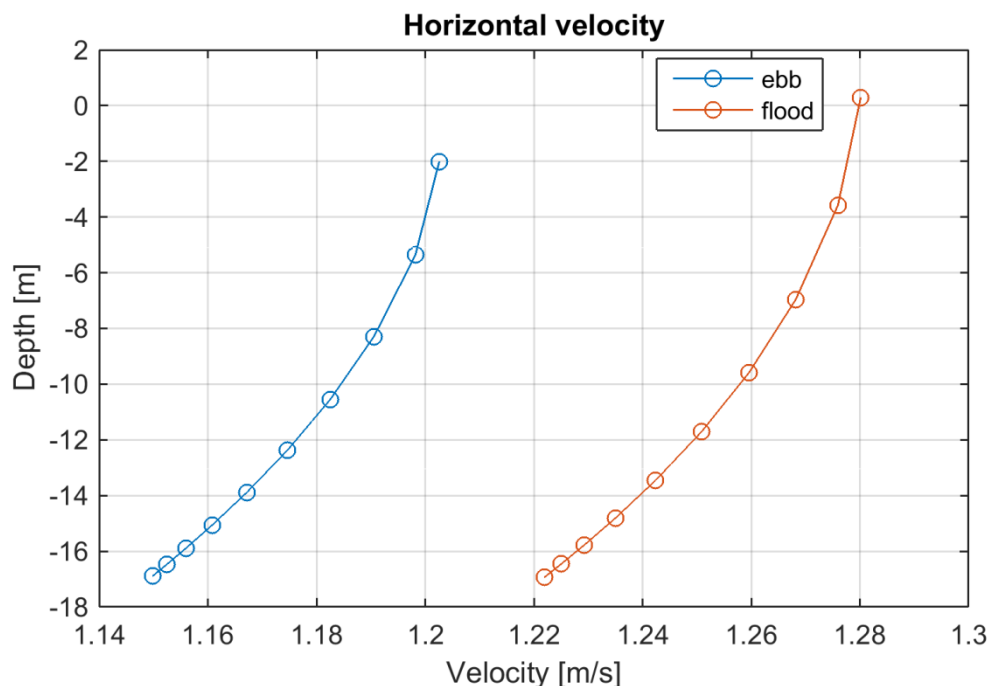


Figure 7.6: Horizontal velocity for point P1 (in the middle of the sediment accretion) over depth

The secondary effect in the 3D model is not significantly different compared to the 2DH model. The erosion/sedimentation pattern is not very different from the pattern found in the depth-averaged model. This suggests the secondary effects are not the main cause of sediment transport. However, to model the exact processes the effect of the estuarine circulation in the model should be investigated further.

## 7.5 Mud

The soil samples from the IJkdijkexperiment in the gap showed the presence of a significant amount of mud. Mud is the combination of the silt and clay fraction with a particle size smaller than  $63 \mu\text{m}$ . In the middle of the gap the percentage of mud is 16.5% after 3 months. On the north side this percentage goes to 43.8% (Mastbergen, 2015). A clearly stratified sequence of mud and fine sand layers is found in the opening in the tidal flat three months after the flow slide. The sediment deposited in the channel is expected to be a mixture of sand and mud.

In the original model only sand fractions are used. To examine the effect of mud on the sediment transport a non-cohesive sediment fraction is implemented in the model. In this model the default values are used. For a more realistic mud fraction the mud percentage of Van Kessel et al. (2006) is used. The thickness of the mud fraction and of the sand fraction in the model is determined. The percentage of the mud content is given in Figure 7.7. Near the banks of the estuary the percentage of mud is the highest, while in the channel the presence of mud is negligible, as expected. Figure 7.8 gives the erosion and sedimentation in the area after approximately half a year. The largest difference compared to the situation, where only sand is modelled is the infilling of the gap. With the inclusion of mud the gap gets filled in, while this was not the case for the situation without mud. The sediment settled in the gap is mostly the cohesive mud fraction. The gap behaves like a small harbour, with calmer conditions to make it possible for the mud to settle.

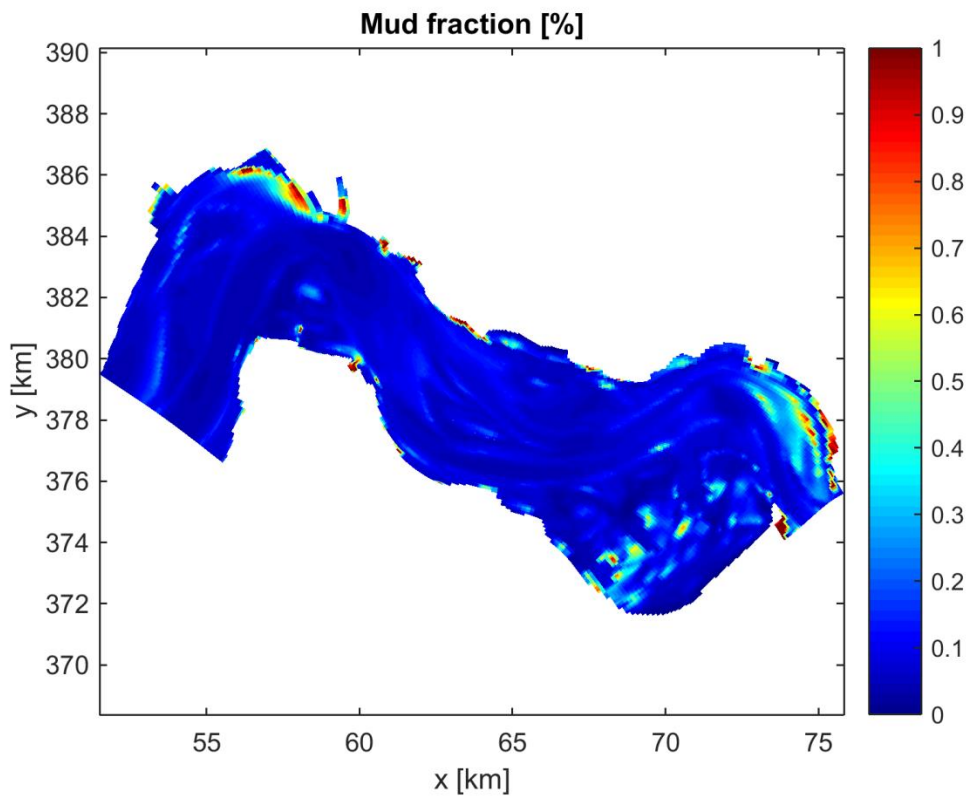


Figure 7.7: Mud percentage used in the model

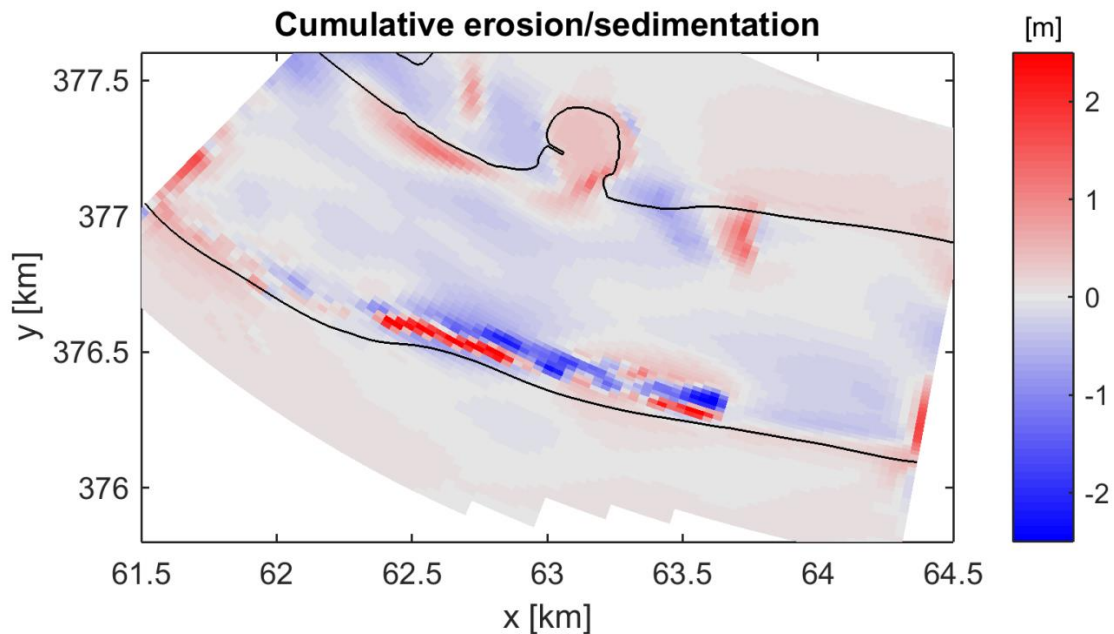


Figure 7.8: Erosion/sedimentation pattern after implementation of a mud fraction over the whole domain

## 7.6 Discussion

The effect of the non-cohesive sediment is a rough estimation. A realistic sediment fraction is used, but the default settings are used for the non-cohesive sediment fraction. These settings are not validated for this specific model. The same is applicable for the 3D simulation. This is

also mostly based on default setting, providing a simple 3D model, suitable for a qualitative analysis. Therefore, only the qualitative result of these effects should be interpreted.

The Engelund-Hansen formulation for sediment transport does not use a critical value. Therefore, it is not unexpected that only the magnitude of the transport changes. If, for example, van Rijn (2004) would be used the effect would be slightly different. However, since this gave small discrepancies at the boundaries this formulation is not chosen.

One of the important processes for sediment transport, the waves, is not implemented in the model. This is possibly a contributing factor to the sediment transport pattern. However, the wave grid for the Western Scheldt first needs to be extended before it can be implemented in the Walsoorden model. Therefore, the effect of the waves cannot be tested in the model yet.

## 7.7 Conclusion

The sensitivity of the model is tested for the sediment diameter, the sediment transport formulation, the secondary effect and the effect of non-cohesive sediment, in order to find an explanation for the discrepancy between the sediment transport and morphological changes in the model and the measurements.

Since Engelund-Hansen is used the sediment diameter only had effect on the magnitude of the transport rate. Sediment with a smaller diameter is transported further throughout the domain than sediment with a large diameter. The direction of this transport is not affected by the sediment diameter.

Different sediment transport formulations are used in the model to examine the effect. All formulations show the same sediment transport pattern. The effect of the formulation on the total sediment transport is very similar for all formulations and did not give a large difference in morphological development.

The tidal asymmetry in the model gave different results compared to the measurements. This was changed using tidal constituents, for the horizontal and vertical tide. These constituents are changed to examine the sensitivity of the model for the tidal asymmetry. However, this gave no change in the transport direction.

The secondary effect on the 2DH model is tested using a 3D model. This model is setup using the Walsoorden model. However, the morphological development did still show a discrepancy with the observations. In the model the effect of the estuarine circulation is hardly found. This could be a possible explanation for the sediment transport pattern difference, but this should be investigated further.

The implementation of non-cohesive sediment fraction gave an effect on the sedimentation in the gap. With only a cohesive sediment fraction there was almost no sedimentation in the gap. After the non-cohesive sediment fraction was implemented the gap became filled in, as was shown in the measurements.

Based on the sensitivity analysis of the model an explanation is found for the infilling of the gap; this is due to the effect of non-cohesive sediment. A clear explanation for the difference in morphological development in the model and the observations is not found. Probably the tidal asymmetry and the estuarine circulation have some influence, but this needs to be investigated further.

## 8 Conclusions and recommendations

### 8.1 Conclusions

The objective of this thesis is to determine, understand and model the fate of the sediment of the July 2014 flow slide on the tidal flat of Walsoorden. During this flow slide approximately 800,000 m<sup>3</sup> flowed from the tidal flat in the navigation channel, leaving a large gap in the tidal flat. In Figure 8.1 the location of the gap and the channel is indicated. From June 2014 the bathymetry is measured monthly, providing a unique dataset, with lots of possibilities for model validation. This data, together with velocity, sediment transport and sediment composition measurements, is analysed to determine the fate of the sediment and the important processes. Afterwards this information is used for the setup and validation of a Delft3D model. The determination, understanding and modelling of the fate of the sediment is based on several research questions, which are answered in the next sections.

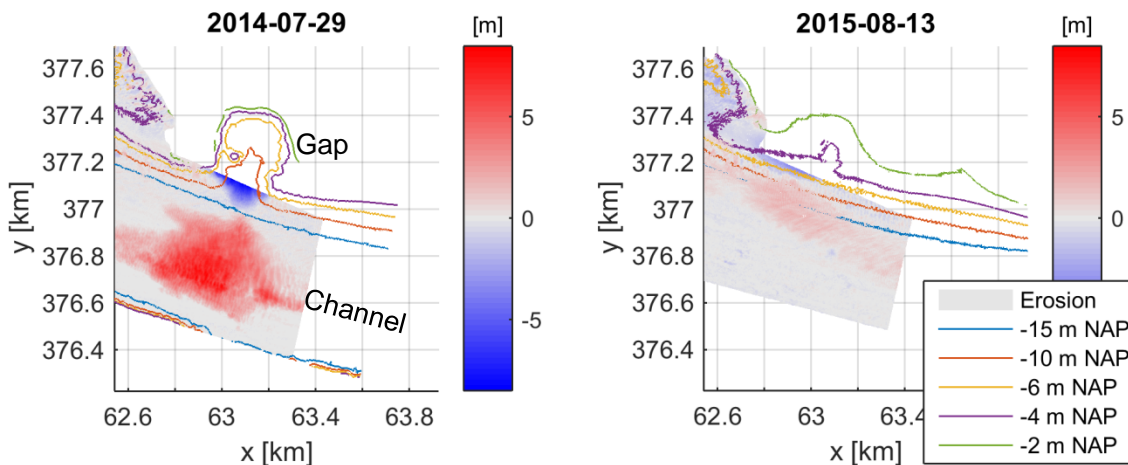


Figure 8.1: The erosion with respect to June 2014, the lines represent the bathymetry of the 29<sup>th</sup> of July 2014 and the 13<sup>th</sup> of August 2015

#### 1 What is the fate of the deposited sediment in the channel and which processes are responsible for this morphological development?

During the flow slide 800,000 m<sup>3</sup> was deposited in the navigation channel. In the left panel of Figure 8.1 the deposited sediment is given in red. The sediment is transported both as bed load and suspended load. The sediment on the channel bed after the flow slide is transported eastwards, as bed load. The volume of the deposited sediment reduces in time, with approximately 25% per month. This follows an exponential behaviour with a recovery time of about 9 months. The reduction in time of the deposited sediment volume suggests the sediment has gone partly into suspension; the direction of this transport is not measured. It is reasonable to assume that this sediment accumulates on the sills, which accrete naturally. However, there was no significant increase of sediment observed on the sills near the tidal flat during the maintenance dredging of November 2014. In the right panel of Figure 8.1 it is observed that the bed returned to the exact same bathymetry in the middle of the channel. This indicates the presence of an immobile bed layer in the channel. In the meantime gradual sedimentation on the northern part of the channel is observed (right panel).

The tidal force is the most important component for the sediment transport in the Western Scheldt. However, the net transport due to the tidal force in the Zuidergat channel is expected

to be in ebb direction, since the discharge is ebb dominant. The bathymetry measurements indicate bed load transport in flood direction, so there must be another force of importance for the sediment transport in the channel.

The estuarine circulation gives an increase in velocity near the bed during flood and a decrease during ebb. This gives more net bed load transport in flood direction. In the channel there is an asymmetry of the horizontal tide. The maximum velocity for flood is higher than the maximum velocity for ebb. The sediment transport measurement showed a critical velocity for sand transport of approximately 0.6 m/s, which is rather high compared to the critical velocity based on Shields. During flood this velocity is exceeded, while during ebb this is not always the case. Altogether this leads to a net sand transport near the bed in flood direction.

Directly after the flow slide the top is dredged, because it exceeded the navigation depth. This was the only dredging operation of the deposited sediment and it concerned only a minor part of the volume. The bathymetry measurements and the model show clearly that the tidal force is large enough to erode the sediment accretion and the channel naturally returned to its original state within a year.

## **2 How does the gap in the tidal flat develop after the flow slide and which processes drive this development?**

During the flow slide a gap with a diameter of 300 m developed in the tidal flat. This gap is indicated by the bathymetry lines in the left panel of Figure 8.1. An exponential behaviour is showed for the infilling of the gap. The recovery time is found using extrapolation and is approximately 1.5 to 2 years. After one year the gap is for a large part filled in already, as can be observed by the bathymetry lines in the right panel of Figure 8.1.

The infilling occurs mainly due to the tidal force. This can be observed by the pattern of infilling, on the eastern side the most sedimentation occurs. The gap is partially (~20 - 40%) filled up with mud, indicating calm conditions in the gap. In the model the implementation of mud was essential for the infilling of the gap. Without mud there was no sedimentation in the gap. The sediment found in the gap has a smaller diameter than the sediment in the channel. This also indicates calm conditions in the gap. From the measurements it can be concluded that the gap in the tidal flat is restored naturally, without the need of human interferences.

## **3 How can we model the morphological evolution and the underlying processes?**

With Delft3D a model is setup to simulate the behaviour of the sediment after the flow slide. The Walsoorden model, used in this study, is based on the Delft3D-NeVla model. The grid is partially used; local refinement with domain decomposition is applied. With this smaller resolution the bathymetry of the measurements is better implemented in the model. The sediment transport is calculated with the Engelund-Hansen equation, since the Van Rijn equation gave some discrepancies with the domain decomposition.

The hydrodynamic results of the model are sufficient compared to water level, discharge and velocity measurements around the tidal flat. The morphological development after the flow slide shows a different pattern than observed in the measurements. In the measurements a transport of the sediment is showed in eastern direction, while in the model the sediment is transported in western direction. The infilling of the gap in the tidal flat is not given in the model. The difference was tried to explain by the sediment diameter, the tidal asymmetry, the 3D effect and the implementation of mud. The implementation of mud resulted in the infilling of the gap. The variation in sediment diameter, tidal asymmetry and the 3D effect did not result in a significant reduction of the difference between the measurements and the model.

## 8.2 Recommendations

The measurements show a natural and relatively quick recovery of the system. In the channel the sediment from the flow slide is almost completely eroded after one year. The gap in the tidal flat is for a large part filled in again. This shows the capacity of the system to recover itself naturally after such a large event. For navigation purposes the depth needs to be guaranteed and some incidental dredging needed to be executed. No signs of enhancement of the disturbance due to the flow slide were found, the gap in the tidal flat is not enlarged and there has been no deposition on the deposited sediment in the navigation channel. It is recommended to dredge the top of the sediment accumulation to guarantee the navigation depth. The recovery of the system is a natural process, but needs to be monitored.

Sediment transport measurements are scarce in the Western Scheldt. The last time sediment transport was measured close to the tidal flat of Walsoorden was in 2005. This data gives a good approximation of the sediment transport; nevertheless, this data only covers one tidal cycle. Since these measurements are scarce, it is hard to get a complete overview of the sediment transport in the Western Scheldt. A transport measurement directly after the flow slide would have been very useful to determine the transport direction and magnitude. In this measurement also the difference between suspended and bed load transport should be measured.

From the sensitivity analysis it was found that mud is important for the infilling of the gap. This is supported by the sediment measurements performed by Stichting FloodControl IJkdijk (2014). In the model used in this research this is only examined using a rough assumption. To get a better understanding of the influence of mud a new model has to be made, making use of the interaction between mud and sand. This would lead to a more realistic infilling of the gap. These model results should be compared with observations in the gap. When the gap is completely filled up it is recommended to perform new sediment composition measurements. If these measurements are compared with the observations in October 2014 the sedimentation process in the gap can be studied in more detail.

In the sensitivity analysis a rough estimation is made using a 3D model. In this model the estuarine circulation was not represented very well. Therefore, further research should be done on the effect of the secondary circulations and the response of the (suspended) sediment on it. This can be done by adding more layers and by using 3D boundary conditions instead of a logarithmic assumption.

To overcome the uncertainties of the nesting and domain decomposition in the future the software D-Flow FM could be used. With this new modelling program the domain can be locally refined without using different domains. This provides the possibility of using the Van Rijn formulation for sediment transport, where the distinction between suspended and bed load transport can be made.

## 9 References

- Aantjes, H. (2014). *Memo, Beoordeling sedimentbezwaar vaargeul Westerschelde nav zettingsvloeiingsproef Plaat van Walsoorden*. Delft: Deltares
- Arcadis (2013a). *Ontwikkeling mesoschaal Westerschelde (factsheets)*.
- Arcadis (2013b). *LTV Veiligheid en Toegankelijkheid, Simulaties V&T met effectanalyse op mesoschaal*.
- Arcadis (2014). *Ecotopen in de Westerschelde – LTV Veiligheid en Toegankelijkheid*.
- Arends, A.A., van Maldegem, D.C. (1999). *Grootschalige effecten Westerschelde dor havenuitbreiding Vlissingen*. Middelburg: Rijkswaterstaat.
- Baeyens, W., van Eck, B., Lamber, C., Wollast, R., Goeyens, L. (1998). General description of the Scheldt estuary. *Hydrobiologia*, 366.
- Beinssen, K., Neil, D.T., Mastbergen, D.R. (2014). *Field observations of retrogressive breach failures at two tidal inlets in Queensland, Australia*. Australian Geomechanics.
- Van den Berg, J.H., Jeuken, C.J.L, Van der Spek, A.J.F. (1996). Hydraulic processes affecting the morphology and evolution of the Westerschelde estuary. *Estuarine Shores: Evolution, environments and human alternations*. John Wiley & Sons.
- Besio, G., Blondeaux, P., Brocchini, M., Vittori, G. (2004). On the 65odelling of sand wave migration. *J. Geophys. Res.*, 109, C04018.
- Bolle, A., Wang, Z.B., Amos, C., de Ronde, J. (2010). The influence of changes in tidal asymmetry on residual sediment transport in the Western Scheldt. *Continental Shelf Research*, 30, pp 871-882.
- Bosboom, J., Stive M.J.F., (2015). *Coastal Dynamics 1, Lecture notes CIE4305*. Delft: Delft Academic Press.
- Cleveringa, J. (2013). *Grootschalige sedimentbalans van de Westerschelde*. Consortium Deltares, IMDC, Svašek, Arcadis, report G2.
- Dam, G. (2013). *Harde lagen Westerschelde*. Consortium Deltares, IMDC, Svašek, Arcadis, report A28.
- Dam, G., Poortman, S., Bliet, A., Plancke, Y. (2013). *Long-term modelling of the impact of dredging strategies on morpho- an hydrodynamic developments in the Western Scheldt*. Brussel: World Organisation of Dredging Associations.
- De Groot, M.B., Stoutjesdijk, T, Meijers, P., Schweckendiek, T. (2007). Verwekingsvloeiing in zand. *Geotechniek*, oktober 2007, pp 54-59.

De Groot, M.B., van der Ruyt, M.B., Mastbergen, D.R., van den Ham, G.A. (2009). Bresvloeiing in zand. *Geotechniek*, 32, juli 2009, pp 32-37.

De Kramer, J. (2002). *Waterbeweging in de Westerschelde, een literatuurstudie*. Utrecht: Universiteit Utrecht.

Delft Cluster (2009). *Oeverstabiliteit bij verdieping waterbodem, rekenmodel HMBreach*.

Deltares (2014). *Delft3D-FLOW, User Manual*. Delft: Deltares.

Departement Mobiliteit en Openbare Werken (n.d.). *Uitvoering 3<sup>de</sup> Scheldeverdieping | Maritieme toegang*. <http://www.maritiemetoegang.be/uitvoering-3de-scheldeverdieping> Retrieved 17 September 2015.

Ebbens, E.H. (1980). *Aanzanding van de bij de plaatval van 1977 ontstane verdieping in de Platen van Ossensisse*. Vlissingen: Rijkswaterstaat.

Flemish government, department Mobiliteit en Openbare Werken (2015). *Maandelijkse bodemmetingen*.

Van den Ham, G.A., Mastbergen, D.R., Koelewijn, A.R., ter Brake, C.K.E., Zomer, W.S. (2015). *Eindrapport validatie experiment zettingsvloeiing, Meten aan zettingsvloeiing*. Amersfoort: STOWA/FloodControl Ijkdijk.

Van den Ham, G.A., de Groot, M.B., Mastbergen, D.R. (2013). A Semi-Empirical Method to Assess Flow Slide Probability. *Submarine Mass Movements and Their Consequences*, 6<sup>th</sup> Int. Symp., Kiel, p. 213-223, Springer.

Hibma, A., de Vriend, H.J., Stive, M.J.F. (2003). Numerical modelling of shoal pattern formation in well-mixed elongated estuaries. *Estuarine, coastal and shelf science*, 57, pp. 981-991.

Hoekstra, P., Bell, P., van Santen, P., Roode, N., Levoy, F., Whitehouse, R. (2004). Bed form migration and bed load transport on an intertidal shoal. *Continental Shelf Research*, 24, pp. 1249-1269.

IMDC (2014a). *Monitoringsprogramma flexibel storten; Deelopdracht 7: Maandrapport plaastrandstoringen augustus-september 2014*. Antwerpen: Vlaamse overheid, mobiliteit en openbare werken.

IMDC (2014b). *Monitoringsprogramma flexibel storten, Deelopdracht 5: Analyse van de storingen in de diepe delen van de hoofdgeul, fase 3 (najaar 2012-najaar 2013)*.

IMDC (2014c). *Monitoringsprogramma flexibel storten; Deelopdracht 7: Maandrapport plaastrandstoringen december 2014-januari 2015*. Antwerpen: Vlaamse overheid, mobiliteit en openbare werken.

Jeuken, C.J.L., Wang, Z.B. (2000). *Tidal asymmetry and sediment transport in the Westerschelde estuary*. Delft: WL| Delft Hydraulics.

- Kater, B.J. (2005). *Ontwikkelingen in de kennis van de morfodynamica en ecologie van de Westerschelde*. Middelburg: Rijkswaterstaat RIKZ.
- Van Kessel, T., Vanlede, J., Bruens, A. (2006). *Development of a mud transport model for the Scheldt estuary in the framework of LTV*. Report Z4210. WL|Delft Hydraulics.
- Kleinbans, M. G.(2013). *Tuning the tide, dynamics of channels and shoals in estuaries with sands and mud*. RU Utrecht.
- Kranenburg, C. (1996). *Dichtheidsstromen*. Handleiding college b81. Delft: Technische Universiteit Delft.
- Kuijper, K., van der Kaaij, T., de Goede, E. (2006). *LTV O&M actieplan voor morfologisch onderzoek modelinstrumentarium*. Delft: WL| Delft Hydraulics.
- Ligtenberg-Mak, C.E., Krajicek, P.V.F.S, Kuitert, C. (1990). Geological study of flow slide sensitive sediments. *6<sup>th</sup> Int. IAEG Congress*. Rotterdam: Balkema.
- LTV (2001). *Toelichting bij de Langetermijnvisie Schelde-estuarium*. Delft: Projectbureau LTV p.a.
- McLaren (1994). *Sediment Transport in the Western Scheldt between Baarland and Rupelmonde*. GeoSea report, GeoSea Consulting, Cambridge.
- Mastbergen, D.R., Van den Berg, J.H. (2003). Breaching in fine sands and the generation of sustained turbidity currents in submarine canyons. *Sedimentology* 50 (4) pp. 625-637.
- Mastbergen, D.R., Van den Ham, G.A., de Groot, M.B., van der Kaaij, T., Peelen, G.P. (2014) *Retrograding breach flow slides in the Netherlands, observations and numerical modeling*, presentation 19<sup>th</sup> International Sedimentology Congress, Geneva
- Mastbergen, D.R., Van den Ham, G., Cartigny, M., Koelewijn, A., de Kleine, M., Clare, M., Vellinga, A. (2015). Multiple flow slide experiment in the Westerschelde Estuary, the Netherlands. *Submarine Mass Movements and Their Consequences, 7<sup>th</sup> Int. Symp.*, Wellington: Springer.
- Mastbergen, D.R. (2015). *Memo, Korrelverdelingen bodem Westerschelde bij Plaat van Walsoorden*. Delft: Deltares.
- Meire, P., Maris, T. (2008). *MONEOS, Geïntegreerde monitoring van het Schelde-estuarium*. Antwerpen: Universiteit Antwerpen.
- Mol, G. (1995). *De Westerschelde, een resultaat van menselijke ingrepen*. Middelburg: Rijkswaterstaat RIKZ.
- Paridaens, K., Plancke, Y., Schrijver, M., Willems, P. (2001). *Comparison of measurement techniques for monitoring sediment transport, under field conditions, in the Scheldt estuary*. Port of Antwerp Expert Team (2003). *The feasibility of morphological dredging as a tool for managing the Westerschelde*.

Portella, L.I., Neves, R. (1994). Numerical modelling of suspended sediment transport in tidal estuaries, A comparison between the Tagus (Portugal) and the Scheldt (Belgium – the Netherlands). *Netherlands journal of aquatic ecology*, 28, pp 329-3335.

Rijkswaterstaat (2006). *Presentatie Meetresultaten; Debiet- sediment- OSM-meting*. ZLMD-05.N.016.

Rijkswaterstaat (2012). *Handreiking toetsen voorland zettingsvloeiing t.b.v. het opstellen van het beheerdersoordeel (BO) in de verlengde derde toetsronde*.

Rijkswaterstaat (2014). *Memo: Plaatval dd '22 juli 2014' plaat van Walsoorden/Valkenisse*. Middelburg.

Rijkswaterstaat (2015). Opgetreden data. *Vaklodingen, Waternormalen, Waterstanden, Stroming, Windsnelheid, Bodemmetingen, Debietmetingen*. Hydro Meteo Centrum Zeeland, Rijkswaterstaat Zee en Kust.

Van Rijn, L.C. (1984). *Sediment transport, part 1 and 2: bed load and suspended load transport*.

Van Rijn, L.C. (2011). Analytical and numerical analysis of tides and salinities in estuaries, part 1: Tidal wave propagation in convergent estuaries. *Ocean Dynamics*, 61, pp 1717-1741.

Van Rijn, L.C. (2013). *Basic hydrodynamic processes in the coastal zone*.

Savenije, H.H.G. (2012). *Salinity and tides in alluvial estuaries*. Delft: Delft University of Technology.

Schroevers, M. (2013). *Stroming in de Westerschelde, Inventarisatie van de informatiebehoefte en informatievoorziening*. Delft: Deltares.

Stichting FloodControl IJkdijk (2014). *Bodemmetingen tijdens experiment*.

Stichting FloodControl IJkdijk (2014). *Field trial for flow slide in Westerschelde*. <http://www.ijkdijk.nl/en/news/163-press-release-field-trial-for-subsidence-flow-in-westerschelde> . Retrieved March 3, 2015

Svašek Hydraulics (2013). *Actualisatie van het FINEL2D model van de Westerschelde*.

Taal, M., Wang, Z.B., Cleveringa, J. (2013). *LTV Veiligheid en toegankelijkheid, G-13: Synthese en conceptueel model, Basisrapport grootschalige ontwikkeling*. Delft: Deltares.

Tank, F.T.G. (1996). *Het gedrag van drempels in de Westerschelde*. Middelburg: Rijkswaterstaat.

Technische Scheldec commissie (1984). *Verdieping Westerschelde Programma 48/43*. Antwerpen, Middelburg.

Thoolen, P.M.C., Wang, Z.B. (1999). *Sedimenttransport modellering Westerschelde*. Delft: WL| Delft Hydraulics.

- US Army Corps of Engineers (1988). *Retrogressive failures in sand deposits of the Mississippi river*. Mississippi.
- Vandenbruwaene, W., Vos, G., Plancke, Y., Mostaert, F. (2012). Werkgroep O&M – Projectgroep Veiligheid en Toegankelijkheid. *Onderzoek naar de morfologie op meso-schaal ter hoogte van stortlocaties*. Versie 3.0. Antwerpen: Waterbouwkundig Laboratorium.
- Vroom, J., de Vet, P.L.M., van der Werf, J.J. (2015). *Validatie waterbeweging Delft3D-NeVla model Westerscheldemonding, Stand van zaken juni 2015*. Delft: Deltares.
- Wang, Z.B., Jeuken, C.J.L., de Vriend, H.J. (1999). *Tidal asymmetry and residual sediment transport in estuaries*. Delft: WL| Delft Hydraulics.
- Waterbouwkundig Laboratorium (2007). *Morfologische analyse van de bagger en stortintensiteitsdata van de beneden Zee- en Westerschelde van 2000 tot en met 2005*.
- Van der Werf, J.J., Briere, C.D.E. (2013). *The influence of morphology on tidal dynamics and sand transport in the Scheldt estuary*. Delft: Deltares.
- Wiertsema & Partners (2014). *Geotechnisch laboratoriumonderzoek validatie-experiment zettingsvloeiing, Vibrocores*.
- Wilderom, M.H. (1972). Plaatvallen. *OTAR*, 288-305.
- Wilderom, M.H. (1973). *Tussen afsluitdammen en deltadijken, Zeeuwsch Vlaanderen*.
- Wilderom, M.H. (1979). *Resultaten van het vooroveronderzoek langs de Zeeuwse stromen*. Vlissingen: Rijkswaterstaat.



## A Bathymetry measurements

The measurements around the tidal flat of Walsoorden are carried out by different companies. In Table A.1 the date of the measurement and the company are displayed. Also the filename of the data is given, because the filenames of Rijkswaterstaat suggest a different date than the actual date. This is caused by the data saving system of Rijkswaterstaat. In the metadata supplied by the measurements the real date was found.

Table A.1: Bathymetry measurements

Date	Company	Filename
12-06-2014	Flemish government	20140612_PWA_B_MB_300_RD
08-07-2014	Flemish government	20140708_PWA_B_MB_300_RD
09-07-2014	Rijkswaterstaat	Multibeamlodingen-Westerschelde_Plaat_van_Walsoorden-2014-7-11.txt
29-07-2014	Flemish government	20140729_PWA_B_MB_300_RD
21-08-2014	Rijkswaterstaat	Multibeamlodingen-Westerschelde_Plaat_van_Walsoorden-2014-8-12.txt
22-08-2014	Flemish government	20140822_PWA_B_MB_300_RD
22-09-2014	Stichting Floodcontrol IJkdijk	INSURVEY_RD_20140922.txt
23-09-2014	Rijkswaterstaat	Multibeamlodingen-Westerschelde_Plaat_van_Walsoorden-2014-9-13.txt
24-09-2014	Flemish government	20140924_PWA_B_MB_300_RD
02-10-2014	Stichting Floodcontrol IJkdijk	OUTSURVEY_RD_20141002.txt
21-10-2014	Rijkswaterstaat	Multibeamlodingen-Westerschelde_Plaat_van_Walsoorden-2014-10-14.txt
22-10-2014	Flemish government	20141022_PWA_B_MB_300_RD
21-11-2014	Flemish government	20141121_PWA_Z_MB_300_RD
17-12-2014	Flemish government	20141217_PWA_B_MB_300_RD
16-01-2015	Rijkswaterstaat	Multibeamlodingen-Westerschelde_Plaat_van_Walsoorden-2015-1-06.txt
22-02-2015	Rijkswaterstaat	Multibeamlodingen-Westerschelde_Plaat_van_Walsoorden-2015-2-07.txt
24-02-2015	Flemish government	20150224_PWA_B_MB_300_RD
18-03-2015	Flemish government	20150318_PWA_B_MB_300_RD
20-03-2015	Rijkswaterstaat	Multibeamlodingen-Westerschelde_Plaat_van_Walsoorden-2015-3-10.txt
17-04-2015	Rijkswaterstaat	Multibeamlodingen-Westerschelde_Plaat_van_Walsoorden-2015-4-11.txt
17-04-2015	Flemish government	20150417_PWA_Z_MB_300.txt
29-05-2015	Flemish government	20155029_PWA_B_MB_300.txt
15-06-2015	Rijkswaterstaat	Multibeamlodingen-Westerschelde_Plaat_van_Walsoorden-2015-6-15.pts
13-08-2015	Rijkswaterstaat	Multibeamlodingen-Westerschelde_Plaat_van_Walsoorden-2015-8-13.pts

## A.1 Bathymetry

In Figure A.1 till Figure A.3 the bathymetry is given that was obtained in the measurements. The depth is given with respect to NAP. A positive depth is above NAP, while a negative depth is below NAP. The used coordinate system is RD. In the first three measurements the flow slide did not occur yet. The fourth measurement is taken just after the flow slide, but the gap in the tidal flat was not measured. From the fifth measurement (21-08-2014) on the gap is also measured. This gives a complete image of the changes in bathymetry after the flow slide and the recovery of the system.

It can be observed that the deposited sediment in the channel is transported towards the east, so in flood direction. This transport goes quite fast, the channel is almost recovered of the sand deposition in January. The gap is also filled up, but the change in time is smaller than in the channel.

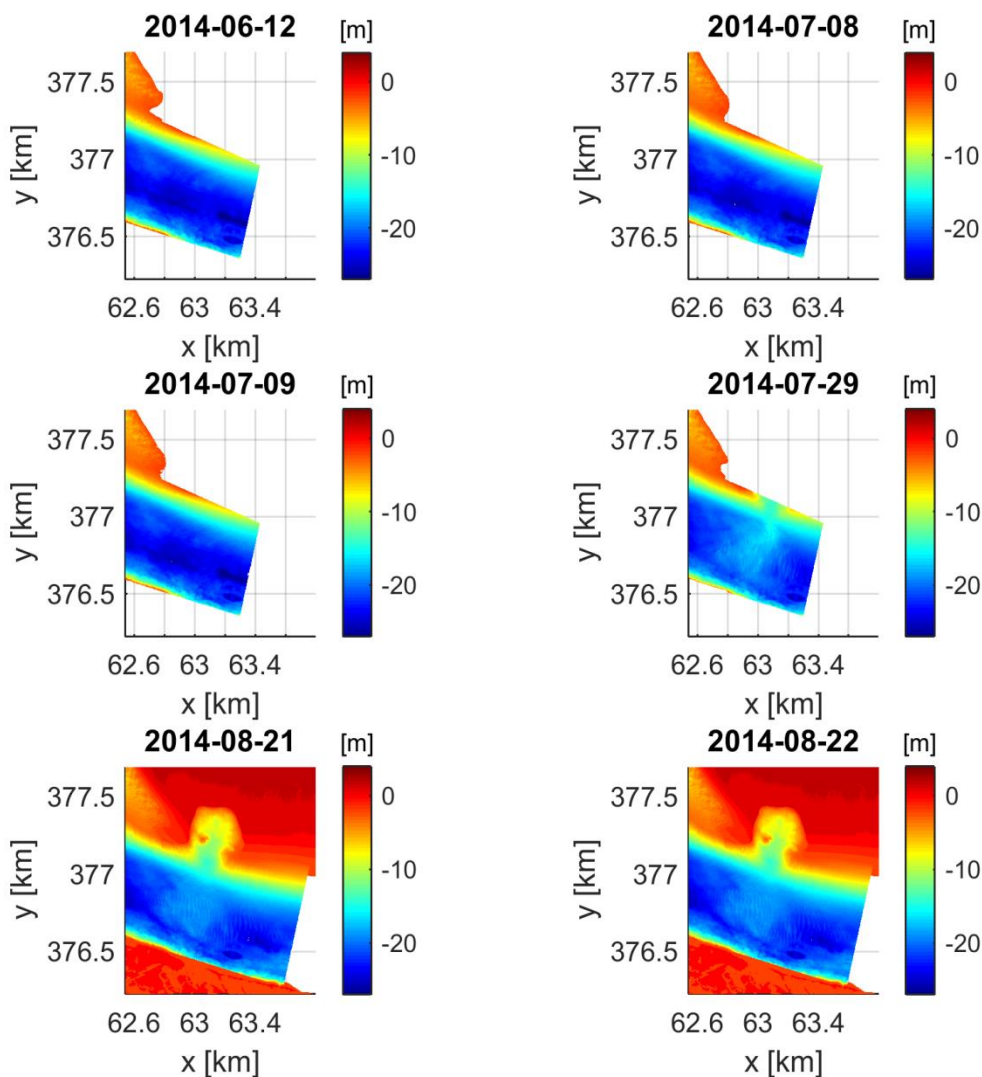


Figure A.1: Bathymetry June 2014 till August 2014

The smaller gap on the east of the flow slide is the initiated flow slide by the Ikdijkexperiment in October 2014. The amount of sediment that flowed down the tidal flat was significantly smaller than during the July 2014 flow slide. The recovery time of the gap of this flow slide is approximately three to four months, based on the bathymetry measurements.

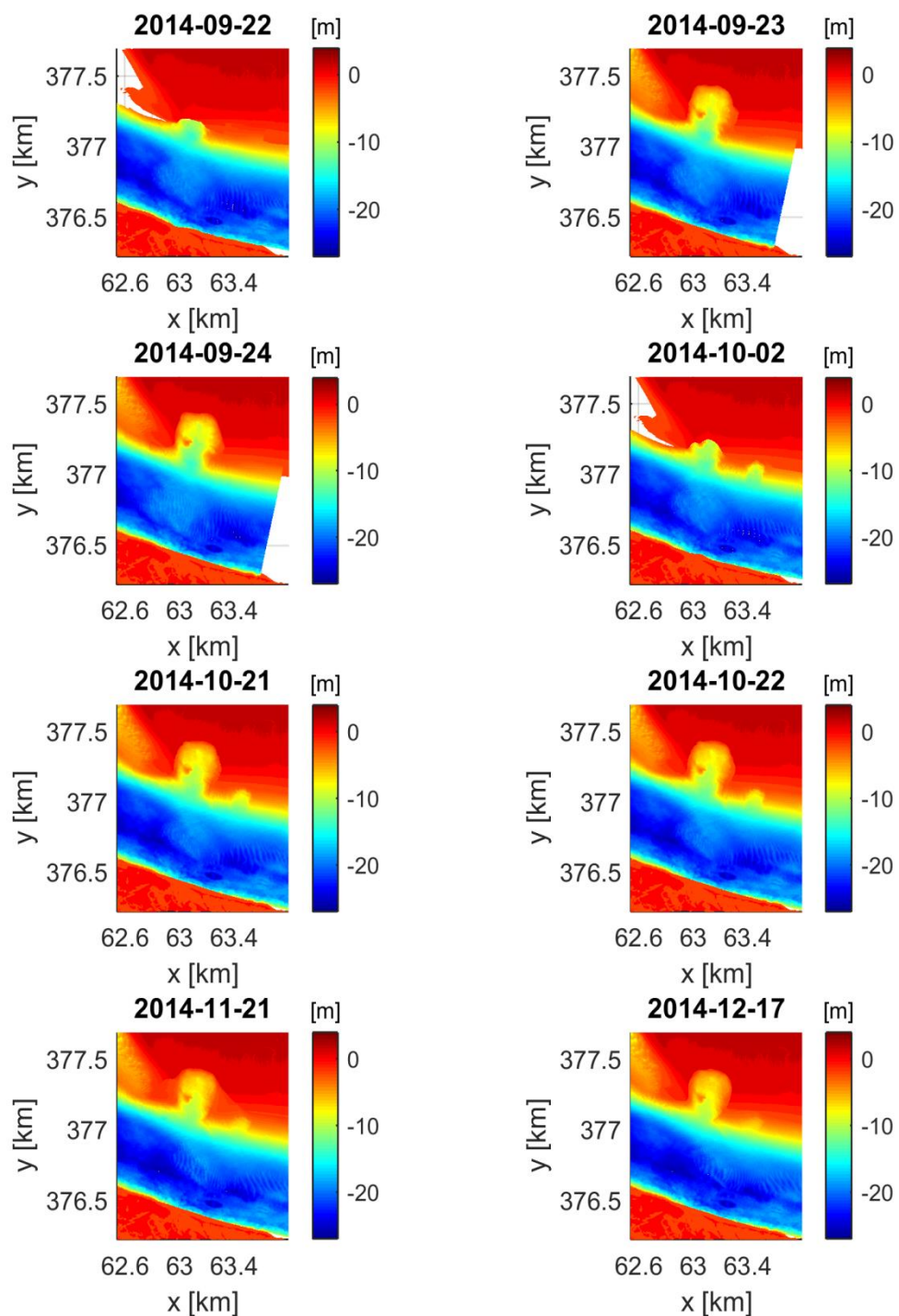


Figure A.2: Bathymetry September 2014 till December 2014

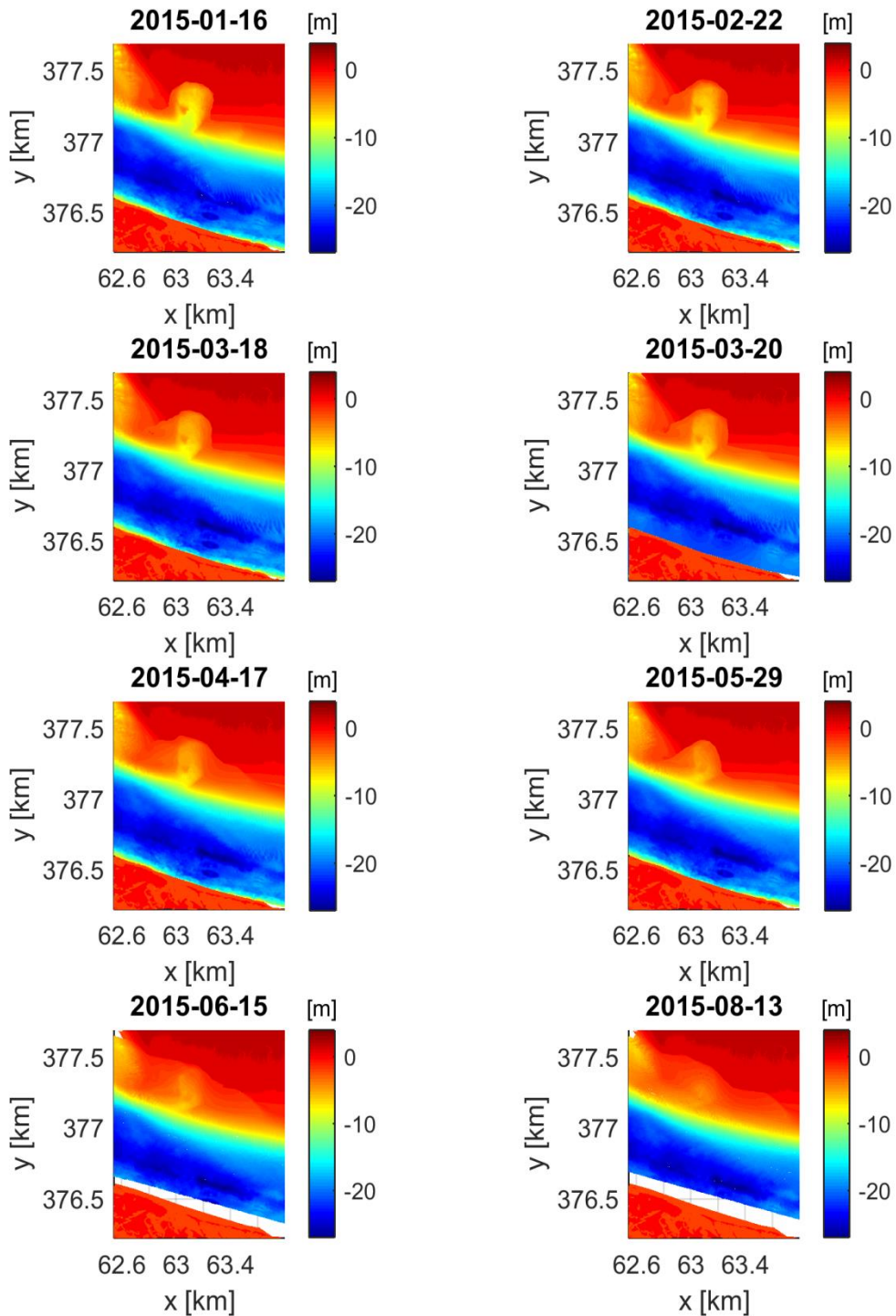


Figure A.3: Bathymetry January 2015 till August 2015

## A.2 Erosion

The erosion is obtained using the difference between the bathymetry measurements. First the difference with respect to June 2014 is shown, indicating the differences with the original situation. After this, in section A.2.2, the difference with August 2014 is shown. From both graphs the travel direction of the sediment is clearly shown, it is directed to the east. The figures showing the differences with August 2014 also show the filling in of the gap. The gap is mainly filled on the east side, suggesting flood dominated flow. In section A.2.3 the monthly erosion is given.

### A.2.1 With respect to June

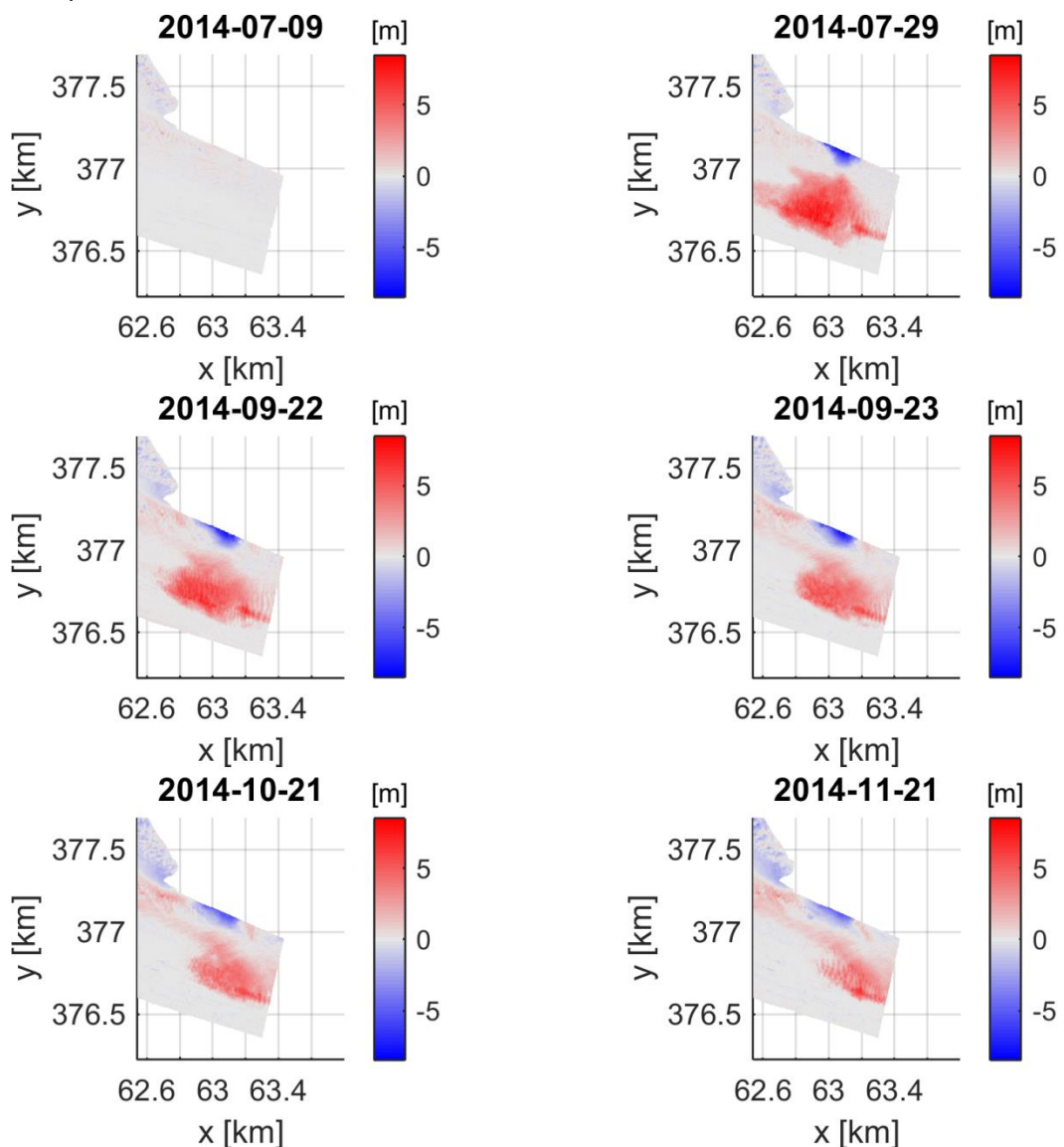


Figure A.4: Erosion with respect to June 2014 for July 2014 till November 2014

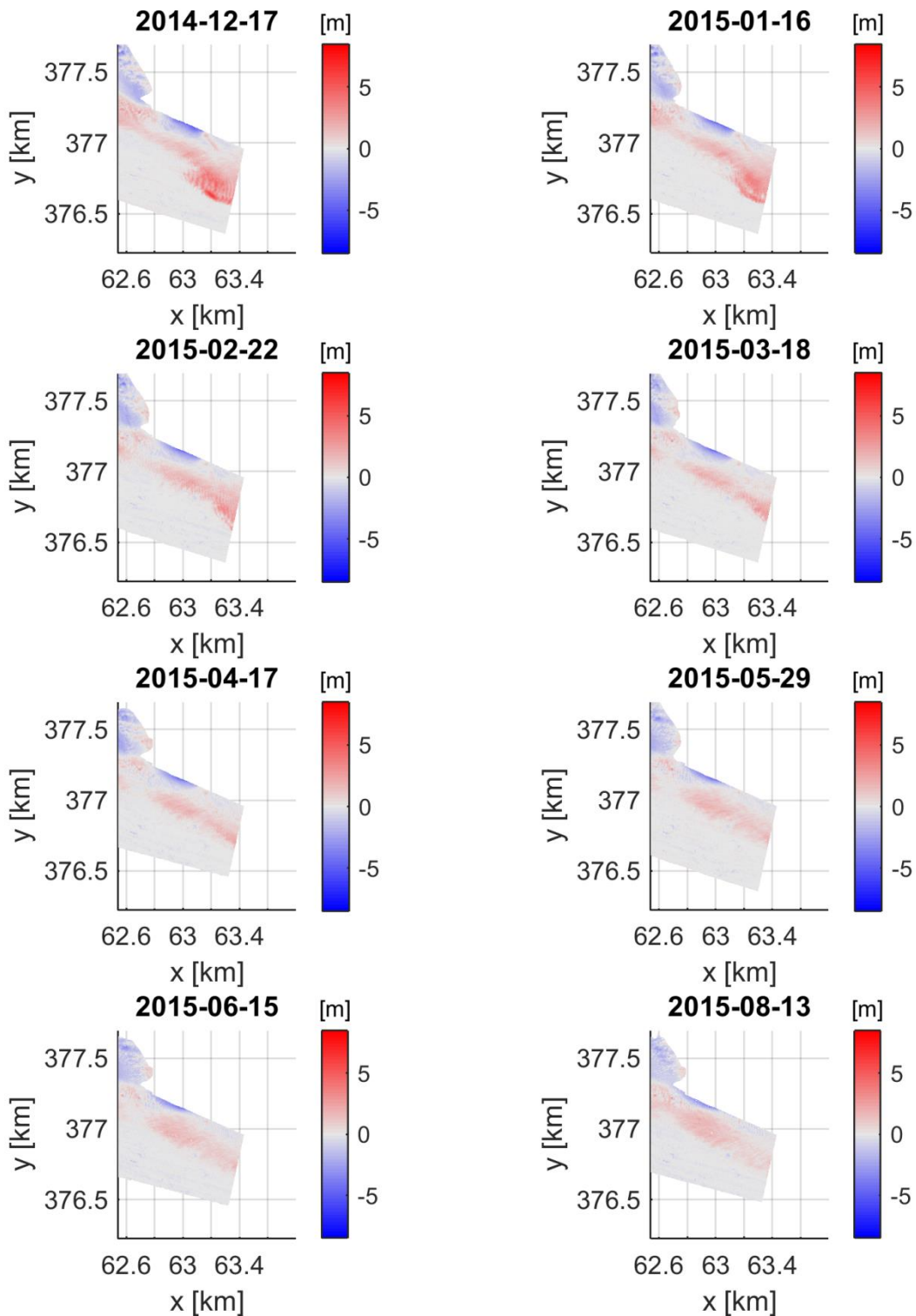


Figure A.5: Erosion with respect to June 2014 for December 2014 till August 2015

## A.2.2 With respect to August 2014

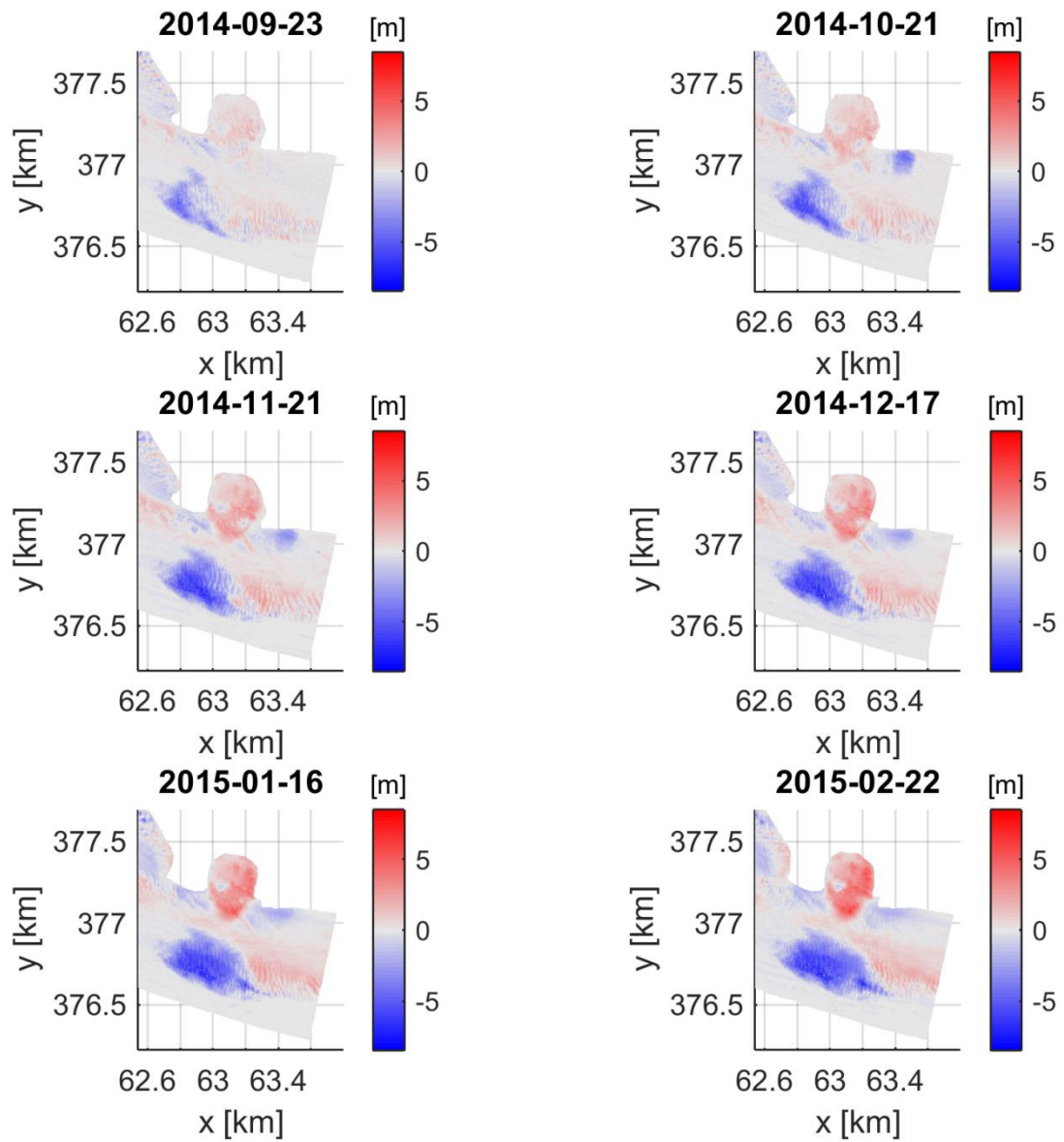


Figure A.6: Erosion with respect to August 2014 for September 2014 till February 2015

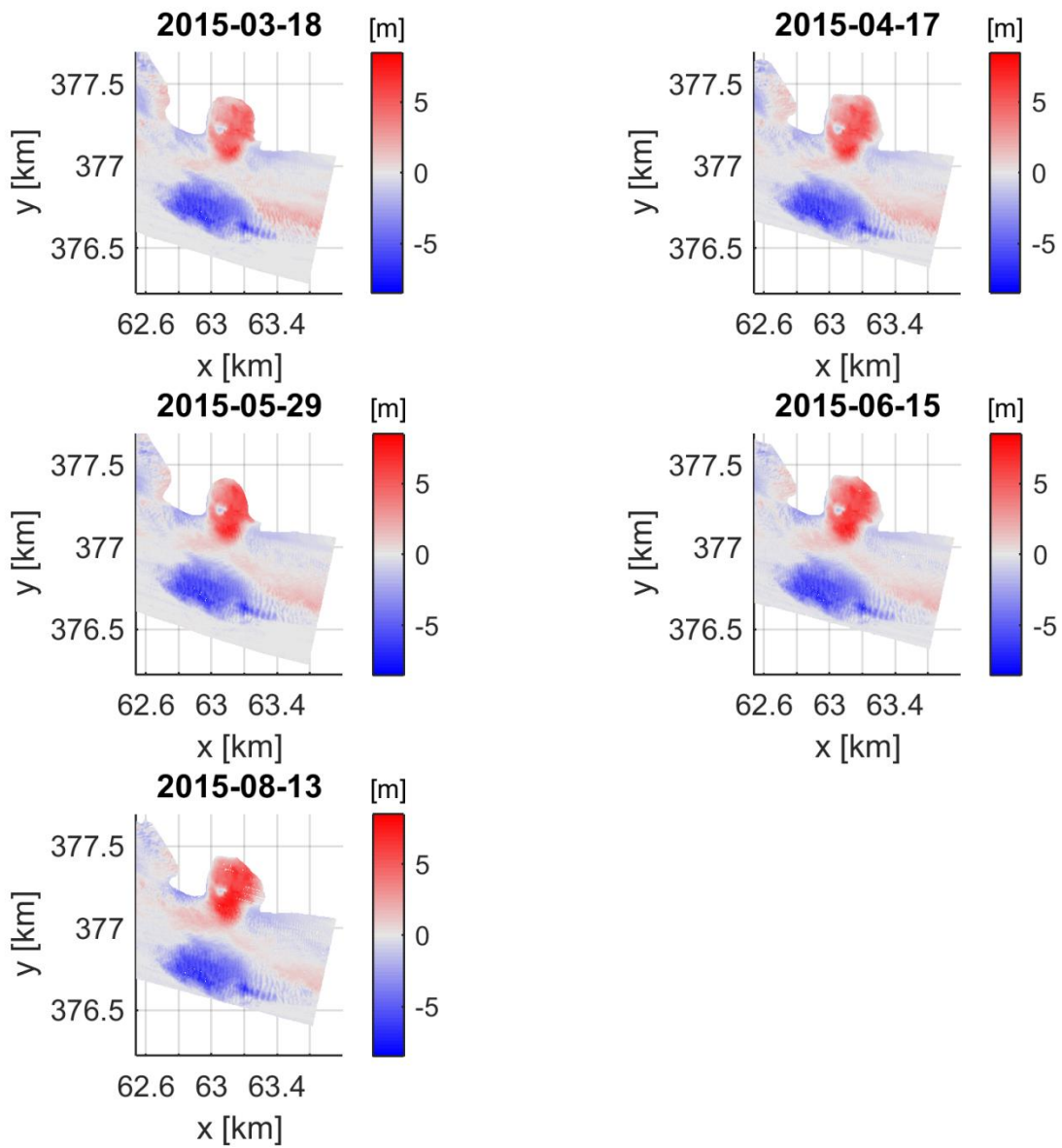


Figure A.7: Erosion with respect to August 2014 for March 2015 till August 2015

## A.2.3 Monthly erosion

The monthly erosion is given in Figure A.8 and Figure A.9. In these figures the difference between two consecutive months is shown. The erosion between September and October 2014 east of the natural flow slide is due to the IJkdijkexperiment, where an artificial flow slide is triggered. This flow slide in the month afterwards already almost filled in.

The erosion front in the middle of the channel is going more and more to the east. In the first month after the flow slide the western part is already almost eroded. Afterwards the erosion is more the east of the flow slide. From March 2015 on the difference in the channel is almost negligible, the channel is returning to its original state. In the gap the most sedimentation occurs on the east side. This indicates infilling during flood.

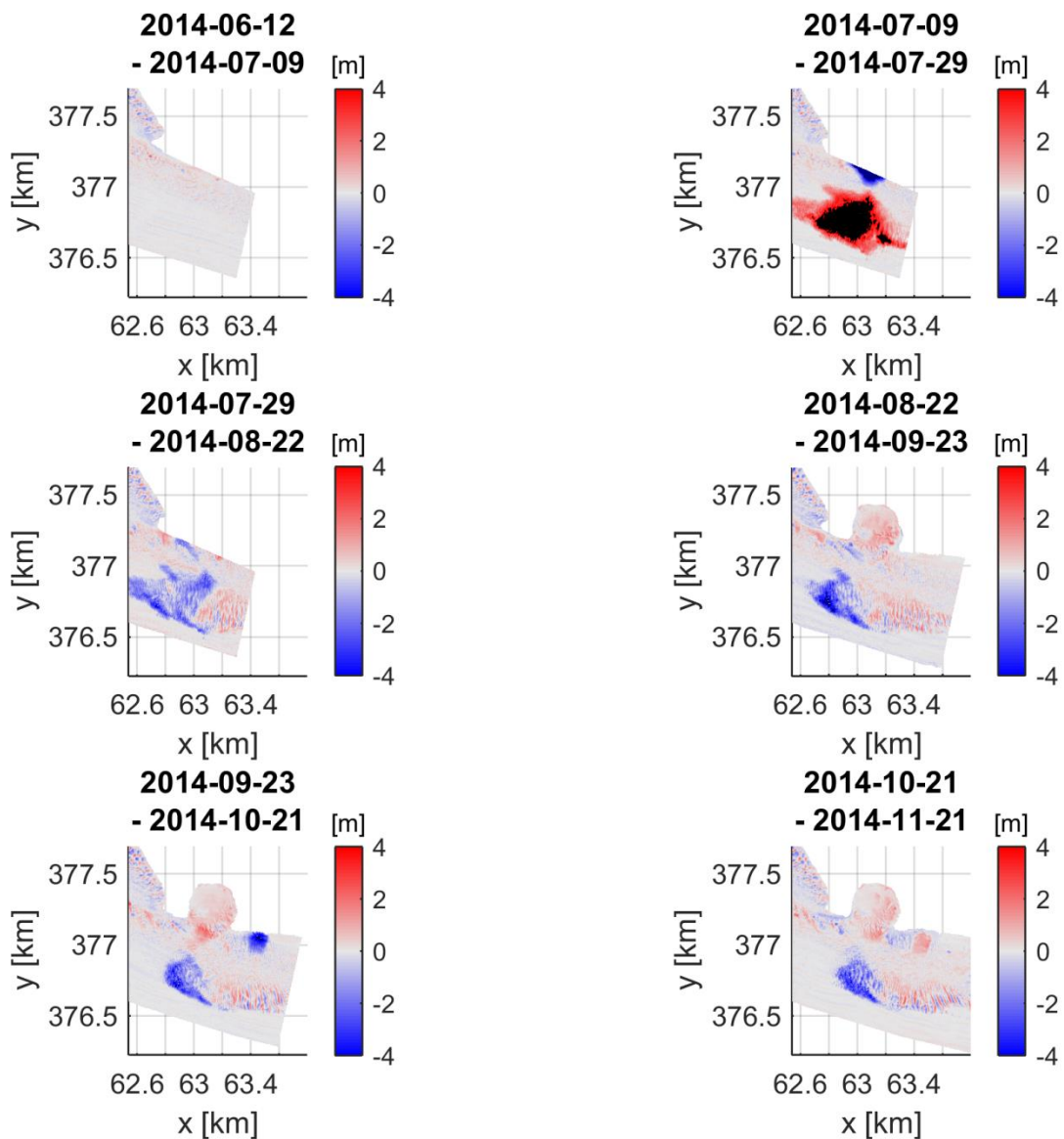


Figure A.8: Monthly erosion from July 2014 till November 2014

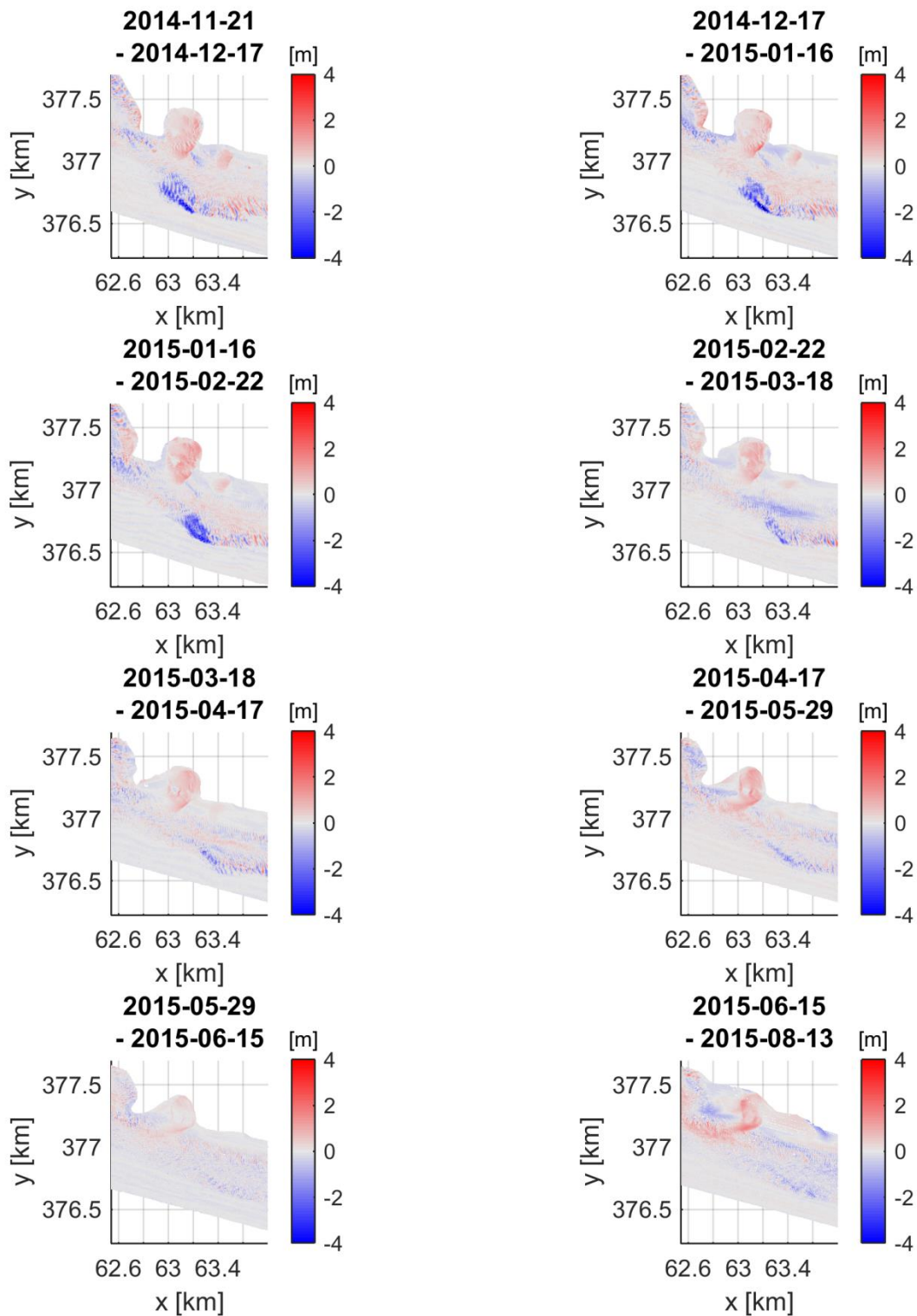


Figure A.9: Monthly erosion from December 2014 till August 2015

## A.3 Cross sections

The locations of the cross sections are given in Figure A.10. In Figure A.11 till Figure A.14 the morphological development along the cross sections is given in somewhat more detail than in Figure 3.9. In these figures the left side is the tidal flat of Walsoorden, the right side is the outer bank. Cross section A-A' is located west of the flow slide, B-B' at the location of the flow slide, C-C' at the east of the flow slide and D-D' somewhat more to the east.

The recovery to the initial profile goes fastest in cross section A-A'. Cross sections C-C' and D-D' show a small increase of sediment in the channel in the first months. After October 2014 there is also a decrease of sediment volume in these cross sections. This indicates net bed load transport in eastern (flood) direction.

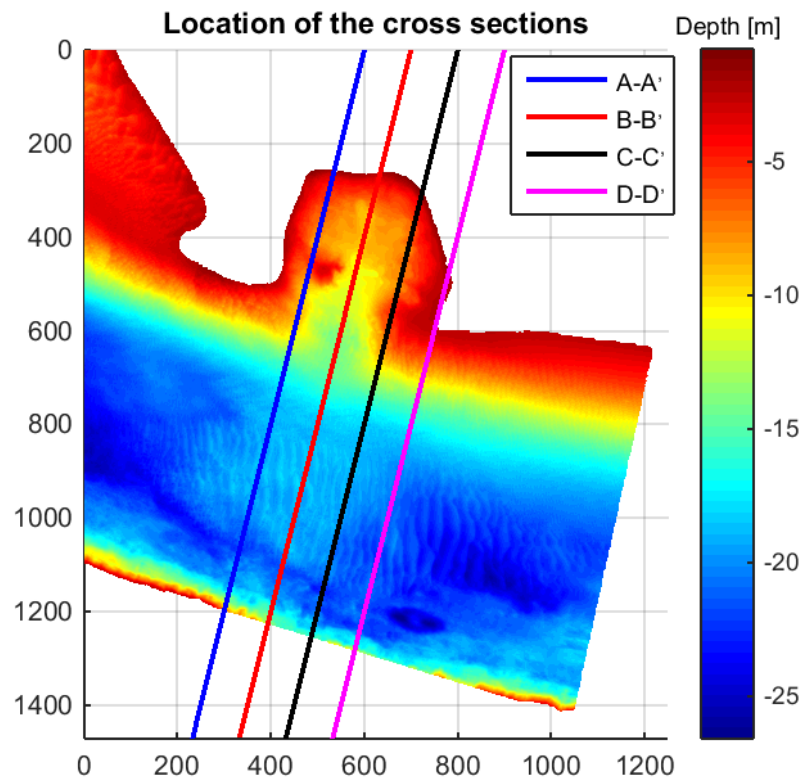


Figure A.10: Locations of the cross sections

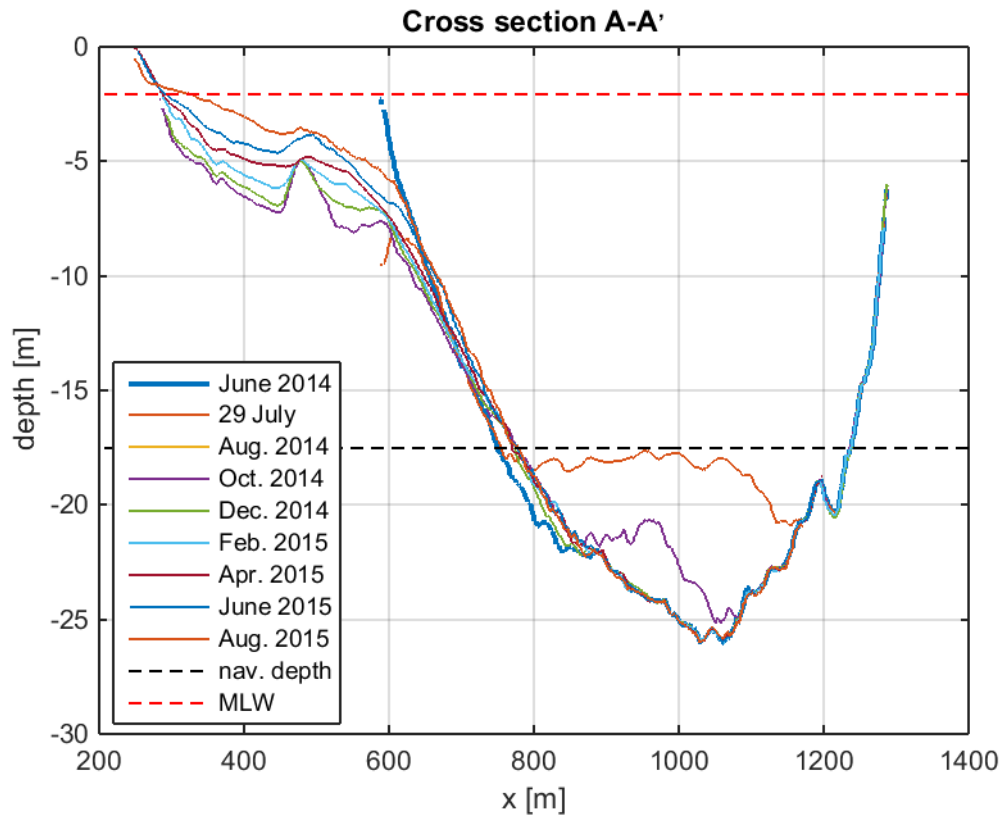


Figure A.11: Morphological development along cross section A-A'

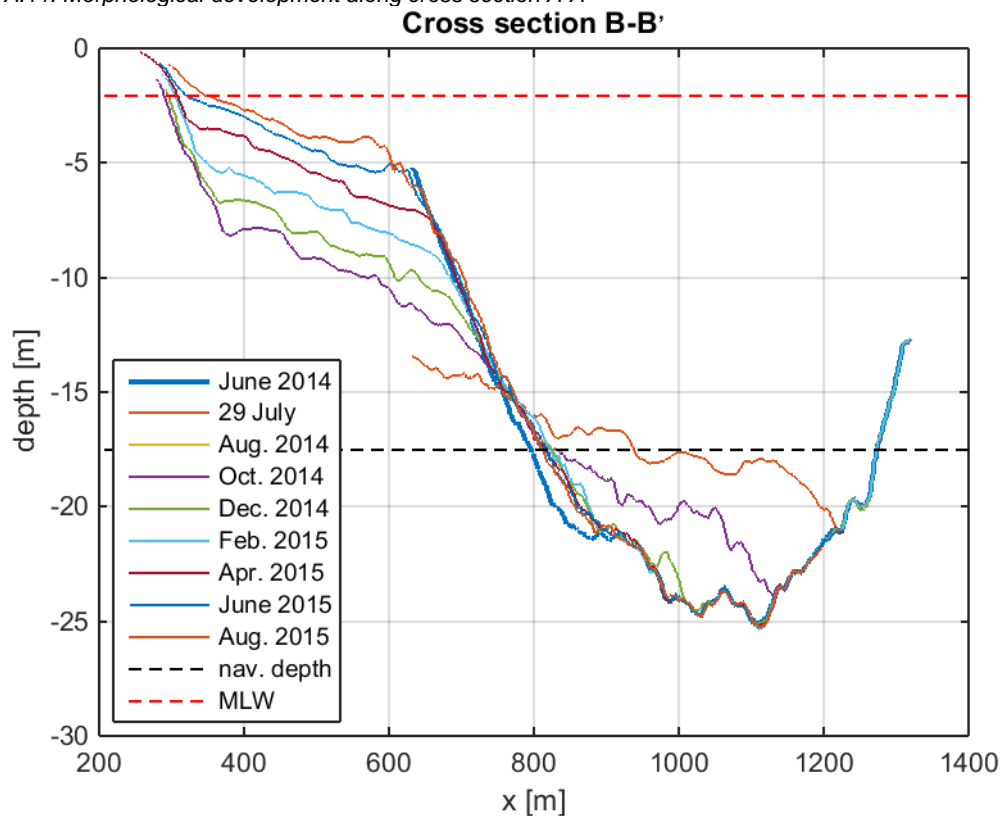


Figure A.12: Morphological development along cross section B-B'

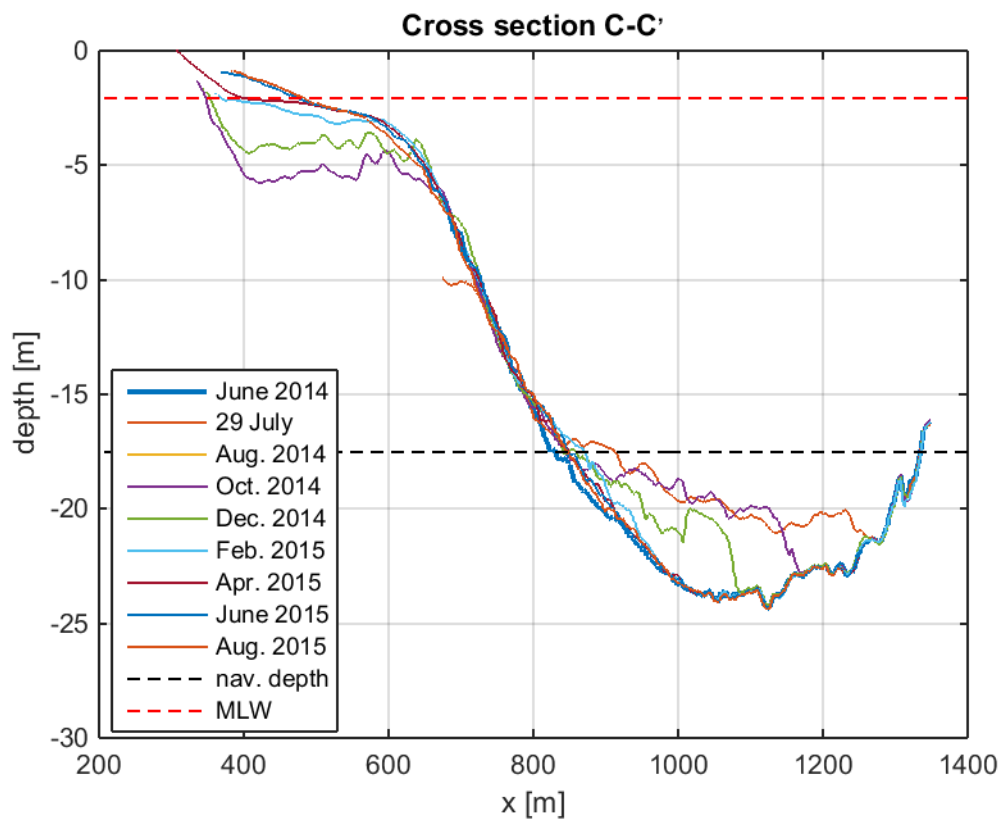


Figure A.13: Morphological development along cross section C-C'

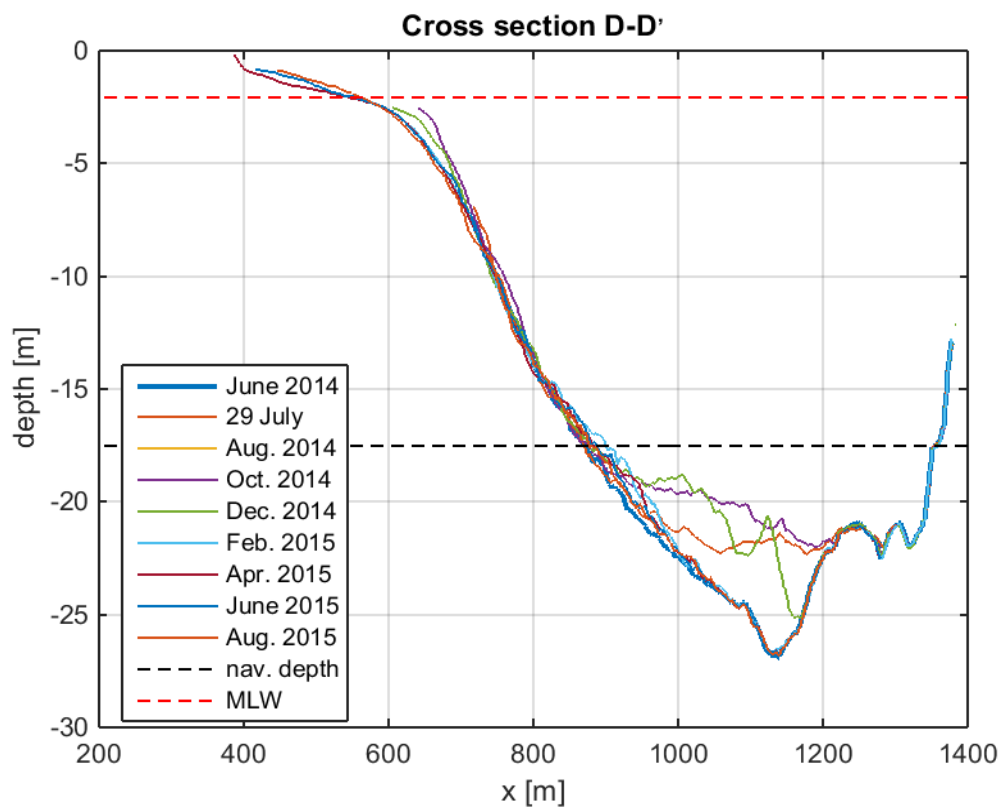


Figure A.14: Morphological development along cross section D-D'

#### A.4 Longitudinal cross sections

To determine if the transport direction is constant along the channel more longitudinal transects are made. Figure A.15 shows the locations of these extra cross sections. The cross section located on the northern side (550) is given in Figure A.16. The deposited sediment is almost equally distributed to both sides of the channel. However, there is a slight dominance towards the west, showing some ebb dominance.

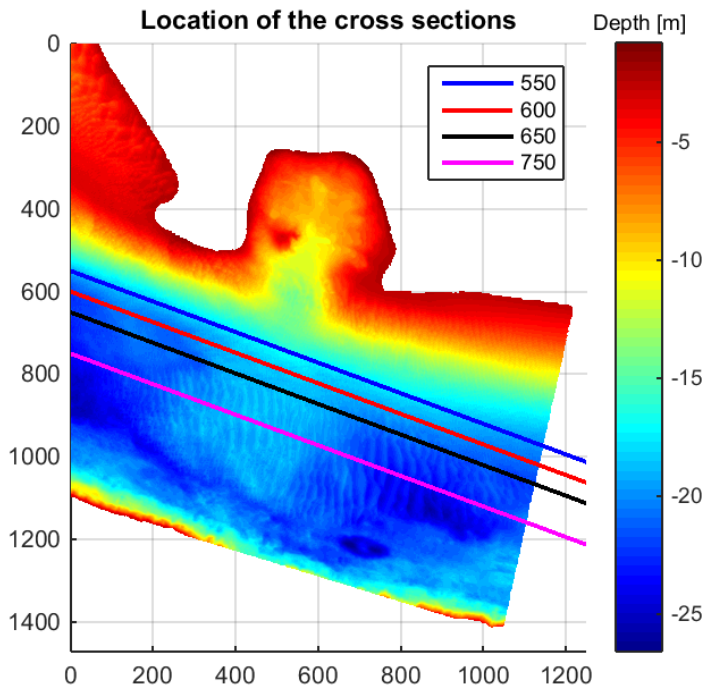


Figure A.15: Locations of the longitudinal sections

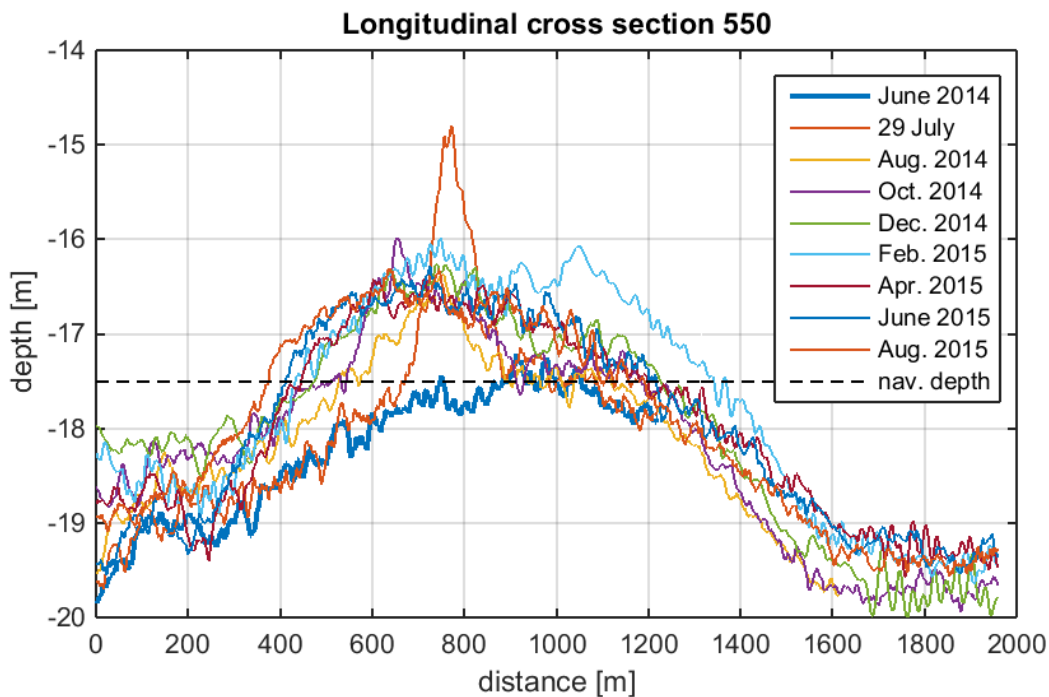


Figure A.16: Cross section 550

The longitudinal cross section more to the south (600) already gives a more dominant transport direction. However, the transport rate is not very high compared to the middle of the channel. Cross section 650 (Figure A.18) gives a quiet clear flood dominated transport direction. From this it can be concluded that the transport direction in the main part of the channel is flood directed. The profile of cross section 750 is already given in section 3.4.2, giving a flood directed transport. On the side near the edge of the tidal flat the transport becomes slightly ebb dominated.

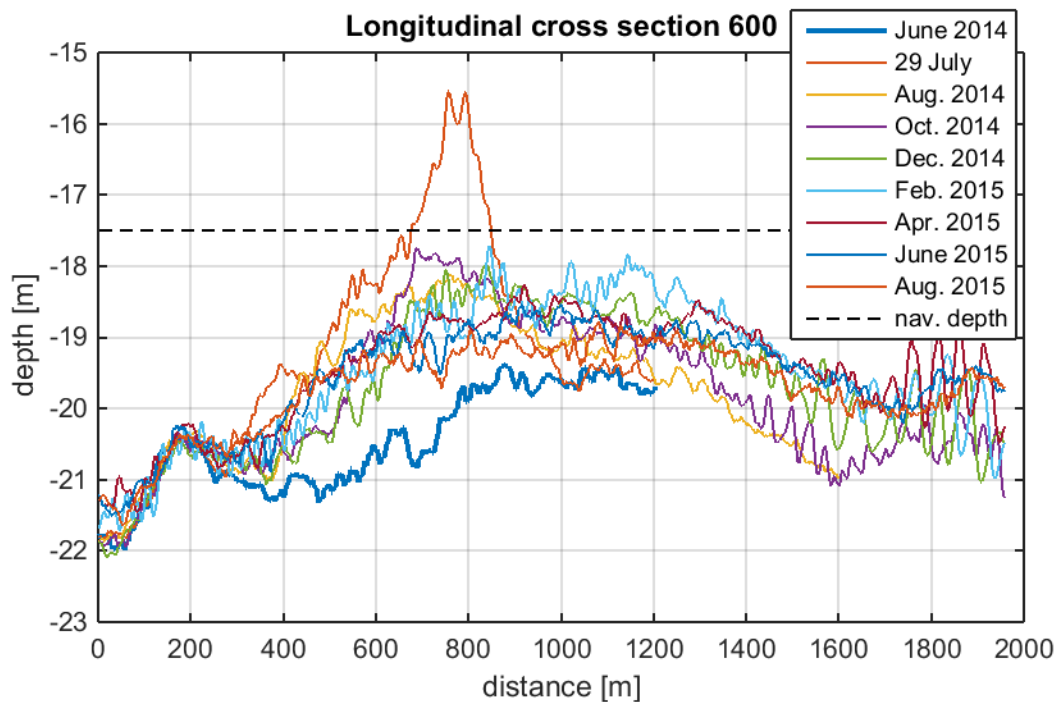


Figure A.17: Cross section 600

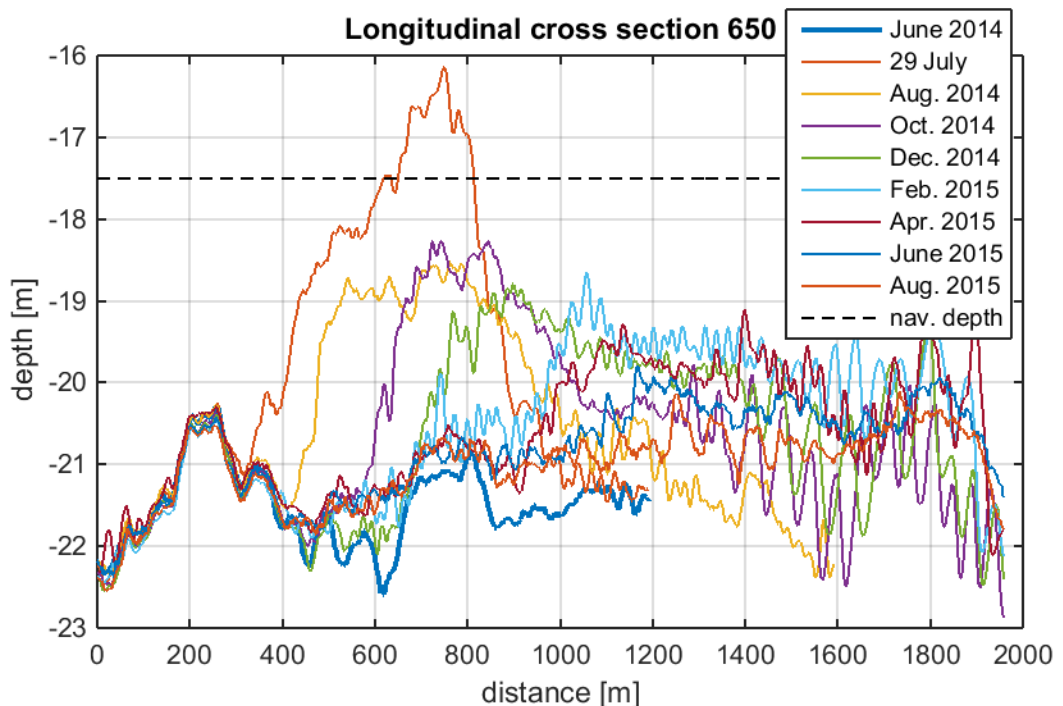


Figure A.18: Cross section 650

### A.5 Location of the sediment accumulation

For the determination of the sediment volume and the amount of sediment that disappeared from the sediment heap, the sediment accumulation is followed. Each month a different polygon is defined based on the position of the sediment heap in the channel. The locations of these polygons are given in Figure A.19. The polygon for the 29<sup>th</sup> of July 2014 is given by the polygon named July 2014.

In the first months (July 2014 till January 2015) the polygons are travelling towards the east. The surface of the polygons is decreasing since the sediment of the flow slide is decreasing. This is already observed in the erosion/sedimentation plots. From February 2015 on the sediment accumulation is situated in the north-eastern part of the channel and the polygons are very similar.

The volumes are based on the difference between the original situation and the bathymetry of that specific month. For the situation of July 2014 till December 2014, the bathymetry of the 9<sup>th</sup> of July 2014 is chosen as the original situation. From January 2015 on this was not possible, since during the July 2014 measurement the eastern part of the channel was not measured sufficiently far away. Therefore the measurement of the 22<sup>nd</sup> September 2014 is used. During this measurement the bathymetry of the eastern part of the channel was measured, but there was no influence of the flow slide in this part of the channel yet.

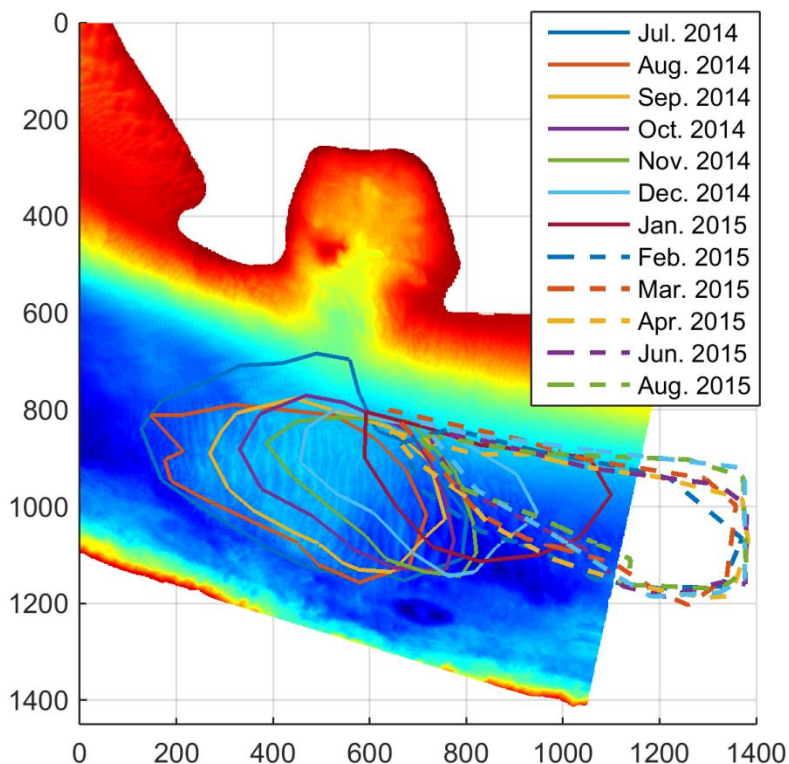


Figure A.19: Locations of the polygons used to determine the floating volume

## B Simulation period

In order to save calculation time a representative period is chosen for the year 2014. This period consists of one spring-neap tidal cycle that is representative for the entire year. Using the measured water level at Baalhoek the different spring-neap cycles are defined (Rijkswaterstaat, 2015). The duration of one spring-neap cycle is determined with equation B.1. In this equation the frequencies of the S<sub>2</sub>- and M<sub>2</sub>-tide are extracted from the water level signal. In total 23 periods are formulated, starting during neap tide. In Figure B.1 these spring-neap tidal cycles are given.

$$T_{spring-neap\ cycle} = \frac{1}{f_{S_2} - f_{M_2}} \quad (B.1)$$

For every period the mean water level is compared with the mean water level over the complete period. This gives the capacity of each period to represent the year 2014. For the periods 3 and 14 the difference is the smallest. Figure B.1 gives the spring-neap tidal cycles and the water level variation in the year 2014.

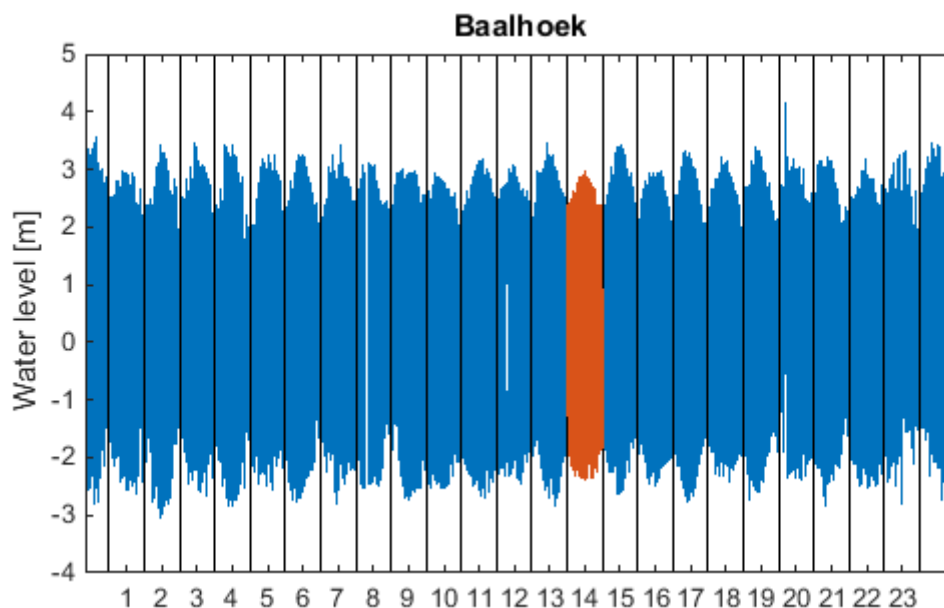


Figure B.1: Spring-neap tidal cycles in the year 2014

After this also the wind for the periods is compared to the annual wind. This is done for the magnitude and the direction by comparing the periods with the annual values (Rijkswaterstaat, 2015). The annual wind shows a somewhat fierce pattern (Figure B.2). Storms are present in almost all periods. However, period 14, in Figure B.3, shows calm and steady conditions. This period represents the situation without storm influence. The storms have a different direction than the normal wind conditions, this gives a large difference in wind rose between annual and periodical result for period 14. If the storms are suggested to have a large influence period 3 should be chosen. However, since waves are not included the influence of storms is almost negligible and period 14 can be chosen.

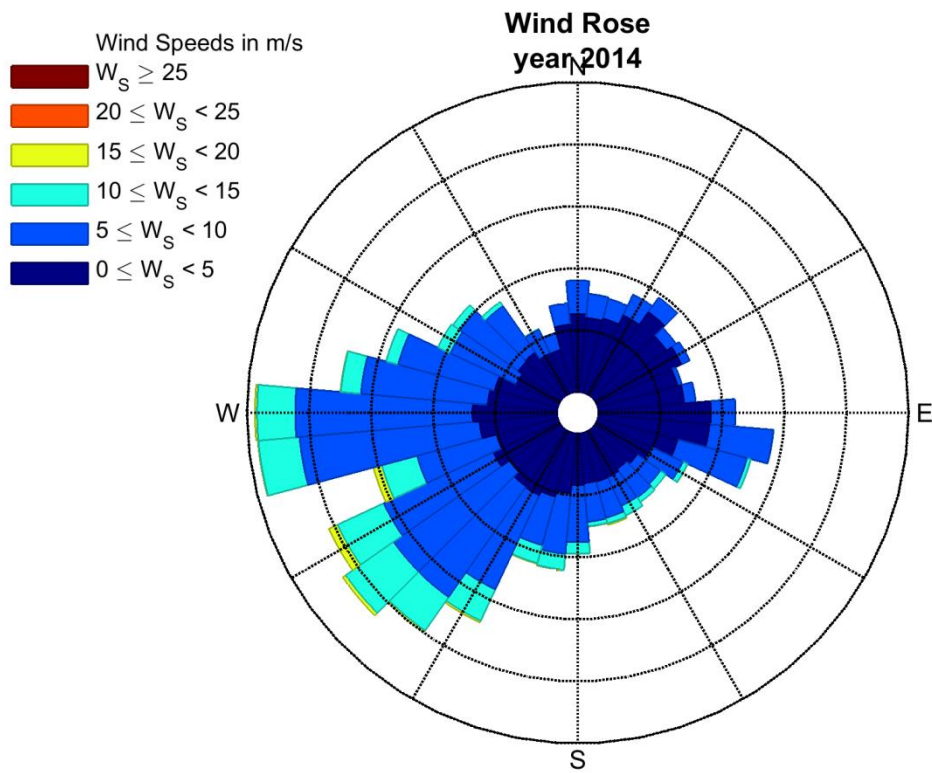


Figure B.2: Wind rose for the year 2014

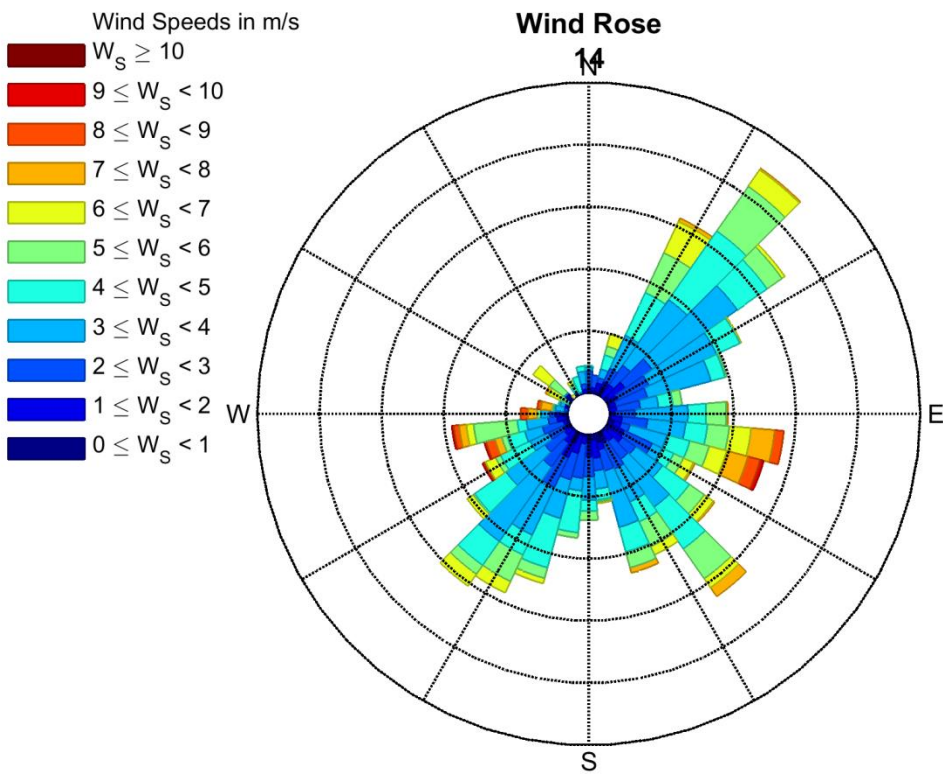


Figure B.3: Wind rose for period 14

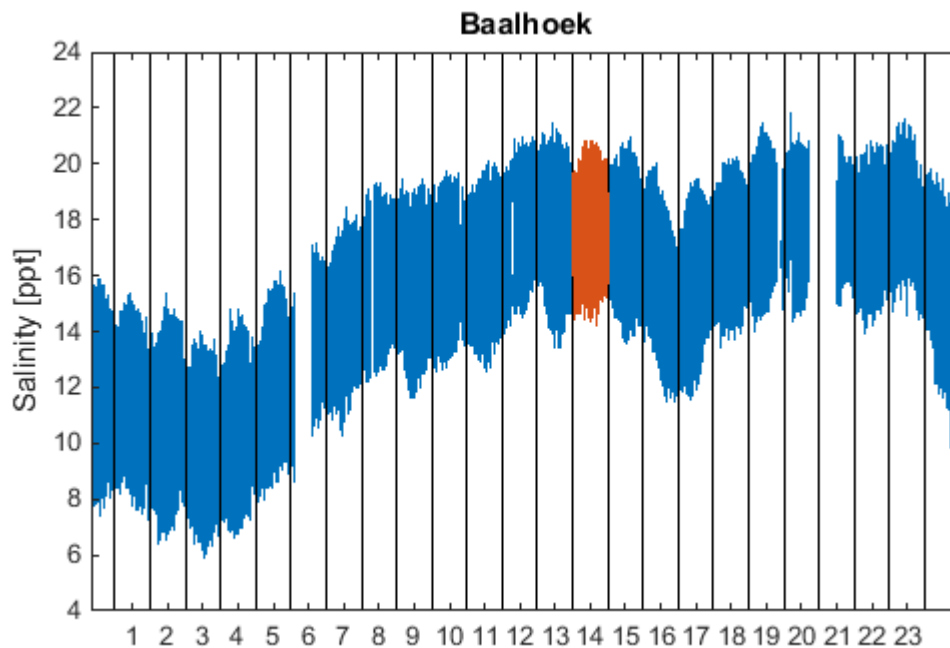


Figure B.4: Salinity distribution over the year 2014 with the indication of the spring-neap tidal cycles

Another parameter that has to be taken into account is the salinity distribution over the year. In Figure B.4 the salinity distribution is given for the year 2014 (Rijkswaterstaat, 2015). There is a large seasonal variability, in summer the salinity is higher than in winter. This is due to the larger river discharge in winter and spring than in summer. Due to this large seasonal variability only the second half year is used to determine the representative period, since this is also the period where the development after the flow slide occurred. When this is used period 14 and 15 are found to be representative for the second half year.

Based on the aforementioned, period 14 is chosen as the representative spring-neap tidal cycle. This period gives a representation of the period after the flow slide for the water level and salinity. For the wind it also gives sufficient results. The only disadvantage of this period is the absence of a storm condition, but since waves are not imported in the model this effect is negligible. The selected tidal cycle occurs between 22-Jul-2014 08:20:00 and 06-Aug-2014 03:20:00.



## C Validation domain decomposition

Through the domain decomposition boundaries information is given from one domain to the other. This technique is very vulnerable for errors and therefore it is important to check if the communication between the domains is correct. This is done using cross sections on both sides of the domain decomposition sections. The locations of these cross sections are given in Figure C.1.

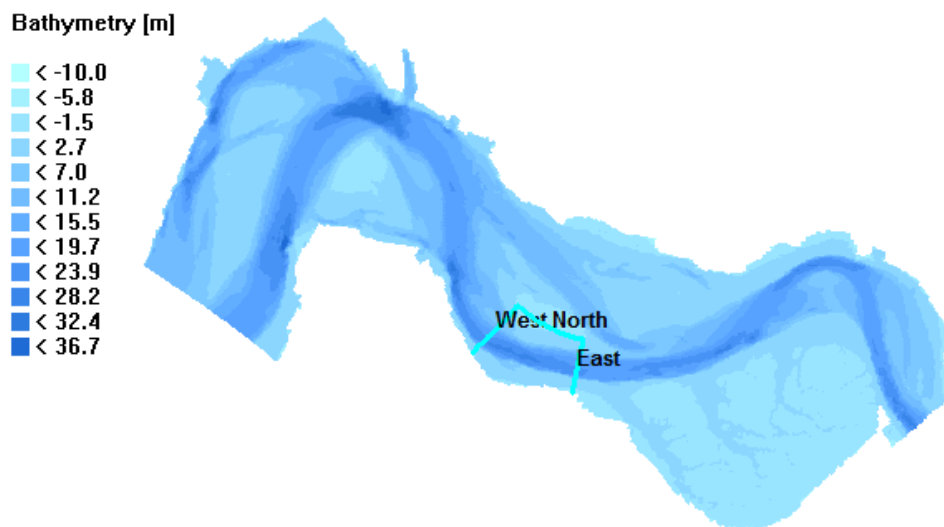


Figure C.1: Location of the cross sections for the domain decomposition

The communication between the two domains is checked on different characteristics. First of all the discharges are compared, see Figure C.2. In this figure dda is the large, overall domain and ddb is the small, refined domain around the location of the flow slide. In the figure only one line can be observed. The other line (dda) is exactly behind the visible line. From this it is concluded that the accuracy of the information transfer for the discharge is sufficient.

The sediment transport through the domain decomposition boundaries is still subject to some discussion. The transport of suspended sediment gives a small inaccuracy, shown in Figure C.4. The bed load transport gives, on the contrary, exactly the same results on both sides of the boundaries. In this model the Engelund-Hansen formula is used. This gives more certainty in the sediment transport in the area near the flow slide, but it also gives better results for the domain decomposition. The Engelund-Hansen method calculates the total transport. This is imposed as bed load transport, giving no problems for the domain decomposition. Therefore this method is better when domain decomposition is used, because it gives negligible errors concerning sediment transport. The total transport for the Engelund-Hansen method through the domain decomposition boundaries is given in Figure C.3. In this figure only one line is shown, the other one is exactly behind it. This indicates a high accuracy for the communication between the domains.

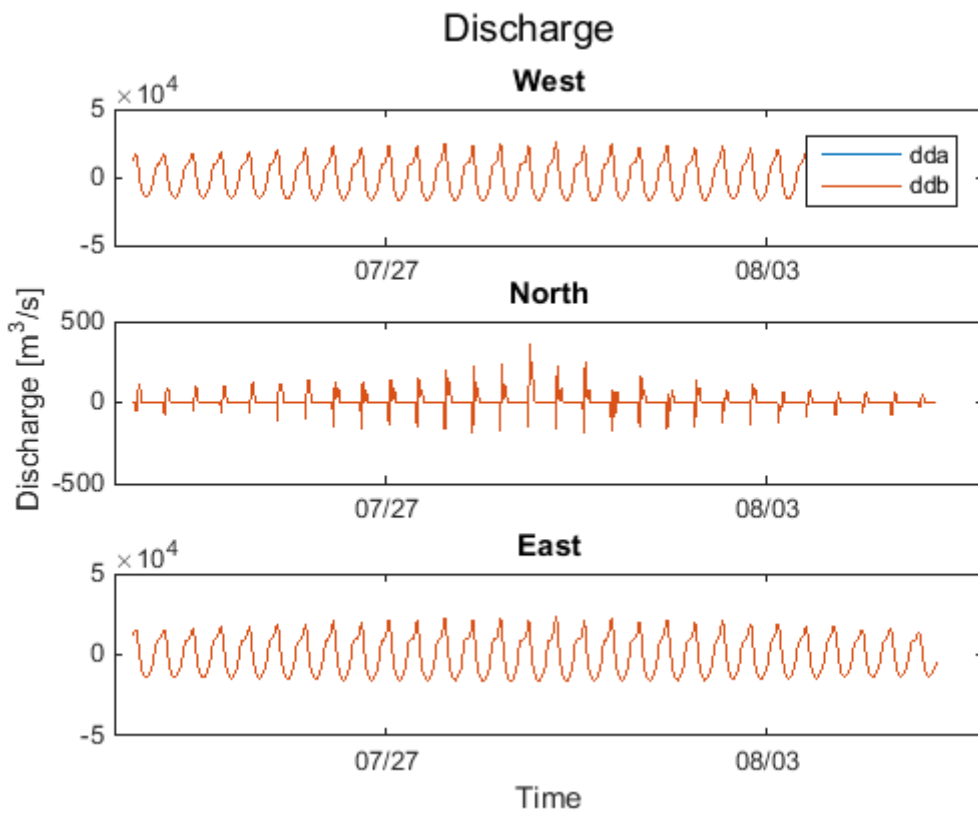


Figure C.2: Discharge on both sides of the domain decomposition boundaries

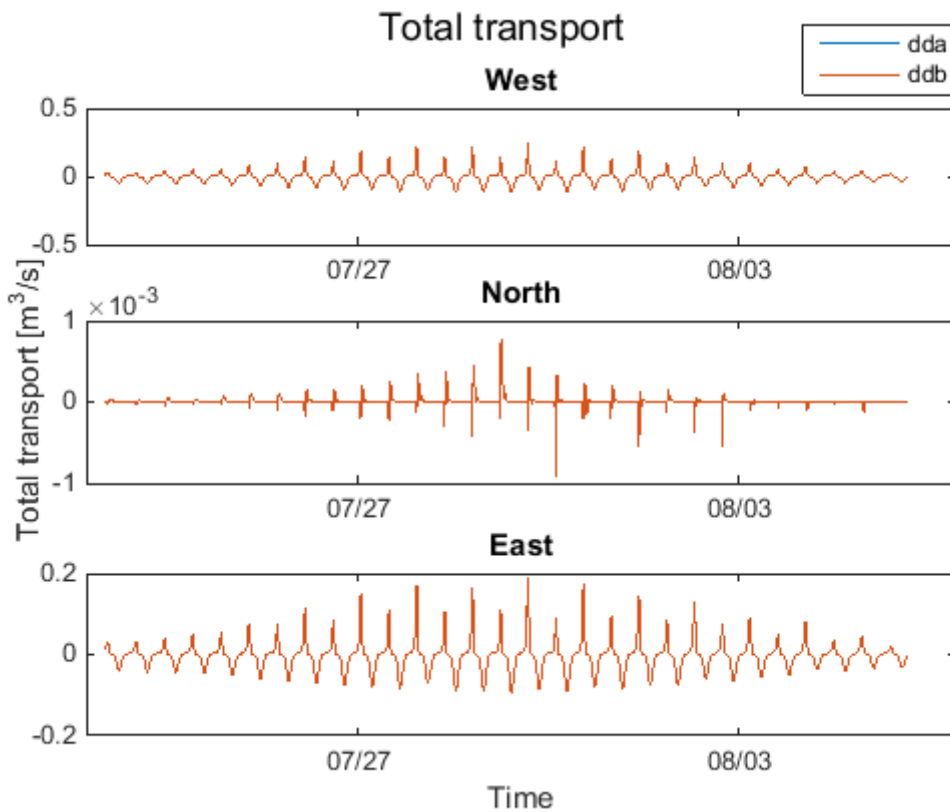


Figure C.3: Total transport through the domain decomposition boundaries for Englund-Hansen

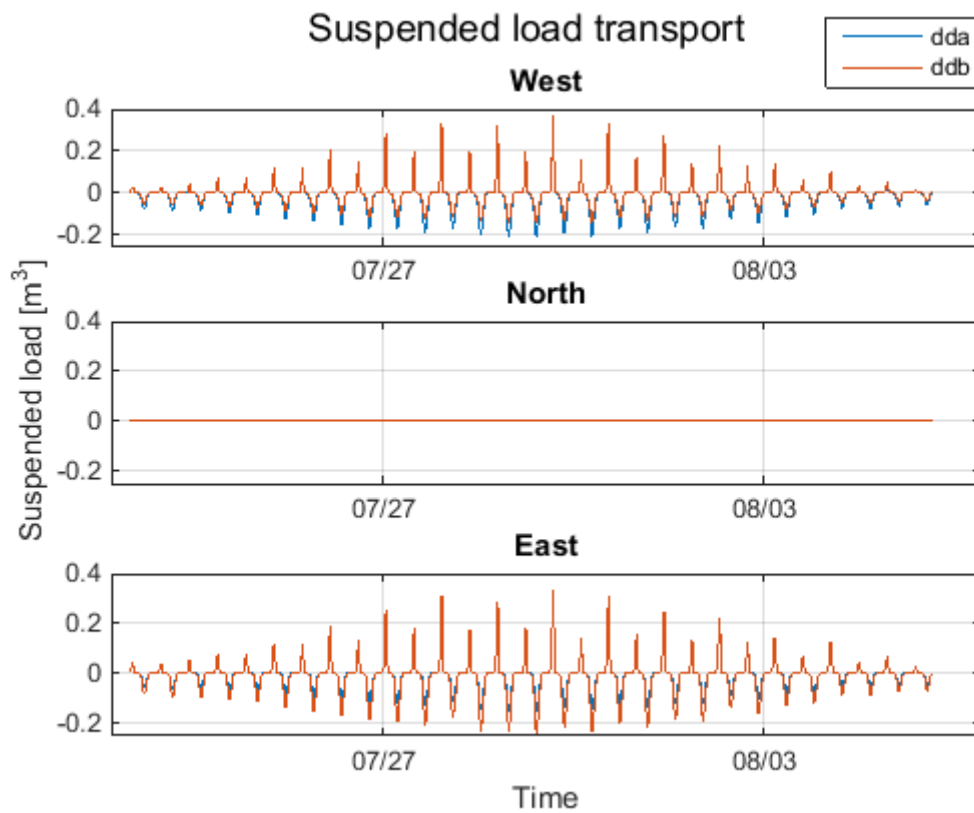


Figure C.4: Suspended load transport for Van Rijn 2004



## D Validation MONEOS measurements

In Chapter 5 the model results are compared with the MONEOS measurements. MONEOS is an abbreviation of Monitoring Effecten Ontwikkelingsschets 2010. During these measurements the flow velocity and direction and water level are measured. This is done using a Nortek AquaDopp Profiler (2 MHz). The points are measured for two spring-neap cycles. The water level is interpolated if the tidal flat runs dry with the (wet) points close by. In Figure D.1 till Figure D.4 the model results are compared with the measurements for all measured points. The water level is given on the left and the velocity on the right. Based on this comparison the model is validated. In these figures maximum flood velocity occurs approximately at 15h00 10-10-2014.

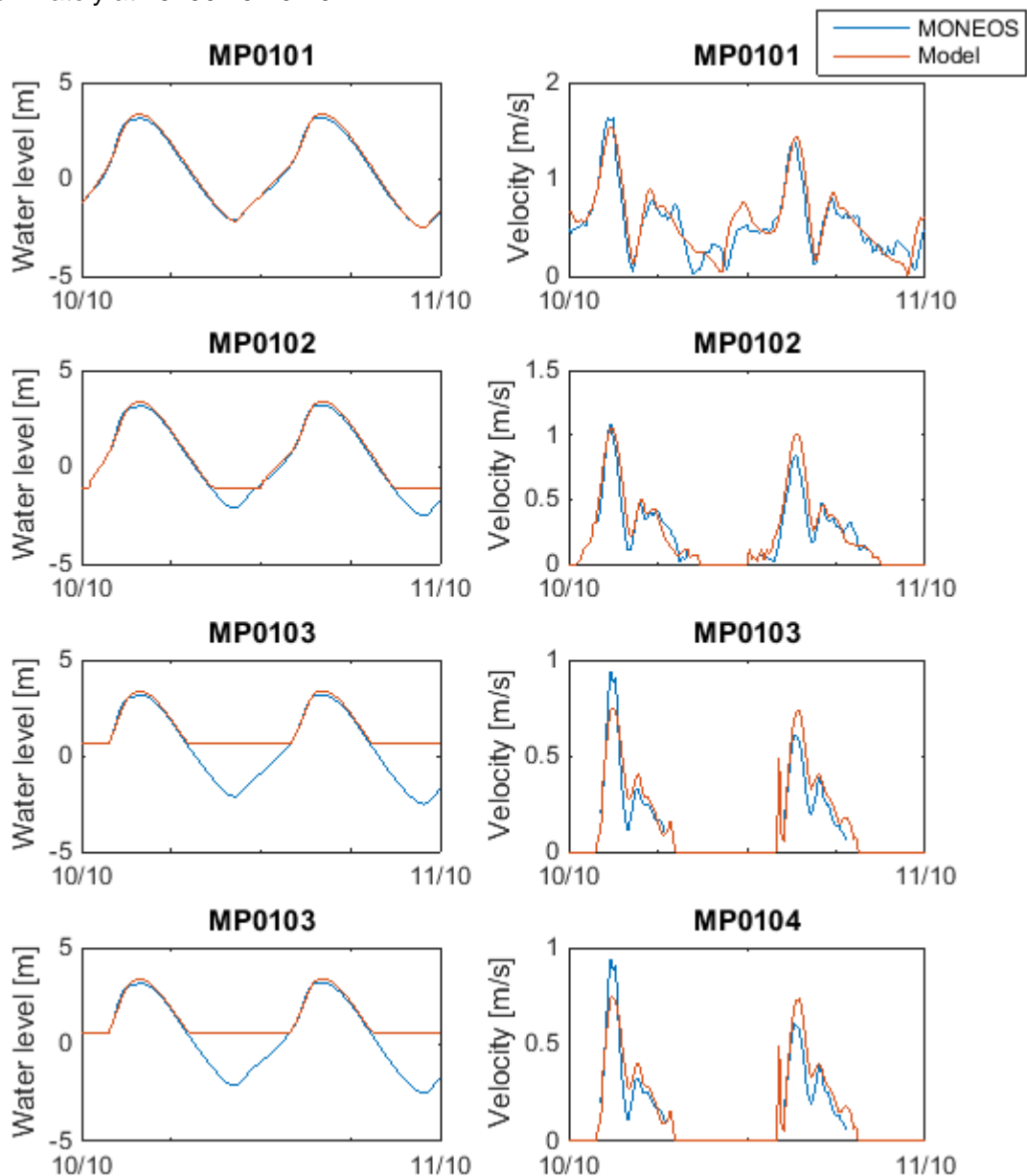


Figure D.1: MP0101 – MP0104

The points MP0101 till MP0104 lay on the northwest side of the tidal flat. The water level shows an overestimation of the high water and a small underestimation of the low water. This difference is seen in all points. The flow velocities perform reasonably well. The same pattern is found in the measurements and the model results.

The same is found in the points MP0309 till MP0312, these points lay on the southwest part of the tidal flat. The water level behaves the same as in the previous points. The velocity from the model follows the measurements very well.

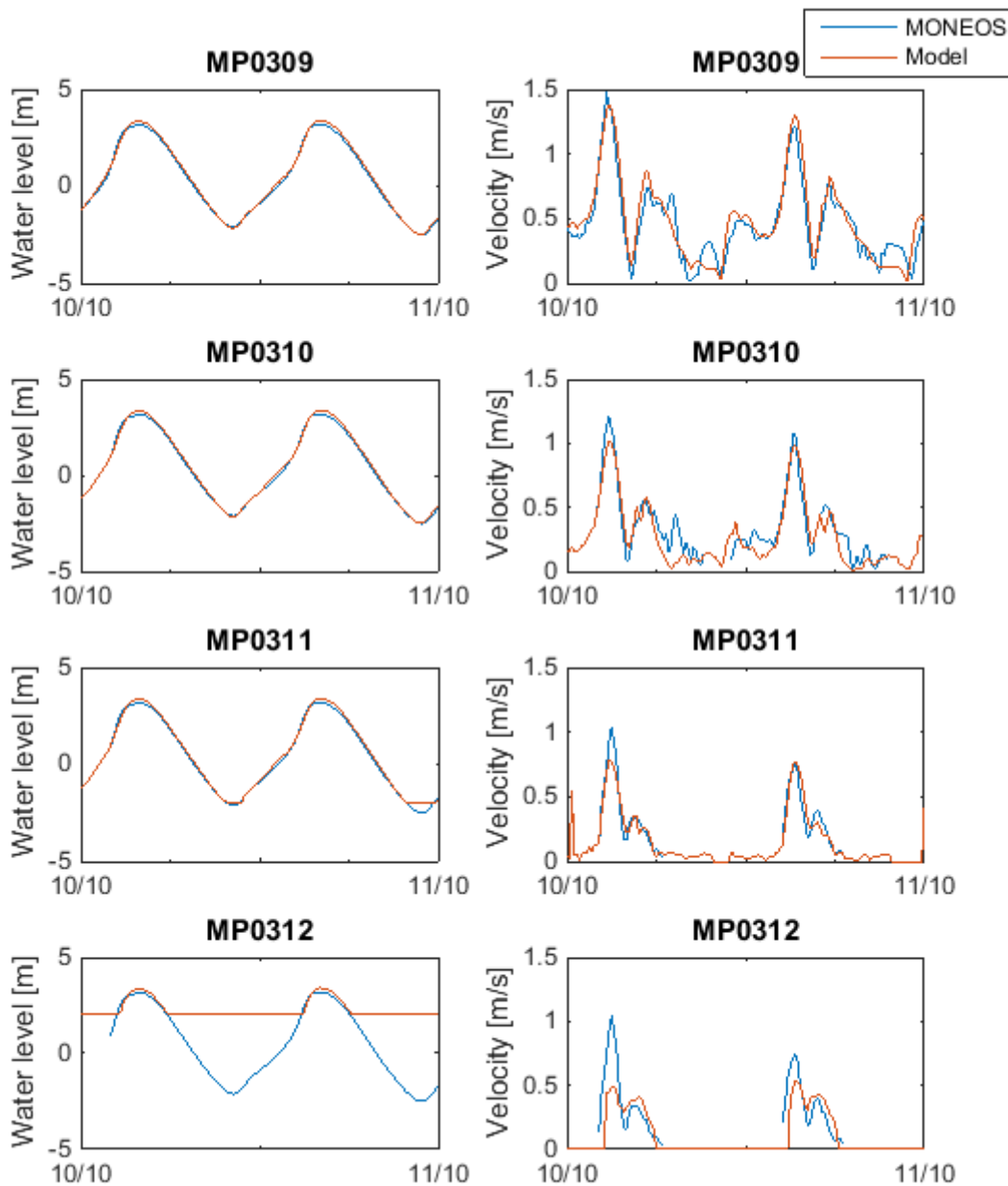


Figure D.2: MP0309 - MP0312

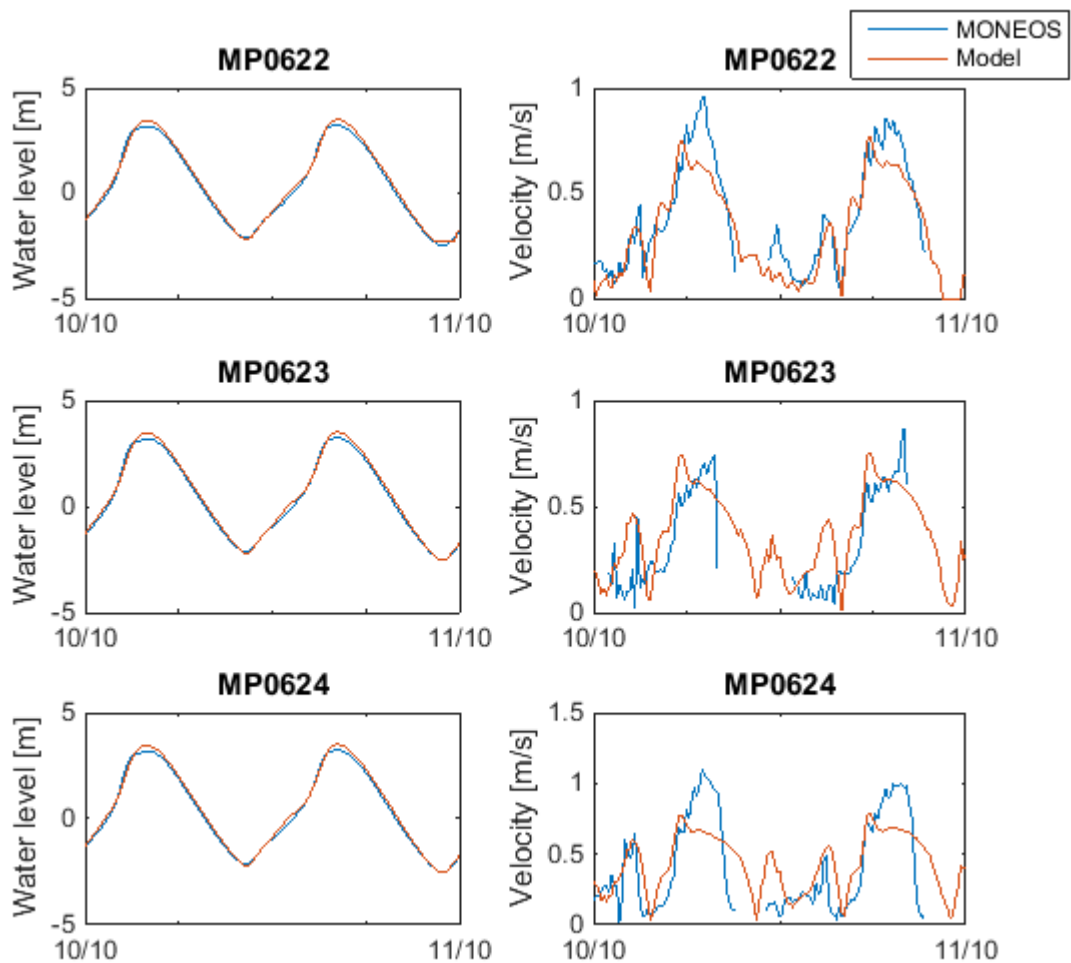


Figure D.3: MP0622 – MP0624

The points MP0622, MP0623 and MP0624 are located on the southeast side of the tidal flat. This part of the tidal flat is very dynamic. The variations in bathymetry give a difference in the velocity magnitude and pattern. The pattern from the model is different from the pattern in the measurements; this is probably due to the difference in depth. The magnitude is approximately equal for the model and the measurements.

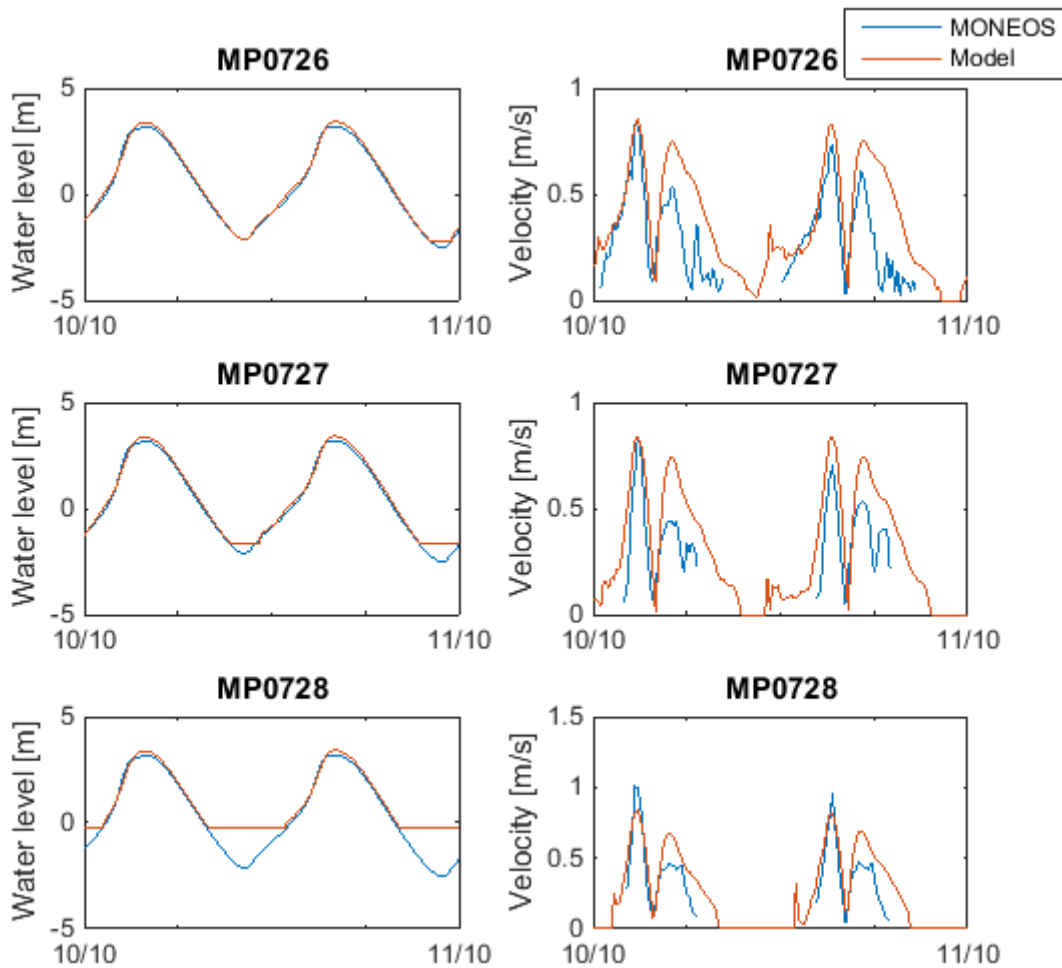


Figure D.4: MP0726 – MP0728

Along the northern channel the points MP0726, MP0727 and MP0728 are located. The water level performs the same as for all the other points. The velocity shows a good approximation during flood, but an overestimation of the ebb velocities. However, these points are located further away from the area of interest, so a small difference is acceptable.

From all the points above it is found that the water level and velocity in the model performs very well compared to the measurements. In all points the same pattern is found and the same order of magnitude for the model and the measurements. This gives sufficient confidence in the behaviour of the model.

## E Modelled sediment transport

In the model the mean total transport is calculated for the situation before and after the flow slide. This is done using the Engelund-Hansen equation and the Van Rijn equation. The situation after the flow slide with Engelund-Hansen is given in Figure E.1. The difference with the situation before the flow slide is very small. The gap in the tidal flat is not importing any sediment. This is due to the fact that Engelund-Hansen is used without lag effects; the sediment will not settle in the gap. In the figures the magnitude is given in the background and by the length of the arrows. The direction is given by the direction of the arrows.

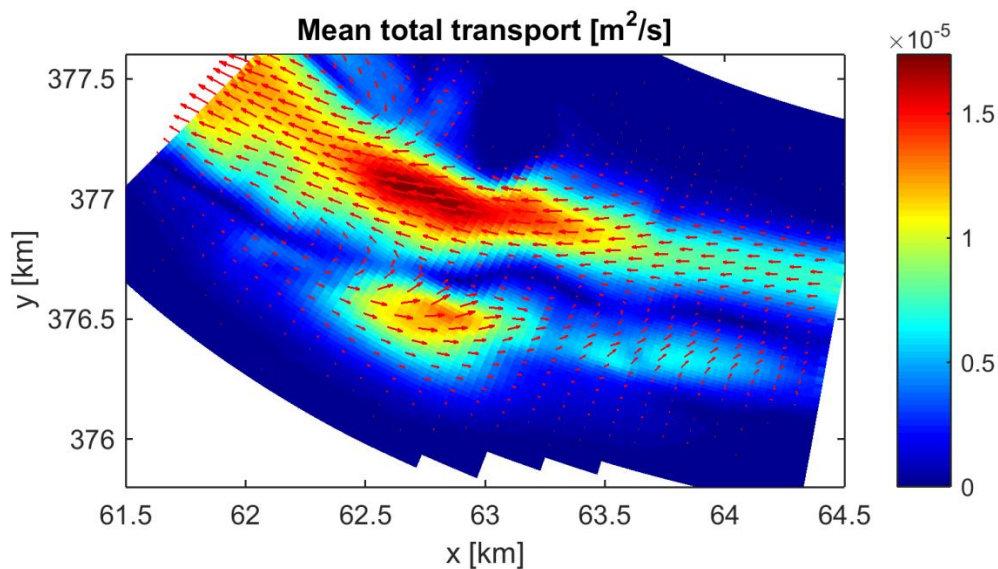


Figure E.1: Mean sediment transport after the flow slide calculated with Engelund-Hansen

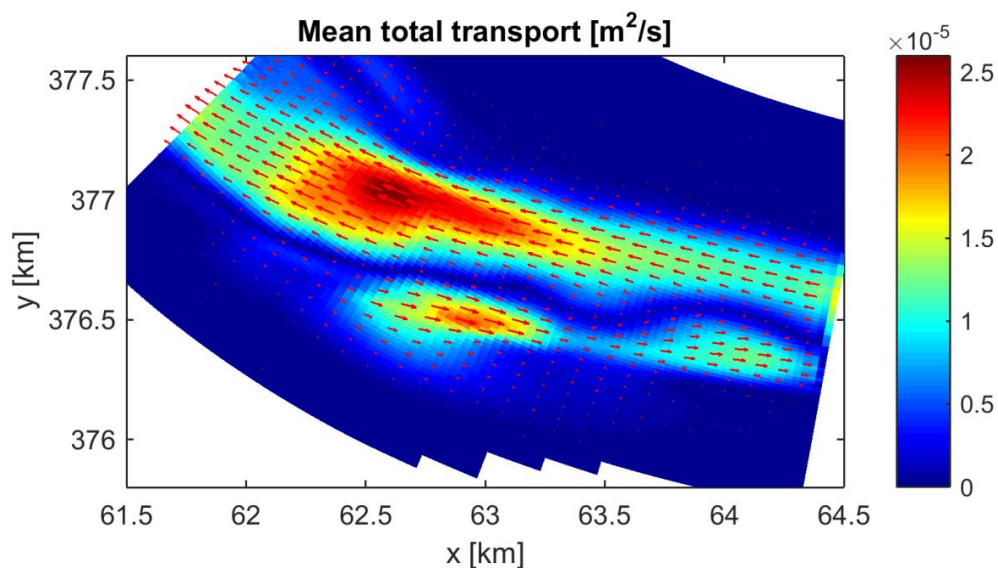


Figure E.2: Mean sediment transport with Van Rijn before the flow slide

Figure E.2 and Figure E.3 show the mean total sediment transport calculated with the Van Rijn equation, before and after the flow slide respectively. Both the patterns are very similar to those calculated using the Engelund-Hansen equation. The magnitudes are slightly higher than with Engelund-Hansen. Unless the inclusion of suspended sediment transport the gap shows no net sediment transport. In Figure E.4 the morphological change over half a year is showed, calculated with the Van Rijn formulation. Compared with the morphological change calculated with the Engelund-Hansen equation (Figure 6.9) the result is very similar.

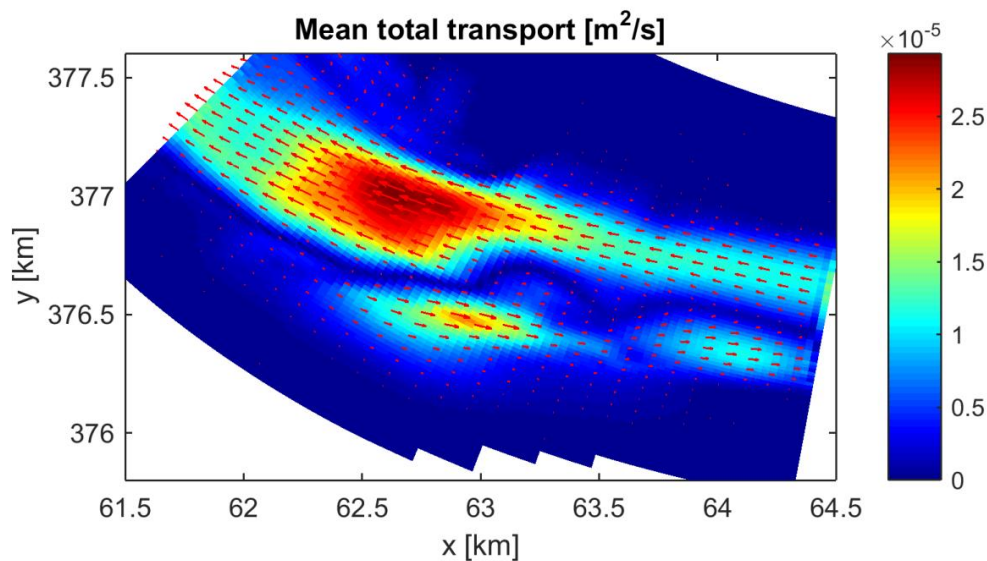


Figure E.3: Mean sediment transport with Van Rijn after the flow slide

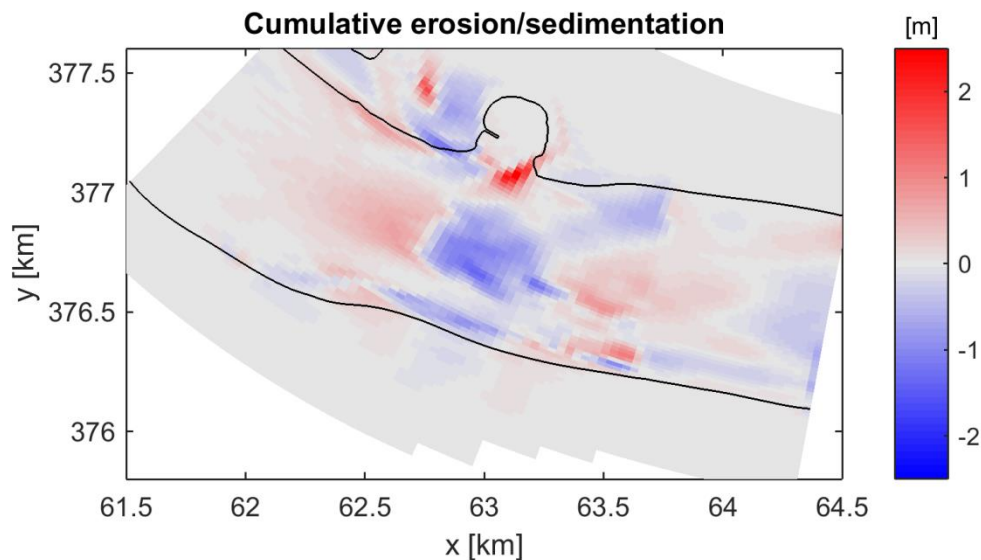


Figure E.4: Morphological change over half a year calculated with Van Rijn (2004)

F Overview channels and shoals Western Scheldt (east)

